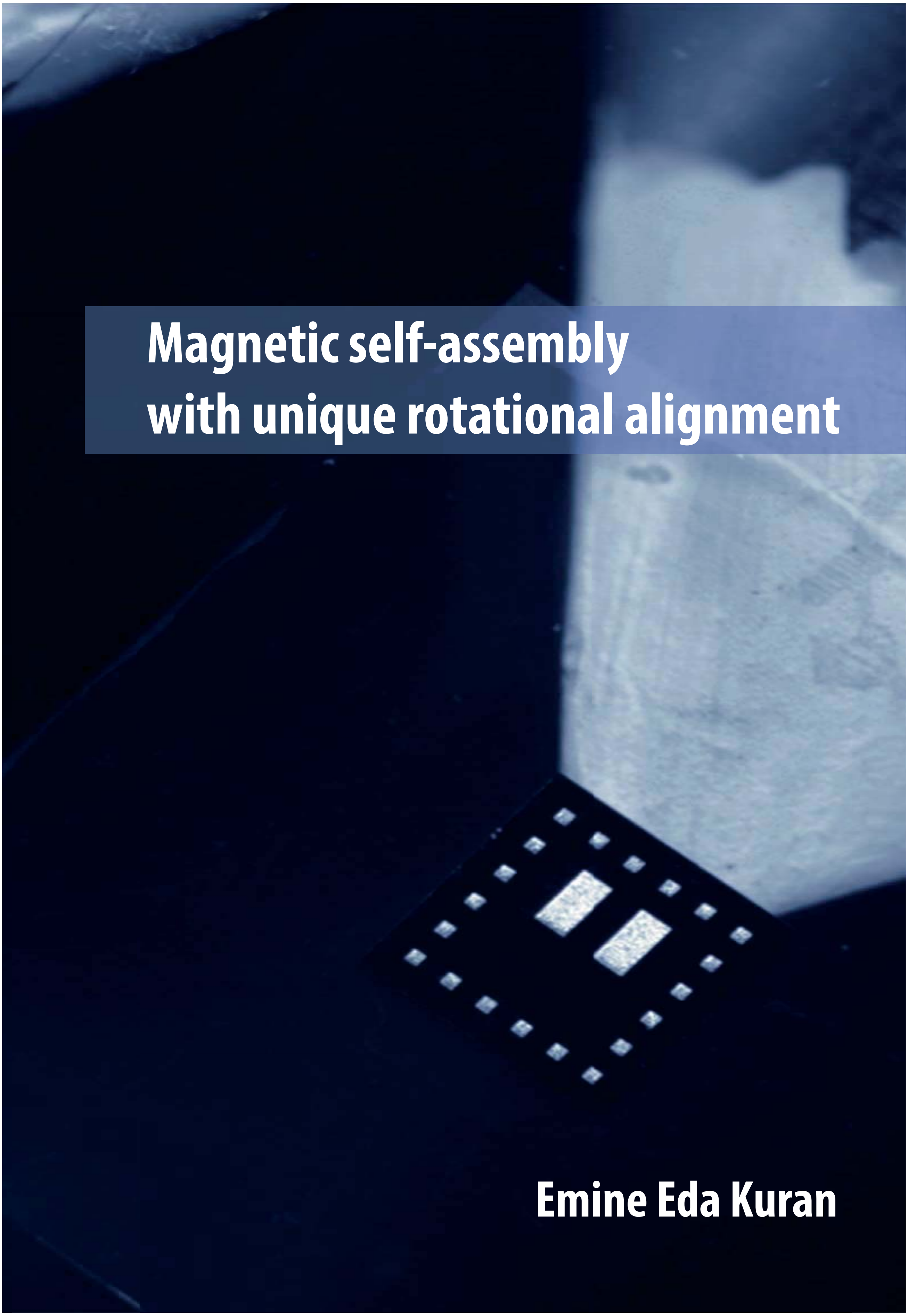

Magnetic self-assembly with unique rotational alignment

Emine Eda Kuran

Propositions

accompanying the dissertation

MAGNETIC SELF-ASSEMBLY WITH UNIQUE ROTATIONAL ALIGNMENT

by

Emine Eda KURAN

1. In self-assembly, regardless of the nature of the force that aligns the parts, using shape asymmetry and shape matching is necessary to reach a unique rotational alignment. (This thesis)
2. Self-assembly can not develop into an advanced process for high-volume manufacturing, unless the researchers start to focus on developing new methods for part presentation and part fixation that are compatible with the physical conditions of an industrial environment. (This thesis)
3. The most important failure mechanism in the manufacturing process of flexible electronics is incompatibility of materials. (This thesis)
4. For assembly of delicate parts, a fast and deterministic part presentation method is more advantageous compared to a stochastic one. (This thesis)
5. Due to the high cost of raw materials, flexible electronics applications that require a silicon chip will never enter the smart packaging market for perishable goods.
6. Writing a thesis is the most enlightening part of the doctoral education.
7. Knowing how to analyze data is more important than the data itself.
8. If you think about money, a precious thing becomes inexpensive when you can afford it. However, time is always precious, even if you have plenty of it.
9. Traffic jams could be resolved, if people would have been more proud of living in a country which is entirely accessible by public transportation, rather than being proud of having a car.
10. Someones comprehension relies more on being interested in a subject than on being smart.

These propositions are regarded as opposable and defendable, and have been approved as such by the supervisor Prof. dr. Urs Staufer.

Stellingen

behorende bij het proefschrift

MAGNETIC SELF-ASSEMBLY WITH UNIQUE ROTATIONAL ALIGNMENT

door

Emine Eda KURAN

1. Bij zelf-assemblage, ongeacht de aard van de kracht waarmee onderdelen uitgelijnd worden, is het gebruik van vorm-asymmetrie en vorm-overeenkomst noodzakelijk voor het bereiken van een unieke rotationele uitlijning. (Dit proefschrift)
2. Zelf-assemblage kan zich niet ontwikkelen tot een geavanceerd proces voor massaproductie, tenzij de onderzoekers zich gaan richten op de ontwikkeling van nieuwe methoden voor het aanbieden en bevestigen van onderdelen. Deze methoden dienen compatibel te zijn met de omstandigheden in een industriële omgeving. (Dit proefschrift)
3. Het belangrijkste faalmechanisme bij de productie van flexibele elektronica is incompatibiliteit tussen materialen. (Dit proefschrift)
4. Voor de assemblage van fragiele onderdelen, geniet een snelle en deterministische onderdeel-aanbiedings-methode de voorkeur boven een stochastische methode. (Dit proefschrift)
5. Vanwege de hoge materiaalkosten zullen flexibele elektronica toepassingen die een silicium chip bevatten nooit gebruikt worden voor slimme verpakkingen van bederfelijke waren.
6. Het schrijven van een proefschrift is het meest verhelderende deel van een promotietraject.
7. Weten hoe data te analyseren is belangrijker dan de data zelf.
8. Wat geld betreft wordt iets kostbaars goedkoop als je het je kunt veroorloven. Maar tijd is altijd kostbaar, zelfs als je er genoeg van hebt.
9. Files kunnen opgelost worden als mensen trotser zijn op wonen in een land dat geheel te bereizen is met het openbaar vervoer, dan op het bezit van een auto.
10. Iemands begrip wordt meer beïnvloed door interesse in een onderwerp dan door intelligentie.

Deze stellingen worden opponeerbaar en verdedigbaar geacht en zijn als zodanig goedgekeurd door de promotor Prof. dr. Urs Staufer.

MAGNETIC SELF-ASSEMBLY WITH UNIQUE ROTATIONAL ALIGNMENT

Magnetic self-assembly with unique rotational alignment

Proefschrift

ter verkrijging van de graad van doctor
aan de Technische Universiteit Delft,
op gezag van de Rector Magnificus prof. ir. K. C. A. M. Luyben,
voorzitter van het College voor Promoties,
in het openbaar te verdedigen op
maandag 9 maart 2015 om 12:30 uur

door

Emine Eda Kuran

Master of Science in Mechanical Engineering
Columbia University, New York, USA
geboren te Hatay, Turkije.

Dit proefschrift is goedgekeurd door de promotor:

Prof. dr. U. Staufer

Copromotor: Dr. Ir. M. Tichem

Samenstelling promotiecommissie:

Rector Magnificus,	voorzitter
Prof. dr. U. Staufer,	Technische Universiteit Delft, promotor
Dr. ir. M. Tichem,	Technische Universiteit Delft, copromotor
Prof. dr. K. F. Böhringer	University of Washington
Prof. dr. H. O. Jacobs	Technische Universität Ilmenau
Prof. dr. rer. nat. A. H. Dietzel	Technische Universität Braunschweig
Prof. dr. ir. J. L. Herder	Technische Universiteit Delft
Prof. dr. ir. F. van Keulen,	Technische Universiteit Delft, reservelid

The research described in this thesis has been financially supported by EU Seventh Framework Programme as a part of the Chip2Foil project (http://www.chip2foil.eu), grant number 248160.

Keywords: magnetic self-assembly, ultra-thin chips, flexible electronics

Printed by: Uitgeverij BOXPress, 's-Hertogenbosch

Front & Back: Chips aligned with magnetic self-assembly.

ISBN 978-94-6186-433-8

An electronic version of this dissertation is available at
http://repository.tudelft.nl/.

dedicated to my father...

CONTENTS

LIST OF FIGURES

LIST OF TABLES

ABBREVIATIONS

DI	Deionized water
DRL	Dynamic release layer
EN	Electroless Nickel
ENIG	Electroless Nickel Immersion Gold
FPFC	Finer pitch flip chip
HDDA	Hexanediol diacrylate
iBOA	Isobornyl acrylate
IC	Integrated Circuit
I/O	Input/Output
LIFT	Laser Induced Forward Transfer
NFC	Near Field Communication
Ni	Nickel
PCB	Printed Circuitry Board
PET	Polyethylene terephthalate
R2R	Roll-to-roll or alternatively reel-to-reel
ROI	Region of interest
Si	Silicon
SMD	Surface Mount Device
UTC	Ultra-Thin Chip
UV	Ultraviolet

1

INTRODUCTION

Those who wish to succeed must ask
the right preliminary questions.

Aristotle

Keep a watch on the faults of the patients,
which often make them lie about
the taking of things prescribed.

Hippocrates, Decorum

Recent improvements in flexible electronics industry require thinner chips to be integrated into cheap polymer substrates. However, handling ultra-thin chips and meeting the precision demands with acceptable throughputs for high volume manufacturing is challenging for pick-and-place machines. Combining the current micro-assembly technologies with new emerging concepts such as self-assembly can ease the precision demand for pick-and-place and eventually increase the throughput.

This thesis is about magnetic self-assembly of thin chips. The aim of this chapter is to give a brief description of the work done in this thesis. The chapter starts with an explanation of the miniaturization trend in electronic devices and the challenges it brought to the industry, with an emphasis on flexible electronics. In Section 1.2, self-assembly is introduced as a potentially advantageous method to overcome these challenges. In Section 1.3, the Chip2foil project, to which the work is affiliated, is presented. A definition of the research goals and the structure of the thesis is discussed in Section 1.4.

1.1. MANUFACTURING OF FLEXIBLE ELECTRONICS

The wide spread use of mobile devices and the desire of users to access information in a compact way, stimulates the electronics industry to develop new technologies for shrinking device sizes. The miniaturization trend allows application of telecommunications into packaging and labeling of the products that people use every day. To establish an interactive connection between the customer and the product, electronic components are integrated into cheap substrates such as plastic and paper. This new technology is called flexible electronics or flex circuits and some of the application areas include, but are not limited to: smart packaging, wearable electronics, implantable medical devices, flexible displays etc. (Figure 1.1).

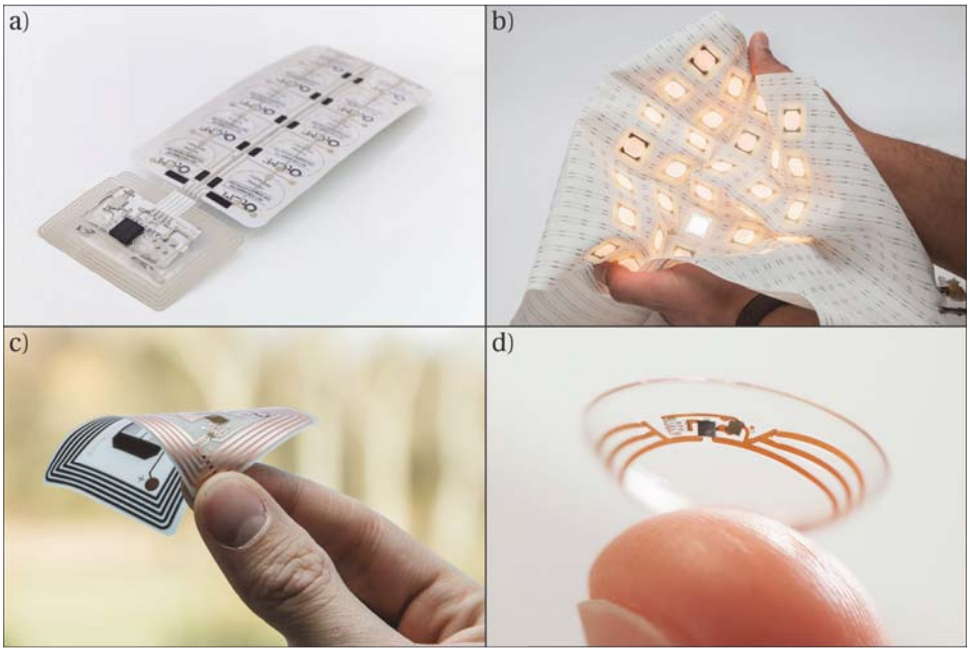

Figure 1.1: Flexible electronics prototypes a) Chip2Foil smart blister [1] b) Direct integration of organic light emitting diodes on textile [2] c) Smart label for sensing applications [2] d) Smart contact lens for measuring glucose level in tears [3]

For instance, smart labeling for food products is one of the forthcoming applications of flexible electronics (Figure 1.1c). Knowing basic information such as expiration date and ingredients is possible with printed labels. However, reading these labels will not help a customer to learn the condition of the product at the time of the purchase. Adding a sensor to the protective package makes it intelligent; the condition of food can be monitored and the price can be changed accordingly. Furthermore, this information can be communicated to the customer and the retailer instantly by a near field communication (NFC) chip embedded in the package which sends signals to a NFC enabled mobile phone.

The electronic components integrated into the packaging of these products should be as bendable as the substrates. It is possible to print flexible layers of some components, such as web circuitry, battery, antenna, resistors, capacitors etc. On the other hand, silicon chips can only provide high performance in bulk form and therefore can not be printed. As a solution, ultra-thin chip (UTC) technology enables thinning down the integrated circuits (ICs) to 50μm or lower thicknesses in order to attain mechanical flexibility [4].

Many of the UTC technology applications require packaging of disposable and relatively inexpensive products that have a high daily consumption rate. Therefore, the manufacturing costs should be kept at a minimum while the throughput is being increased. In particular, the state-of-the-art flexible electronics market requires an adaptation to high volume and low-cost manufacturing techniques where cheap plastic substrates are handled, i.e., roll-to-roll (R2R) processing or web processing. Flexibility in manufacturing is another challenge since the diversity of components to be assembled in one package is increased.

Basic steps of embedding a chip into a polymer electronic package involve: 1) printing of components such as thin film transistors and resistors, i.e web circuitry, 2) direct assembly of components such as the chips. Figure 1.2 shows the general manufacturing process of chip integration into polymer foils.

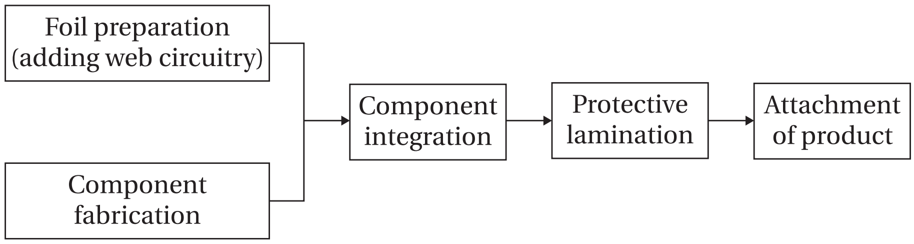

Figure 1.2: General manufacturing process of flexible electronics

At first, a polymer based foil with web circuitry is fed to the manufacturing line. Then the components to be assembled are presented, aligned and interconnected with the web circuitry. In most cases, the assembly layer is protected with lamination of another foil layer. More details on the process flow of manufacturing flexible electronics are given in Section 1.3. In the rest of this section, the difficulties in assembling UTCs with conventional tools is discussed.

1

Robotic manipulation with pick-and-place tools is a standard way of assembling chips to electronic packages. Conventional die bonders used in the industry are evolving in terms of fulfilling the throughput and precision demands for millimeter and sub-millimeter scale components, i.e., high precision pick-and-place reaches up to ±7μm accuracy, and a cycle time of 3 s/chip [5].

However, thinner chips need different handling, i.e., having a high aspect ratio between the surface area and thickness leads to bigger adhesion forces at micro-scale [6–8]. A graph of the scaling between different forces is shown in Figure 1.3.

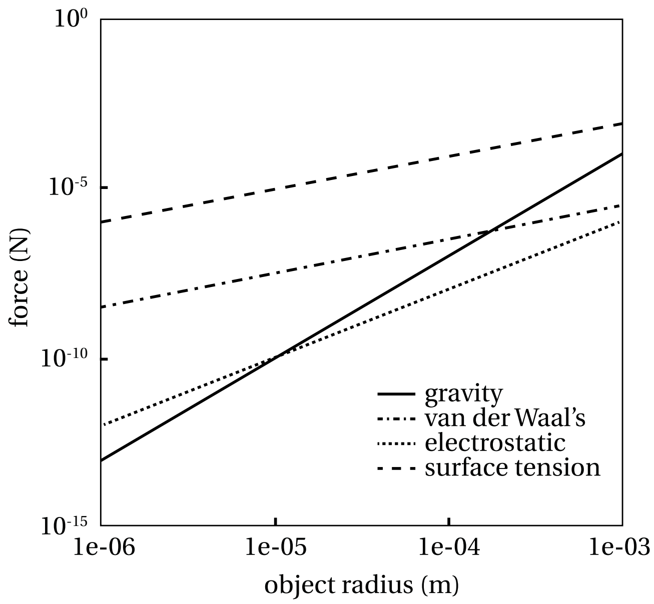

Figure 1.3: Comparison of gravitational, electrostatic, surface tension and Van der Waal's forces at different scales. Reprinted from [6].

As a consequence of the high-adhesion forces between the chip and the pick-and-place tool, the chip placement is accomplished by applying relatively higher forces, e.g., for a vacuum pick-up nozzle a higher air pressure is applied to release the chip. This becomes a major obstacle especially when the chips are assembled into rigid substrates, since the force applied can incur damages and cracks on the chips [9]. Furthermore, usually a die-attach adhesive is used for bonding of the chip after the alignment step. In such cases, contact presentation of a thin chip can cause overflow of adhesive and eventually contaminates the tool and the chip itself.

Another challenge in assembling UTCs is the high precision demand required in chip placement. Some of the flexible electronics applications, e.g., smart packaging of disposable products that requires a small amount of components and electronic functions, aims to combine the activities such as sensing, computation and communication into a single and small chip. This requires an increased number of electrical contacts on the chip. Considering size and complexity of the chip; electrical contacts, a.k.a. Input/Output (I/O) pads, should be distributed into a smaller area which brings complexity in connecting the chip to other components in the package. Therefore, high precision positioning of the chip is required to match the contact pads on the chip to assigned ends of the circuitry on the substrate. Eventually the cycle time per chip increases since the assembly process slows down for a better control of the pick-and-place tool when reaching the substrate.

Machine travel time is another important performance parameter for robotic manipulation. The number of components in a flexible electronics package is relatively low compared to a printed circuitry board (PCB). Additionally, a web of plastic foil may contain multiple packages in one row (Figure 1.4). Sparse population of the assembly positions for the components in a web increases the machine travel time and consequently decreases the throughput.

Figure 1.4: A foil roll that contains rows of "integrated printed biosensors". Courtesy of Acreo Swedish ICT [10].

In conclusion, handling UTCs with robotic manipulation and meeting the precision demands with acceptable throughputs is challenging for manufacturing flexible electronics. Self-assembly is an innovative method that can provide non-contact handling for delicate parts. The benefits of using self-assembly and the details of implementation to industry is discussed briefly in the next section.

1.2. HANDLING UTCS WITH SELF-ASSEMBLY

Self-assembly is the autonomous entrapment and arrangement of small-scale components, without a direct physical contact [11]. The parts to be assembled are passively controlled by using driving forces resulting from gradients created in an external field surrounding the assembly position. Different principles have been used in literature as the source of driving forces in self-assembly; such as shape matching, capillary effects, electrostatics, magnetism etc. [11]. Examples of self-assembly methods using these principles are given in Chapter 2.

Parallelization is one of the biggest advantages of self-assembly, which can improve the throughput for high-volume manufacturing. However, examples of implementation to R2R industrial processes are limited, especially in the case of UTC assembly. The only industrial application known so far is a process developed by Alien Technologies, where sub-millimeter parts are suspended in a fluid and assembled into recesses on a silicon substrate by agitation. The process is claimed to have a throughput of 2,000,000 parts/hour [12].

Both pick-and-place and self-assembly have their own challenges individually. However, a combination of the two methods can overcome the limitations for integration of UTCs to flexible substrates. Using self-assembly as an assisting process can relax the precision required from pick-and-place and consequently decrease the cycle times for chip presentation, i.e., chips can be presented to the bonding area from a significant distance and driven to its final position by the force gradients created by self-assembly.

The work in this thesis is based on a hybrid assembly approach that combines directed presentation of individual chips with magnetic self-assembly. Three main elements are used to manipulate chips in this method:

1. The contact pads on the chips include a nickel layer that makes the chip magnetically susceptible. If necessary, additional magnetic features are added to chips.
2. To eliminate stick-slip effect due to micro-scale adhesion forces between the chip and a foil, a viscous layer is added on top of the foil.
3. An inhomogeneous magnetic field is applied nearby the assembly positions. When released, the chip becomes magnetized and follows the gradient in the surrounding magnetic field.

More details of the concept are reported in Chapter 3. In the following section, the project this research belongs to is discussed briefly.

1.3. CHIP2FOIL: TECHNOLOGY PLATFORM FOR UTC ASSEMBLY

Chip2Foil is an EU funded project that aims to deliver a technology platform for high volume, low-cost placement and interconnection of ultra-thin chips onto thin polymer foils [13]. The platform focuses on developing new methods throughout the total manufacturing process of communicative foil-based packages. Two technical approaches are exploited for chip integration: the first approach uses self-assembly for high speed chip alignment with moderate accuracy, while the second approach creates the interconnection of chips by adaptive circuitry, which compensates initial placement errors up to $\pm 300\mu m$ and $\pm 15°$ (Figure 1.5).

The chosen demonstrator is a smart blister package which monitors a patient's drug taking behavior (Figure 1.1a). Patient non-compliance, the condition where a patient does not adhere to the given prescription, is one of the most important causes of failure

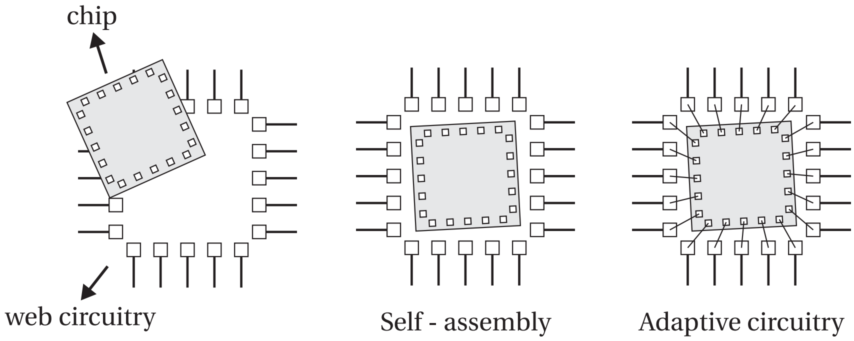

Figure 1.5: Chip2Foil concept

in the long-term treatment of chronic diseases. In developed countries, about half of the patients do not take their drugs according prescriptions. More severely, non-compliance causes causalities: the number rises up to 125,000 per year only in US, with a yearly cost of $300 billion to the health industry [14, 15]. Smart blister tracks the drug taking pattern of a patient by electronics integrated into a traditional plastic blister package. When the patient removes a pill from the package, a resistor at the location is broken. This information is transferred to a receiver in the vicinity, e.g., a mobile phone, by a near field communication (NFC) chip on the package. Monitoring the drug taking process is not only important for the patient and the doctor, but also for several value chains in the health care; such as pharmaceutical companies, pharmacies and insurance companies.

The total process flow of Chip2Foil is shown in the Figure 1.6. The chips are positioned on the foil one-by-one, with their contact pads facing upwards. The process starts with dispensing a die-attach adhesive to the area where the chip will be assembled. After ejection of the chip from the mount tape, a pick-and-place tool is used for presenting the chip to the assembly area. As soon as the release from the tool is accomplished, the self-assembly process captures the chip and aligns it to the target on the foil. Eventually, the chip is mechanically fixed by UV curing of the adhesive. Release and bonding steps are closely related with the performance of self-assembly, and therefore these adjacent steps are addressed more comprehensively in Chapter 4.

The remaining steps in the total process flow are dedicated to interconnection of the chip [16]. First, the position of the chip is optically measured to be able to locate the contact pads for the following processes. Then, a glob-top adhesive is applied to secure the chip and vias are drilled through it by laser to access the contact pads. Subsequently, the vias are filled and the contact pads are connected with web circuitry, by screen printing a conductive patch. In the end, individual interconnections are realized by laser scribing of the patch, thus making unique links between contact lines on the foil with bond pads on the chip.

Although a sheet-based manufacturing scheme was followed for demonstration purposes, the development of each technical concept involves a study on R2R implementation. The R2R application of self-assembly and relative steps in the total process flow is discussed in Chapter 5.

1

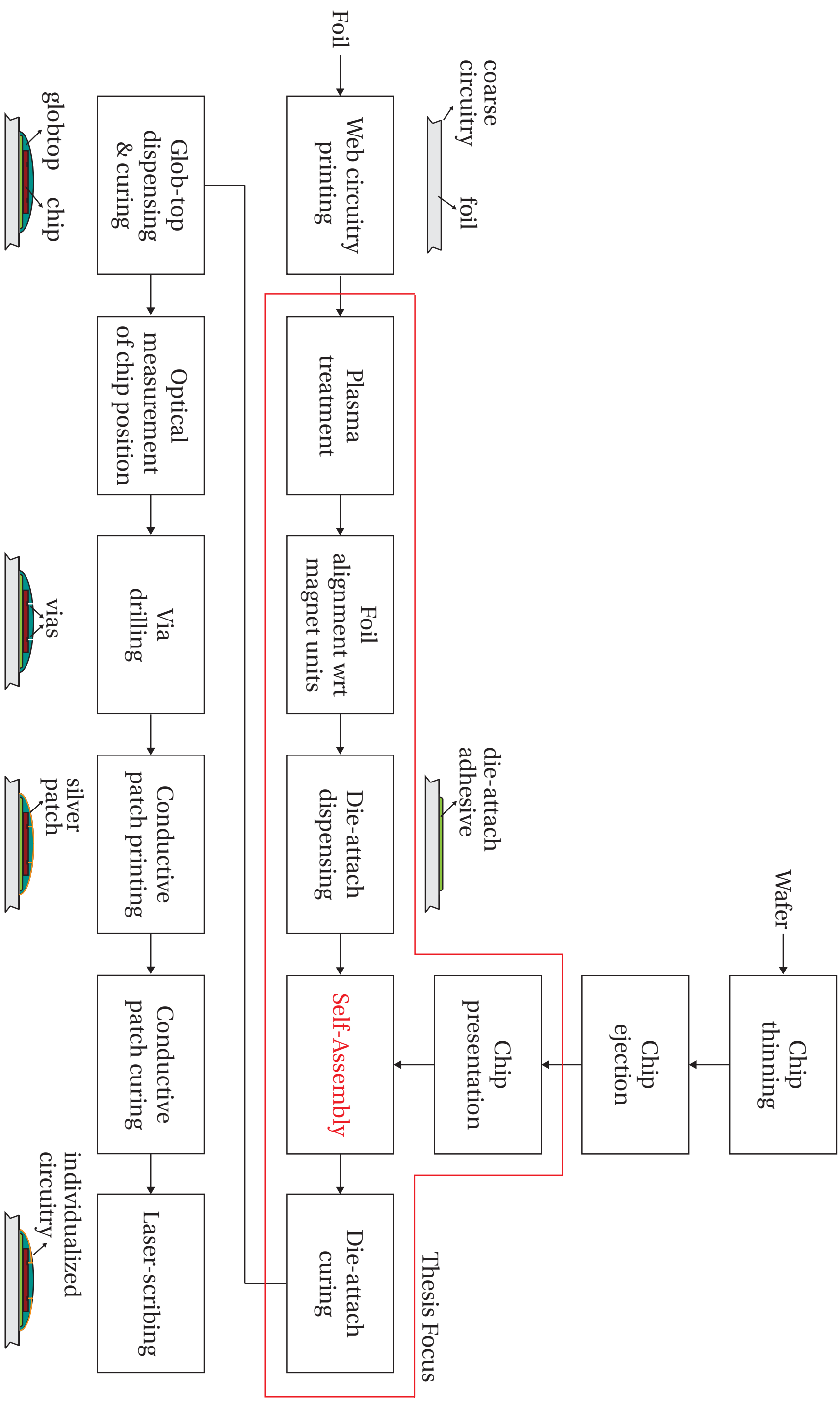

Figure 1.6: Manufacturing process flow of Chip2Foil

1

1.4. Research Goals and Thesis Structure

The work described in this thesis investigates the chip placement by self-assembly using magnetic forces. The overall aim of the research is overcoming the handling difficulties of UTCs and consequently improving the assembly throughput for manufacturing of flexible electronics.

An outline of the thesis accompanied with the research questions that will be answered in related chapters is given in Table 1.1. The thesis is organized as follows: Chapter 2 presents a literature review on self-assembly. Different methods are discussed in this chapter and a classification is made based on the type of the driving forces used to assemble components. The last section of the chapter is devoted to the magnetic self-assembly method; which is the approach taken in this research for exploiting self-assembly. Chapter 3 starts with a general description of the self-assembly method that has been developed, explaining the details and the elements of the concept. The main part of this chapter is dedicated to the investigation of the design parameters related with the motion of the chip by numerical modeling supported with experimental results. In Chapter 4 the fabrication of the components and the research setup used in the experiments is discussed. The chapter continues with the industrial implementation of the magnetic self-assembly. Two different chip presentation methods were studied by experiments carried out in collaboration with industrial partners: pick-and-place method (Besi, Austria) which is an established commercial process and laser die transfer method (Orbotech, Israel) which is at the technology development level. Chapter 5 describes the extension of self-assembly into the roll-to-roll manufacturing. Future work to improve the developed concept and tool designs for implementation of magnetic self-assembly to R2R production lines are discussed. Finally, in Chapter 6 the gain of using self-assembly and future development steps to improve the performance of the self-assembly are discussed.

Outline	Research Questions
Chapter 1: Introduction	What are the requirements for handling UTCs? How can self-assembly contribute to the manufacturing process of flexible electronics?
Chapter 2: State of art	What kind of phenomena can be used as driving-force in self-assembly? What are the advantages of magnetic self-assembly compared to the other methods?
Chapter 3: Physics	What are the design parameters affecting chip alignment? What conditions should be met to achieve a unique stable alignment position and orientation?
Chapter 4: Experimental	What are the failure mechanisms; fabrication, experimental and measurement errors? Which chip presentation techniques can be used for industrial implementation of self-assembly?
Chapter 5: Discussion	Is magnetic self-assembly compatible with R2R fabrication for flexible electronics?
Chapter 6: Conclusion	What are the main advantages of developed method? What kind of future developments could be made to improve the performance of the method

Table 1.1: Thesis structure

1

REFERENCES

[1] http://www.chip2foil.eu/ (Last visited on 30/01/2015).

[2] Holst Centre, http://www.holstcentre.com/ (Last visited on 31/1/2015).

[3] B. Otis and B. Parviz, *Google smart contact lens project,* http://googleblog.blogspot.nl/2014/01/introducing-our-smart-contact-lens.html (Last visited on 31/1/2015).

[4] E. Jung, A. Ostmann, D. Wojakowski, C. Landesberger, R. Aschenbrenner, and H. Reichl, *Ultra thin chips for miniaturized products,* Microsystem Technologies **9**, 449 (2003).

[5] Besi, *Datacon 2200 evoplus,* http://www.besi.com/ (Last visited on 31/1/2015).

[6] R. Fearing, *Survey of sticking effects for micro parts handling,* in *IEEE International Conference on Intelligent Robots and Systems*, Vol. 2 (1995) pp. 212–217.

[7] M. B. Cohn, K. F. Böhringer, J. M. Noworolski, A. Singh, C. G. Keller, K. A. Goldberg, and R. T. Howe, *Microassembly technologies for MEMS,* in *Micromachining and Microfabrication Process Technology IV, SPIE 3511*, Vol. 3511 (1998) pp. 2–16.

[8] M. Wautelet, *Scaling laws in the macro-, micro- and nanoworlds,* European Journal of Physics **22**, 601 (2001).

[9] E. Klaver and P. Huberts, *Two worlds converging: chipshooting and flip-chip bonding,* http://www.assembleon.com/ (Last visited on 30/01/2015).

[10] Acreo Swedish ICT, *Integrated printed biosensor,* https://www.acreo.se/projects/integrated-printed-biosensor-platforms (Last visited on 31/1/2015).

[11] G. M. Whitesides and B. Grzybowski, *Self-assembly at all scales,* Science **295**, 2418 (2002).

[12] E. Snyder, J. Chideme, and G. Craig, *Fluidic self-assembly of semiconductor devices: A promising new method of mass-producing flexible circuitry,* Japanese Journal of Applied Physics **41**, 4366 (2002).

[13] M. Tichem, M. Cauwe, Z. Hajdarevic, E. E. Kuran, B. Naveh, A. Sridhar, and P. Weissel, *Towards reel-to-reel integration of ultra-thin chips to polymer foils,* in *Electronic System-Integration Technology Conference (ESTC)* (2012) pp. 1–6.

[14] D. Smith, *Compliance packaging: a patient education tool,* American pharmacy **NS29**, 42 (1989).

[15] *Adherence to Long-Term Therapies: Evidence for Action* (World Health Organization, Geneva, Switzerland, 2003).

[16] A. Sridhar, M. Cauwe, H. Fledderus, R. H. L. Kusters, and J. van den Brand, *Novel interconnect methodologies for ultra-thin chips on foils,* in *Electronic Components and Technology Conference (ECTC), 2012 IEEE 62nd* (2012) pp. 238–244.

2

State of the Art: Self-Assembly

Out of clutter, find simplicity.
From discord, find harmony.
In the middle of difficulty lies opportunity.

Albert Einstein

It is the harmony of the diverse parts, their symmetry, their happy balance; in a word it is all that introduces order, all that gives unity, that permits us to see clearly and to comprehend at once both the ensemble and the details.

Henri Poincaré

Self-assembly offers "autonomous organization" of the parts, without a direct mechanical contact. This allows handling and manipulation of objects at different scales; from assembly of molecules into monolayers to the assembly of macroscopic components into mobile robots. In electronics packaging, self-assembly can be used for handling of components that are difficult to grasp or release with robotic manipulation. To harvest full potential of self-assembly, all of the manufacturing steps should be considered as a complete logistic chain, starting from the component presentation to the bonding.

2

The aim of this chapter is to make a review of self-assembly methods used in the literature. Based on this review, a self-assembly approach that fulfills the requirements of UTC handling and integration is selected. While making this choice, the entire assembly process, i.e., presentation, alignment and bonding, is studied. The chapter starts with a brief introduction on micro-assembly techniques for embedding chips on flexible substrates. In the following section, the definition of self-assembly and the forces used to create a driving mechanism to align parts are discussed. As mentioned before, this study uses magnetism to employ self-assembly. The rationale behind this choice is explained in the final section. In the next chapters, a comprehensive modeling and experimental study will show how magnetism is used to manipulate thin chips.

2.1. MICRO-ASSEMBLY FOR FLEXIBLE SUBSTRATES

In the scope of precision engineering, the general term “assembly” means arrangement of discrete components into organized structures in a manufacturing process. [1] When micro-scale components are used in the assembly act and the precision is narrowed down to micro-scale, the term becomes “micro-assembly” A classic assembly process involves the following steps: part feeding, part separation/picking, positioning, fixing/joining, interconnection and protection.

Two different approaches exists in terms of manufacturing of components handled in micro-assembly. Monolithic integration creates functions on a single component by a series of fabrication steps applied on the same substrate. Hybrid integration composes a device out of several components created by different fabrication series [2]. Monolithic integration is a serial approach where the risk of failure increases and the compatibility of materials used in each fabrication step becomes a troublesome issue. Therefore hybrid integration is preferred in fabrication of complex devices with multiple functionalities, since it provides better control over the yield by allowing to choose components in good condition.

In the last step of electronic device manufacturing, which is called packaging, the components are enclosed inside a package and mounted on a substrate, e.g., circuit board [3]. The hierarchy in the packaging step of electronic devices is shown in Figure 2.1.

Zero level packaging refers to semiconductor devices within the chip such as diodes and transistors. In the first level a single chip or multiple chips are encapsulated inside a module. Terminology becomes complicated in this level and is divided in terms of scale and characterization of the substrate that the components are integrated into: Chip scale packages (CSP) are composed of a single chip. Multiple chip modules(MCM) contain multiple chips tiled in-plane into one module and act as a single component. System in package (SiP) combines components with different functionalities into a single unit that performs actions related to a system or sub-system [5].

In all of the levels of electronic packaging, the components are electrically connected to each other by means of bonding, i.e., electrical interconnection. The major interconnection techniques used in first and secnd level electronic packaging can be listed as: wire bonding, flip-chip and through-silicon-vias. In flip-chip bonding, the device with solder bumps is flipped and positioned on the connectors of the external circuitry. Bonding is completed with re-flowing, i.e., melting of the solder bumps. Flip-chip bonding is

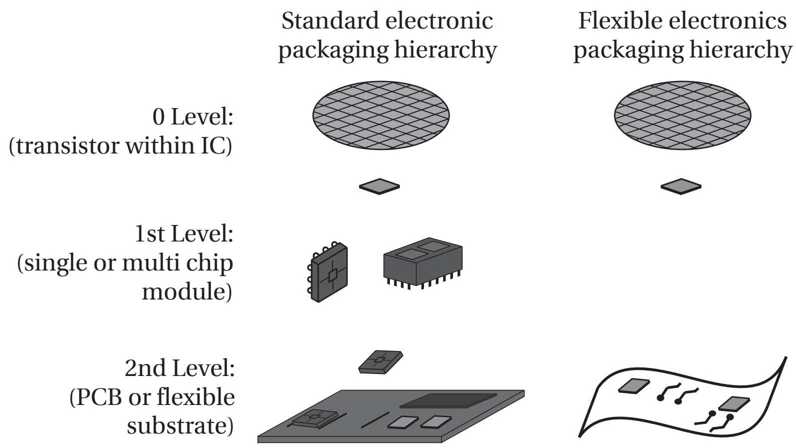

Figure 2.1: Hierarchy of packaging levels in electronic devices, adapted from [4].

used in both first and second level of packaging, where single or multi chip modules are mounted to each other or to printed circuit boards.

In wire bonding, the contact pads on the chip is connected with the external circuitry by thin and conductive wires. Wire bonding is a major interconnection technique in first level packaging, however it is also used in the second level, for interconnection of bare dies to printed circuit boards, which is known as “chip on board” technology [6]. Through silicon vias are used in interconnection of stacked chips. The terminology used in different stages of micro-assembly is summarized in Figure 2.2.

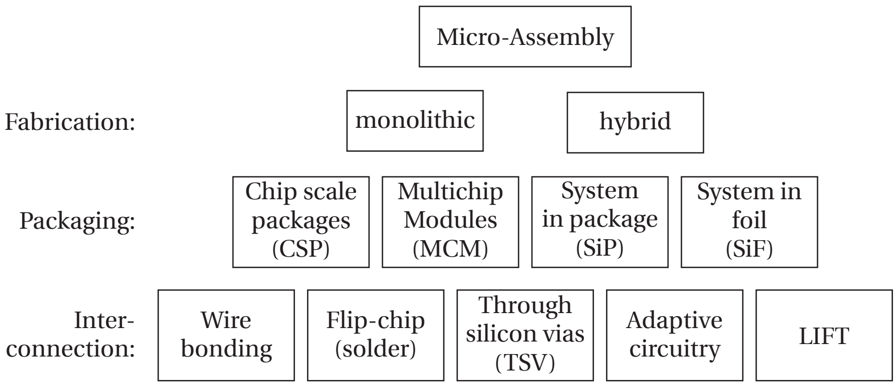

Figure 2.2: Terminology in electronics assembly

The standard electronic packaging hierarchy and fabrication methods used in different scale of packages changes when System-in-Foil (SiF) packaging, a.k.a flexible electronics, is considered (Figure 2.1). Especially, for ultra-thin bare dies assembled on flexible substrates, the first level of packaging is skipped. Furthermore, the compatibility of interconnection materials and techniques is changed, due to the flexibility demand and the polymer substrates that can not withstand high temperatures. New interconnection techniques are developed for these substrates, such as adaptive circuitry [7, 8] where the location of the chip is optically measured in advance and the connection of the contact pads with the circuitry on the substrate is carried out by screen printing and laser scribing. More information on this method can be found in Section 1.3. Laser-induced forward transfer of conductive materials is another emerging technology for adaptive interconnection, where conductive lines are printed between the web circuitry and contact pads by laser-induced-forward-transfer (LIFT) [8].

The new packaging technologies allows shrinking component size both in area and thickness. Especially, the integration of UTCs into flexible electronics brings many new challenges to the industry (Figure 2.3). Some of these challenges are related to the fabrication of UTCs: In the design of the functional blocks of the chips (floorplanning), the mismatches between the CMOS layers initiates chip warping [9]. Besides, stresses resulting from wafer thinning and dicing processes can create micro-cracks on the chips. In addition, the miniaturization trend promotes using a single chip to provide all the functionalities required from the flexible electronics package. The challenges continue in the upper levels of packaging; in the ejection of individualized chips from the wafer carriers, handling of ejected chips, assembly and bonding and finally interconnection.

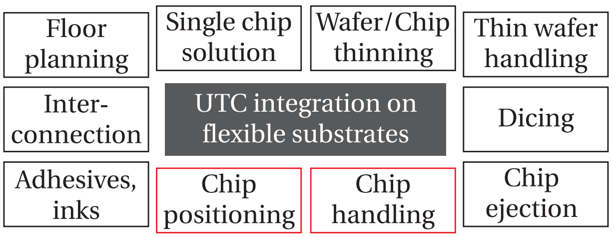

Figure 2.3: Challenges in UTC integration to flexible substrates

In the rest of this section, examples of UTC integration to flexible substrates will be discussed. The first two citations present different methods developed for fabrication and individualization of ultra-thin chips.

IZM's "dicing by thinning" process [10, 11] is a common method used for fabrication of UTCs. The process starts with protection of the active layer on the wafer by coating with a resist. The resist is patterned such that the separation lines, i.e., scribing lines are not covered. Afterwards, trenches are created on the scribing lines by sawing, followed by etching for smoothing the grooves and removing micro-cracks. Then the wafer is transferred to a handling substrate and thinned down from the opposite side until the trenches are reached. Finally, separated chips are transferred to a blue tape, which is a polymer carrier used in the pick-and-place industry. IZM [11] also studies the total integration of the chips to the flexible substrates. The chips are released from the blue tape by local heating of the chip by the pick-up tool, which decreases the adherence of the carrier tape to zero. Then the chip is placed on a die attach adhesive at the flexible polymer substrate surface and bonded by curing. The interconnection is performed by screen printing of conductive material.

Chipfilm technology [12, 13] focuses on fabrication of thin chips by an additive approach instead of the standard chip thinning process of grinding and polishing. Trenches are created on the wafer surface by etching, which leaves the chips to be attached to wafer only at the anchor points. Subsequently, the chips are detached from the wafer by the “pick-crack-place” method, which refers to mechanical cracking of the anchor points with help of a pick-up tool.

IMEC’s UTCP (ultra-thin chip packaging) technology [14] assembles the chips between two polyimide layers. Vias are etched on the top polyimide layer to reach the contact pads and the interconnection is created by deposition of a fan-out metalization layer. Finally, the packaged die is attached to flexible substrates. Since the contact pads are nicely distributed on the polyimide package, the alignment with the substrate is relatively easy.

Banda et. al. [15] uses a flip-chip technique for assembling thinned chips with solder bumps to flexible substrates build of polyimide films bonded to copper foils. The bumping of the chips is done after thinning of the wafer, unlike the common method of metalization and patterning prior to the thinning process. A carrier wafer is used throughout the fabrication including the dicing. The diced carrier wafer layer is used to handle the thinned and bumped chips, which is released with acetone after the assembly of the chip to the substrate. Vacuum fixation is necessary to keep the substrate from buckling during the reflow of the solder bumps. An underfill adhesive is used to decrease the curvature of the chip after release and to have uniform shaped solder joints. Even though this technology uses standard flip-chip mount technologies and has a high-yield, it involves long baking and curing processes and a complex underfill dispensing process, which decreases the chance of applicability to high volume production.

Self-assembly aims to solve the difficulties in handling and integration of the UTCs with the following advantages over the conventional micro-assembly methods:

- Self-assembly enables handling small-scale parts without applying a direct mechanical contact, thus it eliminates sticking and does not damage the components [2, 16].
- Self-assembly enables parallelization. Therefore, it is suitable for high-volume manufacturing [2].
- Self-assembly can handle identical or different parts simultaneously to built hybrid systems [17].
- Assembled parts can be decomposed in-situ, if the direction of the driving force used in self-assembly is reversible.

The chapter will continue with a further explanation of self-assembly, different force fields used in literature to manipulate parts and finally, selection of the self-assembly method studied in this thesis.

2.2. SELF-ASSEMBLY

Self-assembly forms an organized structure out of disordered small scale components autonomously, without a direct mechanical contact, but with an external force that is causing local interactions between the component and the substrate [16]. Self-assembly is a commonly used term for many self-organization concepts, e.g., self-construction of complex structures out of small scale components, self-alignment of 3D hinged structures [18] and self-assembly of molecules into mono-layers (SAM). The work in this thesis deals with discrete parts and aligns them to separated positions on a substrate. The literature covered in this chapter is confined in such manner and it only focuses on 2D-level self-assembly of micron to milli-scale parts.

A typical self-assembly process starts with presentation of chips in the proximity of the force field that drive the parts to desired locations on the substrate. Once the parts are trapped, they follow the gradient in the field until the most energetically favorable position is found. After the alignment is finished, the parts are fixed at the position by bonding (Figure 2.4).

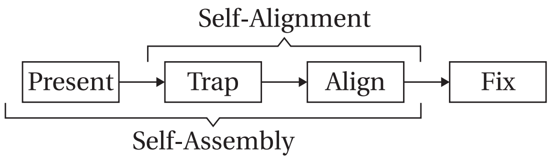

Figure 2.4: Steps of assembly

Different applications require variations of the techniques used in each assembly step. For example, in assembly of complex structures, it is common to present the parts as a cluster agitated in a wet environment. However, in the case of large area electronics the assembly positions are sparsely populated, therefore dipping the whole system inside of a fluid medium may not be efficient. The techniques used in each step affect the competence of the self-assembly method. Parallelization in terms of assembling multiple components at once may not be advantageous at all times, even though the force field used in self-assembly method is capable of handling multiple components simultaneously. However, parallelization of process steps decreases the cycle time, i.e., the time to assemble each chip, and eventually increases the throughput.

At this point, “What should be considered as self-assembly?” becomes a confusing discussion amongst the scientific community. According to most of the researchers working in this area, self-assembly should involve parallelization in terms of stochastic presentation and simultaneous handling of a cluster of unorganized parts [19]. More recently, a new term: “hybrid micro-assembly” is introduced to the literature to define the combination of directed presentation and self-alignment of individual parts [20, 21]. The work done in this thesis assembles ultra-thin chips with the same approach. However, it is still debatable if a distinct terminology should be used to separate the assembly methods that deliberately facilitate “autonomous organization” to manipulate micro-scale components. Likewise, fabrication of “pop-up hinges” does not involve a stochastic distribution of parts in the beginning of the assembly, however they are still considered to be self-assembled. Therefore, the following annotation is suggested: Autonomy in the alignment of parts, i.e., self-alignment, is crucial for self-assembly. Additionally, self-assembly can be performed in a stochastic or deterministic fashion, based on the organization of the parts in the beginning of the assembly action (Figure 2.5). As a consequence, the term "self-assembly" is chosen to describe the assembly method proposed in this thesis, regardless the starting point of the autonomy in the process.

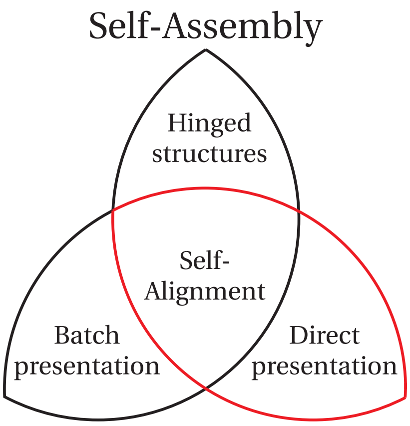

Figure 2.5: The definition of self-assembly. Autonomous alignment of components, i.e., self-alignment, is always present in the founding of self-assembly concepts.

The literature review presented in this thesis highlights the issue of industrial implementation and addresses the compatibility of the chosen self-assembly approach with the total manufacturing flow of flexible electronics, starting from the printing of web-circuitry to the bonding and interconnection of the chips. This analysis is featured in 2.4, and experimentally studied in Section 4.3.

Figure 2.6 summarizes different approaches used to exploit self-assembly. As mentioned before, two different approaches can be taken while bringing the chips in the vicinity of the assembly area: batch presentation in a random fashion and directed presentation of individual chips. In terms of logistics, self-assembly can be exploited in three different ways. Part-to-part assembly refers to the construction of 3D structures by fitting multiple parts to each other. In part-to-template assembly, components are organized into a pattern initially on a template and later transferred to the final substrate. In this method, the alignment should be retained during transfer. On the other hand, in part-to-substrate assembly components are positioned directly on the final substrate, which eliminates the additional step of using an intermediate template. In this thesis a directed chip presentation approach and part-to-substrate assembly is used.

The force fields used in self-assembly and the part or substrate adaptation required in each method is discussed in the following section.

2.3. DRIVING FORCES

The term driving force is used in literature to describe the force field which directs the parts in a self-assembly process. The most common methods that are used to exploit self-assembly can be listed as shape matching, surface tension, electrostatics and magnetism. All of these methods are based on energy minimization, such that the parts en-

2

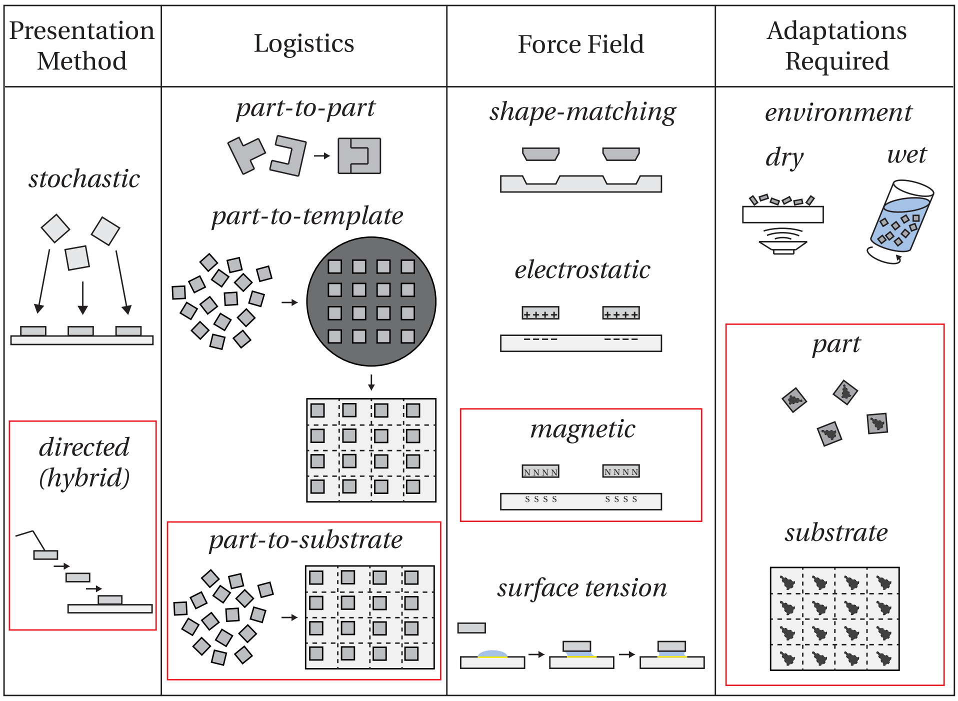

Figure 2.6: Methods to exploit self-assembly. The approaches used in this thesis are marked with red boxes.

tering the system are excited by the applied field and finally settled at the energetically most favorable locations. To narrow down these stability locations into a single one, identical asymmetries should be created both in the parts and the force field. Another way to reduce the stability locations is to control the initial conditions of alignment by limiting process parameters such as release position or release orientation.

For example, surface tension force driven self-assembly is based on minimization of the surface free energy in liquids. The attractive forces between molecules in the surface of a liquid becomes unbalanced when it interferes with another surface. For self-assembly, binding sites matching the shape of the parts are created on the substrate by changing the surface chemistry at desired locations. Lower surface energy at these points leads to increased wettability. To reach the most energetically favorable state, a droplet of liquid dispensed at a binding site changes its form and adjusts its touching area. When a part is presented to the droplet, it is subject to capillary forces applied by the liquid and eventually aligns with the binding site. This method might require surface modifications both on the parts and the substrate, correspondingly the chip and the polymer-based foil for flexible electronics. A unique alignment is reached either by having same asymmetrically shaped patterns on the chip and the foil [22, 23], or by introducing asymmetry with help of an another force field such as magnetism [24]. Surface tension forces have a short working range, therefore the parts to be assembled should touch the liquid at first to initiate the alignment. The parts are brought to the binding sites either by robotic manipulation, i.e., hybrid assembly [20, 21, 25], in air environment or by agitation in a fluidic environment [26]. Template matching [27] and gravitational forces are other assisting methods used to trap parts in surface tension driven self-assembly. Different agents are used as droplets to apply capillary forces such as solder, adhesive or water. Adhesives are used for prior mechanical bonding of the parts, whereas solder assembly [28] provides both fixation and interconnection. When water is used as the fluid medium, it should be removed from the binding site before continuing with the fixing step. The evaporating water leaves traces which can contaminate the substrate and the surface tension of the shrinking droplet may cause misalignment of the chip. Therefore the water should be extracted from the binding site homogeneously as in [20], or a restoring force should be used for repositioning the chip. If the binding sites are individualized for contact pads on the chip and a conductive adhesive is used, interconnection of the chip is also achievable [29].

In electrostatics driven self-assembly, the driving force is generated by attraction between oppositely charged parts and binding sites on the substrate. As in other self-assembly methods, vibration is applied to the substrate or template with binding sites to mobilize the chips in a dry environment [30, 31] and in wet environments agitation was used [32]. The perpendicular force applied on the parts is much greater than the lateral force on this method, therefore the working range is relatively small. Additionally, the risk of damaging chips with active layers is quite high due to the built up charges.

Another method to assemble parts is using mechanical vibration with shape matching. In this method the parts are trapped into recesses built on substrate. The stochastic nature of the process makes it slow and unpredictable. Therefore it is mostly used as a supporting technique to other self-assembly methods.

Micro-manipulation of small-scale parts with magnetic forces is an extensively used approach, i.e., magnetic micro-robots [33] and 3D assembly of complex structures [34–40]. As in other methods, the friction between the parts and the substrate should be eliminated or decreased that the parts become free to move in the surrounding force field. In most cases, the assembly is done in a wet environment, the substrate and a number of parts are dipped in a liquid and mechanical vibration is added to the system to increase the yield [24, 39, 41, 42]. In dry environment mobilization of parts are achieved by vibration of substrate [43] or air pressure [44, 45]. A combination of different self-assembly methods was also used, including shape-matching and gravitational forces [43] and surface tension [24, 38, 46].

The driving force in magnetic self-assembly can be created in two different ways:

I. Interaction between embedded hard magnetic materials on the parts and an externally applied field either by hard magnets [47] or an electromagnet[48];
II. Magnetization of soft magnetic materials on the parts by an externally applied field either by hard magnets [24, 42, 43, 49] or an electromagnet.

2.4. CONCLUSION: SELECTION OF MSA

The requirements needed in the Chip2Foil project was considered for selection of the self-assembly method. It was decided to assemble chips facing bumps up, bonded to a substrate with a die-attach adhesive, in a dry environment. The precision demand is shared between different assembly steps in the Chip2Foil technology. First, the chips are presented with pick-and-place method which brings the chip nearby the desired alignment position. The required precision is in millimeter range at this stage. Then, magnetic self-assembly completes the rest of the alignment process. Finally, the interconnection of the chip is realized by adaptive circuitry which compensates for any alignment errors coming from the self-assembly step up to a precision of $\pm 150\,\mu m$. For demonstration purposes, chips are handled individually in a step-and-go fashion, however compatibility with reel-to-reel manufacturing was required.

A comparison of different force-fields used in self-assembly is shown in Table 2.1. It was concluded that all methods require part and substrate adaptations. Surface tension and magnetic forces appear to be the most promising methods to apply self-assembly based on their compatibility with different environments and their capability to align chips with unique orientation. In terms of scaling, surface tension and electrostatic forces are dominant at micro-scale when compared to other forces as shown in Figure 1.3. However, without additional logistics concepts such as agitation or vibration, these forces can only trap parts from short distances. For instance, in surface tension the size of the binding site matches the size of the part to be assembled, and the self-assembly only takes place when the part is in contact with the droplet on the binding site. Therefore as the part size gets smaller, the precision demand in chip presentation is also gets higher for these forces. For these forces, supplementary logistic concepts are inevitable which is advantageous for batch part presentation, but might be harmful for handling delicate parts. Finally, it was concluded that using magnetic forces is the most suitable method to fulfill the demands of the Chip2Foil process. The selection was made based on the following aspects.

General advantages can be listed as:

	Risk of damage	Adaptations required for part/substrate	Environment	Working range	Unique orientation	Scaling
electrostatic	high	yes/yes	dry/wet	short	yes	$F_\mathrm{e} \propto \frac{1}{2}\varepsilon_0\varepsilon_\mathrm{a} A E_\mathrm{a}^2$
gravitational, template-matching, vibration	high	no/yes	dry/wet	short*	yes	$F_\mathrm{g} \propto G\frac{m_1 m_2}{r^2}$
surface tension	low	yes/yes	dry/wet	short	yes	$F_\mathrm{s} \propto \gamma L cos(\theta)$
magnetic	low	yes/yes	dry/wet	long	yes	$F_\mathrm{m} \propto \frac{1}{2} B^2 \mu_\mathrm{r} / r^3$

* The working range becomes high with the help of vibration or agitation.
F_e electrostatic force, ε_0 permittivity of free space, ε_a relative permittivity of air
A contact area, E_a electric field
F_g gravitational force, G gravitational constant, m_1 mass of first object,
m_2 mass of second object, r distance between the centers of masses
F_s surface tension force, γ surface tension of the liquid medium,
L perimeter of the part, θ contact angle between part and liquid
F_g magnetic force, B magnetic field, μ_r relatie permeability
r distance between part and magnetic field source

Table 2.1: Comparison of driving forces used in self-assembly

- Magnetic forces enable part-to-part bonding, part-to-substrate bonding and selective bonding of heterogeneous components [50].
- The force applied on the parts and working range can be actively controlled [33].
- Heterogeneous components can be manipulates selectively by using different type of magnetic materials [33]. Relatively, both attractive and repulsive forces can be created by using hard magnetic materials magnetized in different directions.
- There is no chance of damaging a chip with magnetic forces, unless the magnetic field is interfering with the active layer on the chips.
- Orientation control can be achieved without creating complex patterns on parts or substrates.

Specific advantages for Chip2Foil include:

- Magnetic forces act on longer ranges compared to other forces. This enables to attract parts from a further distance, which lowers the precision demand in chip presentation step and eventually decreases the cycle time per chip.

- The long working range expands to 3-dimensions, therefore the parts can be released at a relatively further distance above the substrate. This eliminates overflow of adhesive to the active side of chip and protects the pick-and-place tool from contamination.
- Magnetic forces can be applied externally, such that no adaptations are required on the substrate. However to freely move the parts at the substrate surface, a pattern of binding sites were created on the foil by plasma treatment.[1] A die-attach adhesive deposited at these binding sites eliminates sticking and provides mechanical bonding.
- Scaling of parts can be compensated without changing the force field or adjusting binding sites (Chapter 3).
- The nickel bond pads already present on the chip, provides enough magnetic material to manipulate the parts. If the layout of the bond pads is fulfilling the requirements for reaching a unique orientation, no additional magnetic material is added to the chips (Chapter 3).

[1] The size of the binding sites is much bigger than the chip size, therefore surface tension forces does not play a role in the alignment of the chip.

REFERENCES

[1] S. Ratchev and S. Koelemeijer, eds., *Micro-Assembly Technologies and Applications*, Fourth International Precision Assembly Seminar (IPAS) (Springer, 2008) pp. 6–7.

[2] J. Fang and K. F. Böhringer, *Self-Assembly,* in *Comprehensive Microsystems*, edited by Y. B. Gianchandani, O. Tabata, and H. Zappe (Elsevier, Oxford, 2008) Chap. 1.14, pp. 403 – 429.

[3] J. W. S. M. Datta, Tetsuya Osaka, *Microelectronic Packaging* (CRC Press, 2004).

[4] *IEEE components, packaging, and manufacturing technology society, press images and visuals,* http://www.ewh.ieee.org/soc/cpmt/press/pressimage.html (Last visited on 20/11/2014).

[5] ITRS, *The next step in assembly and packaging: System level integration in the package (SiP),* (2007).

[6] J. H. Lau, *Chip On Board: Technology for Multichip Modules* (Springer Science & Business Media, 1994).

[7] M. Tichem, M. Cauwe, Z. Hajdarevic, E. E. Kuran, B. Naveh, A. Sridhar, and P. Weissel, *Towards reel-to-reel integration of ultra-thin chips to polymer foils,* in *Electronic System-Integration Technology Conference (ESTC)* (2012) pp. 1–6.

[8] H. Schulte-Huxel, R. Bock, S. Blankemeyer, A. Merkle, and R. Brendel, *Aluminum-based mechanical and electrical laser interconnection process for module integration of silicon solar cells,* IEEE Journal of Photovoltaics **2**, 16 (2012).

[9] M.-U. Hassan, E. Angelopoulos, H. Rempp, S. Endler, and J. Burghartz, *Packaging challenges associated with warpage of ultra-thin chips,* in *Electronic System-Integration Technology Conference (ESTC)* (2010) pp. 1–5.

[10] C. Landesberger, G. Klink, G. Schwinn, and R. Aschenbrenner, *New dicing and thinning concept improves mechanical reliability of ultra thin silicon,* in *International Symposium on Advanced Packaging Materials: Processes, Properties and Interfaces* (2001) pp. 92–97.

[11] M. Feil, C. Adler, D. Hemmetzberger, M. Konig, and K. Bock, *The challenge of ultra thin chip assembly,* in *Electronic Components and Technology Conference*, Vol. 1 (2004) pp. 35–40 Vol.1.

[12] J. Burghartz, W. Appel, H. Rempp, and M. Zimmermann, *A new fabrication and assembly process for ultrathin chips,* IEEE Transactions on Electron Devices **56**, 321 (2009).

[13] J. N. Burghartz, W. Appel, C. Harendt, H. Rempp, H. Richter, and M. Zimmermann, *Ultra-thin chip technology and applications, a new paradigm in silicon technology,* Solid-State Electronics **54**, 818 (2010).

2

[14] J. Govaerts, W. Christiaens, E. Bosman, and J. Vanfleteren, *Multiple chip integration for flat flexible electronics,* in *IEEE Conference on Polymers and Adhesives in Microelectronics and Photonics* (2008) pp. 1–5.

[15] C. Banda, R. Johnson, T. Zhang, Z. Hou, and H. Charles, *Flip chip assembly of thinned silicon die on flex substrates,* IEEE Transactions on Electronics Packaging Manufacturing **31**, 1 (2008).

[16] G. M. Whitesides and B. Grzybowski, *Self-assembly at all scales,* Science **295**, 2418 (2002).

[17] K. S. Park, J. H. Hoo, R. Baskaran, and K. Böhringer, *Parallel heterogeneous integration of chip-scale parts by self-assembly,* Journal of Microelectromechanical Systems **21**, 1273 (2012).

[18] R. Syms, E. Yeatman, V. Bright, and G. M. Whitesides, *Surface tension-powered self-assembly of microstructures,* Journal of Microelectromechanical Systems **12**, 387 (2003).

[19] M. B. Cohn, K. F. Böhringer, J. M. Noworolski, A. Singh, C. G. Keller, K. A. Goldberg, and R. T. Howe, *Microassembly technologies for MEMS,* in *Micromachining and Microfabrication Process Technology IV, SPIE 3511*, Vol. 3511 (1998) pp. 2–16.

[20] V. Sariola, M. Jaaskelainen, and Q. Zhou, *Hybrid microassembly combining robotics and water droplet self-alignment,* IEEE Transactions on Robotics **26**, 965 (2010).

[21] B. Chang, A. Shah, I. Routa, H. Lipsanen, and Q. Zhou, *Low-height sharp edged patterns for capillary self-alignment assisted hybrid microassembly,* Journal of Micro-Bio Robotics **9**, 1 (2014).

[22] C. Lin, F.-G. Tseng, and C.-C. Chieng, *Orientation-specific fluidic self-assembly process based on a capillary effect,* Journal of Micromechanics and Microengineering **19**, 115020 (2009).

[23] U. Srinivasan, D. Liepmann, and R. Howe, *Microstructure to substrate self-assembly using capillary forces,* Journal of Microelectromechanical Systems **10**, 17 (2001).

[24] K. S. Park, J. H. Hoo, R. Baskaran, and K. F. Böhringer, *Orientation-controlled parallel assembly at the air-water interface,* Journal of Micromechanics and Microengineering **22**, 105028 (2012).

[25] G. Arutinov, M. Mastrangeli, E. Smits, G. van Heck, J. Toonder, and A. Dietzel, *Foil-to-foil system integration through capillary self-alignment directed by laser patterning,* Journal of Microelectromechanical Systems (2014), 10.1109/JMEMS.2014.2321013.

[26] H. O. Jacobs, A. R. Tao, A. Schwartz, D. H. Gracias, and G. M. Whitesides, *Fabrication of a cylindrical display by patterned assembly,* Science **296**, 323 (2002).

[27] J. Fang and K. F. Böhringer, *Parallel micro component-to-substrate assembly with controlled poses and high surface coverage,* Journal of Micromechanics and Microengineering **16**, 721 (2006).

[28] W. Zheng, J. H. Chung, and H. Jacobs, *Non-robotic fabrication of packaged microsystems by shape-and-solder-directed self-assembly,* in *IEEE International Conference on Micro Electro Mechanical Systems* (2005) pp. 8–11.

[29] N. Boufercha, J. Sägebarth, M. Burgard, N. Othman, D. Schlenker, W. Schäfer, and H. Sandmaier, *Fluidassem - a new method of fluidic-based assembly with surface tension,* IFIP International Federation for Information Processing **260**, 149 (2008).

[30] K.-F. Böhringer, K. Goldberg, M. Cohn, R. Howe, and A. Pisano, *Parallel microassembly with electrostatic force fields,* in *IEEE International Conference on Robotics and Automation*, Vol. 2 (1998) pp. 1204–1211.

[31] I. Kurniawan, M. Tichem, and U. Staufer, *Dry self-alignment for batch-assembly of chips,* in *Solid-State Sensors, Actuators and Microsystems Conference (TRANSDUCERS2009)* (2009) pp. 212–215.

[32] J. Tien, A. Terfort, and G. M. Whitesides, *Microfabrication through electrostatic self-assembly,* Langmuir **13**, 5349 (1997).

[33] R. S. M. Rikken, R. J. M. Nolte, J. C. Maan, J. C. M. van Hest, D. A. Wilson, and P. C. M. Christianen, *Manipulation of micro and nanostructure motion with magnetic fields,* Soft Matter **10**, 1295 (2014).

[34] J. Judy and R. Muller, *Magnetically actuated, addressable microstructures,* Journal of Microelectromechanical Systems **6**, 249 (1997).

[35] T. Ebefors, E. Kalvesten, and G. Stemme, *New small radius joints based on thermal shrinkage of polyimide in v-grooves for robust self-assembly 3d microstructures,* Journal of Micromechanics and Microengineering **8**, 188 (1998).

[36] M. Boncheva, S. A. Andreev, L. Mahadevan, A. Winkleman, D. R. Reichman, M. G. Prentiss, S. Whitesides, and G. M. Whitesides, *Magnetic self-assembly of three-dimensional surfaces from planar sheets,* Proceedings of the National Academy of Sciences of the United States of America **102**, 3924 (2005).

[37] A. J. Nichol, P. S. Stellman, W. J. Arora, and G. Barbastathis, *Two-step magnetic self-alignment of folded membranes for 3d nanomanufacturing,* Microelectronic Engineering **84**, 1168 (2007).

[38] C. J. Morris, B. Isaacson, M. D. Grapes, and M. Dubey, *Self-assembly of microscale parts through magnetic and capillary interactions,* Micromachines **2**, 69 (2011).

[39] F. Ilievski, M. Mani, G. M. Whitesides, and M. P. Brenner, *Self-assembly of magnetically interacting cubes by a turbulent fluid flow,* Phys. Rev. E **83**, 017301 (2011).

[40] M. Poty, G. Lumay, and N. Vandewalle, *Customizing mesoscale self-assembly with three-dimensional printing,* New Journal of Physics **16**, 023013 (2014).

[41] J. Rumpler, J. Perkins, and J. Fonstad, C.G., *Optoelectronic integration using statistical assembly and magnetic retention of heterostructure pills,* in *Conference on Lasers and Electro-Optics*, Vol. 2 (2004) p. 2.

[42] Q. Ramadan, Y. S. Uk, and K. Vaidyanathan, *Large scale microcomponents assembly using an external magnetic array,* Applied Physics Letters **90**, (2007).

[43] S. Shet, V. Mehta, A. Fiory, N. Ravindra, and M. Lepselter, *The magnetic field-assisted assembly of nanoscale semiconductor devices: A new technique,* JOM **56**, 32 (2004).

[44] B. Van Leeuwen, *Passive Airflow Based Self-assembly of Silicon Chips on Foils*, Master's thesis, Delft University of Technology (2009).

[45] T. Poiesz, *Magnetic Alignment of Ultra-thin Chips*, Master's thesis, Delft University of Technology (2010).

[46] D.-A. Wang and H.-H. Ko, *Magnetic-assisted self-assembly of rectangular-shaped parts,* Sensors and Actuators A: Physical **151**, 195 (2009).

[47] S. Shetye, I. Eskinazi, and D. Arnold, *Magnetic self-assembly of millimeter-scale components with angular orientation,* Journal of Microelectromechanical Systems **19**, 599 (2010).

[48] T. Inoue, Y. Hamasaki, I. Shimoyama, and H. Miura, *Micromanipulation using a microcoil array,* in *IEEE International Conference on Robotics and Automation*, Vol. 3 (1996) pp. 2208–2213.

[49] D. I. Cheng, J. J. Rumpler, J. M. Perkins, M. Zahn, C. G. Fonstad, E. S. Cramer, R. W. Zuneska, and F. J. Cadieu, *Use of patterned magnetic films to retain and orient micro-components during fluidic assembly,* Journal of Applied Physics **105**, (2009).

[50] S. Shetye, I. Eskinazi, and D. Arnold, *Part-to-part and part-to-substrate magnetic self-assembly of millimeter scale components with angular orientation,* in *IEEE 22nd International Conference on Micro Electro Mechanical Systems* (2009) pp. 669–672.

3

PHYSICS AND MODELING

The purpose of models is not to fit the data
but to sharpen the questions.

Samuel Karlin

The consequences of every act are
included in the act itself.

George Orwell, *1984*

In the proposed self-assembly process, the chip is released above the substrate into an externally applied magnetic field. At that instant, the nickel layer present on the chip becomes magnetized, which generates a magnetic force and a magnetic torque that drive the chip to the target position on the substrate. A viscous layer is added to the substrate surface in advance, which acts as a buffer that mobilizes the chip. The gradient in the applied magnetic field guides the chip along its travel through the air and on the viscous layer.

Parts of this chapter is based on article E. E. Kuran, M. Tichem, *Magnetic self-assembly of ultra-thin chips to polymer foils*, IEEE Transactions on Automation Science and Engineering, **10**, 536 (2013).

This chapter is dedicated to understanding the fundamentals of the magnetic self-assembly method developed in this thesis. The first section introduces the building blocks of the assembly process. The chapter continues with an explanation of the physics behind the concept and the description of the initial conditions that are required to reach a unique rotational alignment. In the next section, the interactions between the chip, the magnetic field gradient and the viscous layer are studied on the basis of an experimental study, where the design and process parameters (e.g., magnetic field, contact pad arrangement, release position etc.) are varied to examine the changes on the alignment of the chip.

3.1. ALIGNMENT OF CHIP IN TWO STEPS

The main components in a self-assembly process are the parts to be assembled, the substrate and the surrounding medium. The self-assembly action is driven by the interactions between these three components. The magnetic self-assembly method studied in this thesis uses the interactions between an external magnetic field, a chip with a soft-magnetic material layer and a viscous layer on top of the substrate. The chip's motion

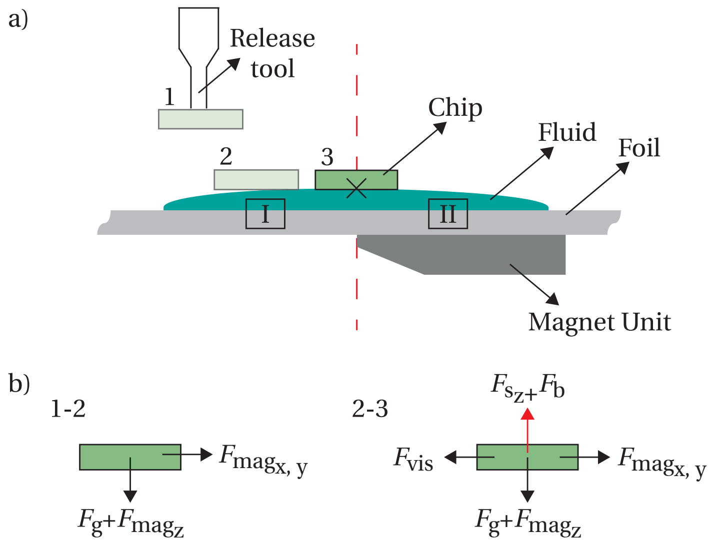

Figure 3.1: Illustration of magnetic self-assembly concept a) Chip's motion in two steps 1-2: The chip is released above the substrate and reaches the viscous layer. 2-3: The chip is traveling on the viscous layer and reaches the final position. b) 1-2: Forces applied to the chip during its travel.

is divided into two steps, as seen in Figure 3.1. The first step refers to chip's trajectory in the air; starting at the separation of the chip from the release tool, until the moment where the chips bottom surface is completely wetted by the viscous layer. At this step, the chip is exposed to a complex set of forces such as the adhesion between the tool and the chip, e.g., electrostatic attraction and the momentum coming from the release of the chip. It should also be noted that, the viscous layer only acts as a buffer that lubricates the substrate surface and occupies an area more than twice of the chip's size. Therefore, capillary forces applied at the first contact of the chip with the viscous layer do not play a role on the chip's alignment process. In the following sections, the forces that are applied to the chip in the first step of assembly are ignored while explaining the chip's alignment. The given equations assume that the chip is completely wetted and stabilized (floating) on the viscous layer and has no initial velocity.

The second step is the motion of the chip on the viscous layer until it reaches a final stable position. The three main forces applied to the chip at this step are (Figure 3.1b):

I. The in-plane magnetic force, which acts as a locomotive in the chip's alignment process,
II. The in-plane viscous forces, i.e., the viscous drag applied against the movement of the chip,
III. The sum of the out-of plane forces including the weight of the chip, the vertical component of the magnetic force, the buoyancy and the vertical component of the surface tension force.

The magnetic and viscous forces applied on the second step of alignment are extensively studied in the following sections, since these are the dominant forces that are defining the chips final trajectory along with the final position and the orientation.

3.2. PHYSICS

The physics behind the chips motion involve two main disciplines: magnetism and fluid dynamics. In this section, the basic principles such as formation of the magnetic field gradient, magnetization of the nickel layer on the chip and the viscous drag forces are explained. Additionally, numerical calculations of the out-of plane viscous forces and the weight of the chip are discussed in Section 3.2.3.

3.2.1. DRIVING FORCE IN MAGNETIC SELF-ASSEMBLY

Magnetic properties of materials are dependent on the electron pairing of their atoms, and the net magnetic dipole moments applied to these electrons [1]. The magnetic dipoles inside a magnetic material are oriented randomly in the absence of a magnetic field. When the material is placed in an external magnetic field, each dipole experiences a torque which is called magnetic dipole moment and tends to align itself in the direction of the applied field.

The magnetic dipole moment can be represented as a current loop, which is inducing a magnetic field of its own. In atoms with only paired electrons, the net magnetic moment equals to zero since in each pair, the electrons spin in opposite directions and the magnetic fields induced by the current loops of these electrons cancel each other. Nonetheless, the atoms with unpaired electrons generate a net magnetic moment.

The density of the net magnetic moments (m) inside a material is called magnetization (M), which is which is defined by

$$M = \frac{1}{V}\sum_{i=1}^{N} m_i \tag{3.1}$$

where N represents the number of atoms in volume V of the material.

When placed inside a selonoid which applies a magnetic field B_0, the material becomes magnetized and the magnetic fields generated by the current loops of atoms inside the material contribute to the external field. The following equation enables distinguishing the contribution of magnetization (M) of the material to the magnetic field inside the solenoid (B) from the field (B_0) applied by the solenoid itself.

$$B = B_0 + \mu_0 M \tag{3.2}$$

3

The field that magnetizes the material and which is generated by the external currents, i.e., the magnetic field intensity (H), can also be represented as

$$H = \frac{1}{\mu_0} B_0 \tag{3.3}$$

Eventually, the equation 3.2 becomes;

$$B = \mu_0 (H + M) \tag{3.4}$$

It is possible to classify the materials according to their susceptibility (χ_m) to an external magnetic field [2]. For linear magnetic materials,

$$M = \chi_m H \tag{3.5}$$

and

$$B = \mu_0 (1 + \chi_m) H = \mu_0 \mu_r H = \mu H \tag{3.6}$$

where μ is the permeability of the material to the magnetic fields. The relative permeability μ_r is a constant that represents the permeability of the material with respect to the permeability in free space.

The materials that have atoms with only paired electrons are called diamagnetic. These materials have a linear magnetization and they response weakly to the magnetic field ($\chi_m < 0$ and $\mu_r < 0$). The paired electrons in diamagnetic materials spin in opposite direction and therefore they have no net magnetic moment. Additionally, the magnetization of paramagnets is in the opposite direction of the applied field, therefore they repel the magnetic fields.

The other type of materials that are also linearly magnetic and have a weak response to magnetic fields are called paramagnets ($\chi_m > 0$ and $\mu_r < 1$). In paramagnetism, the unpaired electrons in the orbitals of the atoms create a net spin and tend to realign with the direction of external field. Therefore the paramagnets are attracted to the magnetic fields.

The magnetic materials that show non-linear magnetization are called ferromagnetic. Ferromagnets give a strong response to the magnetic field due to their atoms with unpaired electrons. ($\chi_m >> 0$ and $\mu_r >> 0$) In ferromagnetism, the magnetic dipoles with the same orientation create domains inside the material. In the absence of the magnetic field, these domains are randomly oriented and when exposed to the magnetic field the domains are oriented almost to the same direction with the applied field. Ferromagnetic materials gets saturated at sufficiently high fields, i.e., the magnetization of the material can not increase further with a higher external field after saturation. At magnetic saturation, all the domains inside the material are aligned with the applied field.

In addition, ferromagnets can retain their magnetization in the absence of the applied field, which is called hysteresis. To remove the residual magnetization in the material, a magnetic field in the opposite direction of magnetization should be applied. The behavior of the magnetization (M) of the material versus the magnetizing field (H) along the full cycle of magnetizing and demagnetizing can be represented as a closed loop as shown in Figure 3.2), i.e., the hysteresis loop [1].

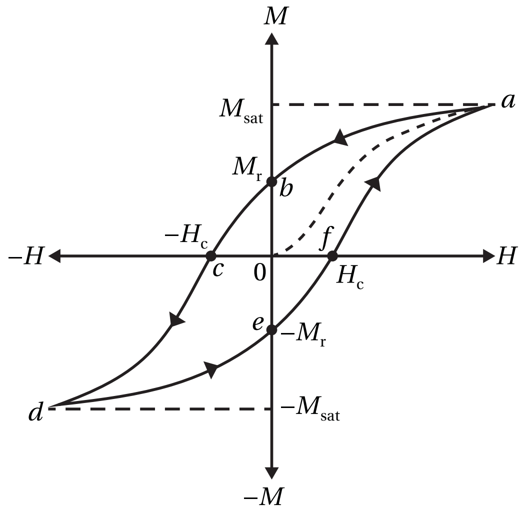

Figure 3.2: M versus H hysteresis curve

The dashed curve in the figure shows the first step of the hysteresis loop ($0-a$), where a ferromagnetic material with zero net magnetization is placed inside of an magnetic field increasing in the positive direction. In this step, the magnetization of the material increases until it reaches magnetic saturation (M_{sat}), where all of its domains are aligned with the applied field. In the second step ($a-b$), the applied field is decreased to zero. At this step, the magnetization decreases, however it does not vanish and a residual magnetism (M_r) remains in the ferromagnetic material. After this point ($b-c$), a magnetizing field increasing in the negative direction is applied to fully demagnetize the material. At this step, a coercive force is applied to the magnetic domains and the magnetic field required to reduce the net magnetization back to zero is called coercive field (H_c). If the demagnetizing field is decreased even further ($c-d$), the material reaches magnetic saturation in the opposite direction. When the magnetizing field is reduced back to zero ($d-e$), the material retains a negative residual magnetization ($-M_r$). The magnetizing field should be in positive direction after point e, in order to reach zero magnetization. Finally, the curve is closed by increasing the applied field in positive direction ($f-a$), until magnetic saturation is reached.

The work done to move a ferromagnetic material in an inhomogeneous magnetic field is compensated with the change in the magnetic potential energy of the system. For an ferromagnetic material with volume V, the applied magnetic force F_{mag} can be described by

$$F_{\text{mag}} = -\frac{dPE}{dr} \tag{3.7}$$

where r is the displacement of the material.

For linear materials, in which the magnetic flux density B is linear with the magnetizing field H, the total energy stored in a steady magnetic field is

$$PE = \frac{1}{2}\int_{\text{vol}} B \cdot H dv \tag{3.8}$$

The equation 3.6 can be used to rewrite the equation 3.8

$$PE = \frac{1}{2}\int_{\text{vol}} \frac{B^2}{\mu} dv \tag{3.9}$$

To be able to use the above equations for nonlinear material, the following situation is considered. For a electromagnet which has a soft-magnetic core with constant permeability, the magnetic field in the air gap can be considered to be same as the field in the core. If we consider the core is consisting of two pieces just touching each other (Figure 3.3, the work done to separate these two pieces would be equal tot the potential magnetic energy change in the air gap. Assuming a magnetic core with cross sectional area S is separated for a distance of dl, the magnetic force would be equal to

$$F_{\text{mag}} dl = -dW = \frac{1}{2}\frac{B^2}{\mu_0} S dl \tag{3.10}$$

$$F_{\text{mag}} = \frac{1}{2}\frac{B^2}{\mu_0} S \tag{3.11}$$

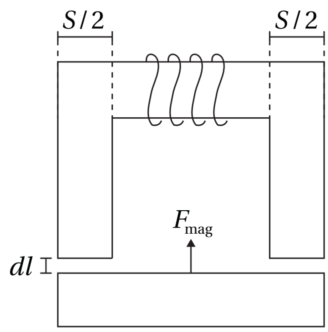

Figure 3.3: An electromagnet with a two core pieces. The virtual work done to separate the pieces is equal to the potential energy change in the air gap.

The nickel on the contact pads of the chips, shows a ferromagnetic behavior; the stray flux coming out of the magnet unit prefers to be concentrated on the nickel layer, rather than dispersing into the air. Eventually, the chip is forced to relocate, until the least resistant path for the magnetic flux to follow is found.

The magnetic field coming out of the magnet unit can be represented with field lines. In a homogeneous external field, the distance between the field lines are equal as shown in Figure 3.4a. When the chip is released into the homogeneous magnetic field, the nickel layer on the chip guides the field lines, and the chip is rotated to decrease the bending in the field lines. If a gradient is present on the applied field, the density of the field lines changes and the chip follows this gradient in order to capture the maximum amount of magnetic flux (Figure 3.4b). By changing the shape of the gradient in the field, one can guide the chip and locate it to a desired position.

The shape of the magnetic field gradient is defined by the geometry of the magnetic circuit, i.e., the shapes of the yoke and pole pieces that are guiding the stray field coming out of permanent magnets. For instance, a tapered pole piece is used to focus the field lines to the self-assembly area. The magnetic field gradients created with different shape of pole pieces are discussed further in Section 3.3.1.

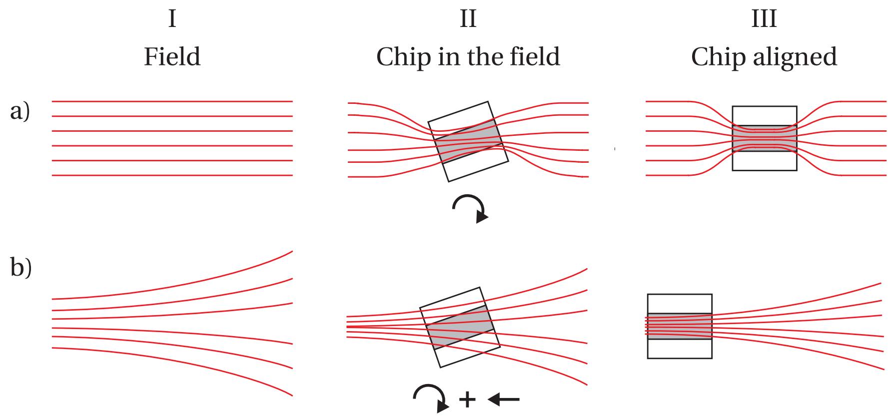

Figure 3.4: Chip with an anisotropic magnetic material feature exposed to different magnetic field gradients. a) The chip in a homogeneous field tends to rotate and aligns itself with the magnetic field lines. b) The chip in a gradient field rotates and relocates itself to capture maximum amount of flux.

3.2.2. MAGNETIZATION OF ELECTROLESS NICKEL

The nickel layer on the contact pads is added by electroless nickel/immersion gold (ENIG) deposition. Magnetic properties of electroless nickel (EN) depend on the percentage of the phosphorus content in the deposited layer. Deposits with 3–4 % phosphorus show ferromagnetic behavior, whereas deposits that have more than 8% phosphorus become non-magnetic [3, 4]. The contact pads of the chips that are used in this thesis have a content of 4-6% of phosphorus, which is within the ferromagnetic regime.

In addition,the micro-structure of the materials also plays a significant role in their magnetization [5, 6]. Ferromagnets typically posses different magnetic characteristics along different crystal directions, which is called magnetocrystalline anisotropy [1]. When placed in an external field, the electron spins inside ferromagnetic atoms prefer to align along one of the preferred crystal directions, which is referred as easy direction of magnetization. Eventually, the magnetic domains inside the material magnetize along the easy direction and align with the applied field.

For thin films, it is common to have an in-plane magnetic easy-axis due to the longitudinal anisotropy [7–9]. However, Huang et al. [10] shows that for EN thin films with columnar structure 420–520 nm, there is a microscopic effect of out-of plane magnetization on the macroscopic in-plane anisotropy.

The magnetization of the EN layer used in the contact pads was measured with an SQUID magnetometer (Quantum Design Inc., MPMS XL Magnetic Property Measurement System) to confirm the ferromagnetic behavior and to define the magnetic easy-axis. The quality of the measurements were low, due to the difficulties in fixing the thin chip to the sample holder. The chip was misplaced during the experiments which caused noise in the measured magnetization curves. The details of these measurements are discussed in Appendix B.

3.2.3. OUT-OF-PLANE FORCES (BUOYANCY, SURFACE TENSION)

The viscous forces applied on the chip is not limited to the viscous drag; the buoyancy and the surface tension lifts and mobilizes the chip on the viscous layer. The balance of the out-of plane forces which makes the chip float on the viscous layer is represented with Equation 3.12. The sum of the buoyancy (F_b) and the vertical components of the surface tension force ($F_{\mathrm{s_z}}$) is equal to the sum of the vertical force applied by the magnetic field ($F_{\mathrm{mag_z}}$) and the weight of the chip (F_g).

$$F_\mathrm{b} + F_{\mathrm{s_z}} = F_\mathrm{g} + F_{\mathrm{mag_z}} \tag{3.12}$$

$$\rho_{\mathrm{fluid}} V_{\mathrm{fluid}} g + \gamma L cos(\theta) = mg + F_{\mathrm{mag_z}} \tag{3.13}$$

where ρ_{fluid} is the density of the fluid, V_{fluid} is the volume of displaced fluid, g is the gravitational constant, γ is the surface tension of the fluid, L is the characteristic length (the perimeter of the chip) and m is the mass of the chip.

Water ($\rho = 1000\,\mathrm{kg/m^3}$ and $\mu = 1\,\mathrm{mPa \cdot s}$) has a surface tension of $71.97\,\mathrm{mN\,m^{-1}}$ against air at 25 °C [11]. The contact angle of water on silicon wafers cleaned with various standard pretreatment processes differs between 10 – 60° [12]. This creates an out-of-plane surface tension force that is greater than 0.1 N, which can compensate the vertical magnetic force and the weight of the chip. The simulation results shows that the vertical component of the pulling force is approximately 0.003 N at the tip of the pole piece where it reaches the maximum value.

3.2.4. VISCOUS DRAG

The viscous drag force arises from the internal friction between the layers of a moving fluid: as the chip starts aligning, the fluid layers between the chip and the substrate rub against each other, which creates a resistance against the motion of the chip (Figure 3.5).

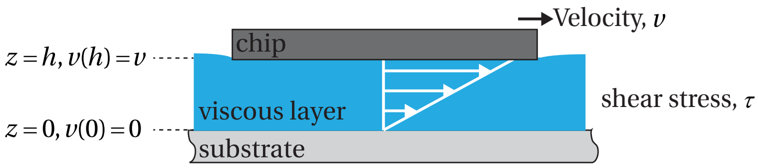

Figure 3.5: Laminar shear stress

At first, the Reynolds number is calculated to determine whether the fluid flow is laminar or turbulent. For a fluid with constant density (ρ) and dynamic viscosity (η) the Reynolds number is defined by;

$$Re = \frac{\rho v L}{\eta} \tag{3.14}$$

in which v is the velocity of the chip relative to the viscous layer and L is the characteristic length. For $Re < 1$, the flow is laminar and for $Re > 1$ the flow becomes turbulent. With the observed velocities from the experiments (approximately 14 mm/s) and small characteristic length (perimeter of the chip = 4 mm) the flow is expected to remain laminar during the alignment.

The density of the fluid remains constant during the alignment process, therefore the fluid flow is considered to be incompressible. For an incompressible and Newtonian fluid, the laminar shear stress between two parallel plates at a separation distance of h is given by;

$$\tau = \eta \frac{\partial v}{\partial h} \tag{3.15}$$

where η is dynamic viscosity coefficient and v is the velocity of the fluid.

The drag force applied on the chip is calculated by integration of the laminar shear stress over the wetted area of the chip. Thus, the drag force can be written as

$$F_{\text{drag}} = \int \tau \, dA = \eta A \frac{\partial v}{\partial h} \tag{3.16}$$

3.3. REACHING A UNIQUE ROTATIONAL ALIGNMENT

The ability to reach a unique alignment with magnetic self-assembly is a major goal in this research. According to the principle of minimum potential energy, a chip exposed to a magnetic field tries to relocate itself into a state, such that the system reaches the energetically most favorable situation. Having only one global minimum state is essential to reach a unique stability, which means that the chip always ends up in the same final position and orientation. Many process parameters play a role in achieving such a condition, but most importantly a resemblance between the shape of the magnetic material pattern on the chip and the gradient of the external field is required. However, unique alignment on the basis of shape matching only is not feasible. As this work will show, geometrical symmetries on the shape of the field or the shape of magnetic pattern will result with multiple stable orientations. For such cases, the unique alignment can be reached by changing the initial conditions, such as the release position and angle. By doing so, one actually alters the proportion of the magnetic and viscous forces applied on the chip, which individually controls the path that the chip follows in the external magnetic field. The parameters that affect the alignment performance are summarized in Figure 3.6. Four pillars stands out as the foundation of the magnetic self-assembly process:

I. The gradient in the three dimensional magnetic field surrounding the assembly point
II. The region of interest in this magnetic field gradient which has boundaries that are defined by the initial position of the substrate and the chip
III. The magnetic material on the chip
IV. The viscous layer

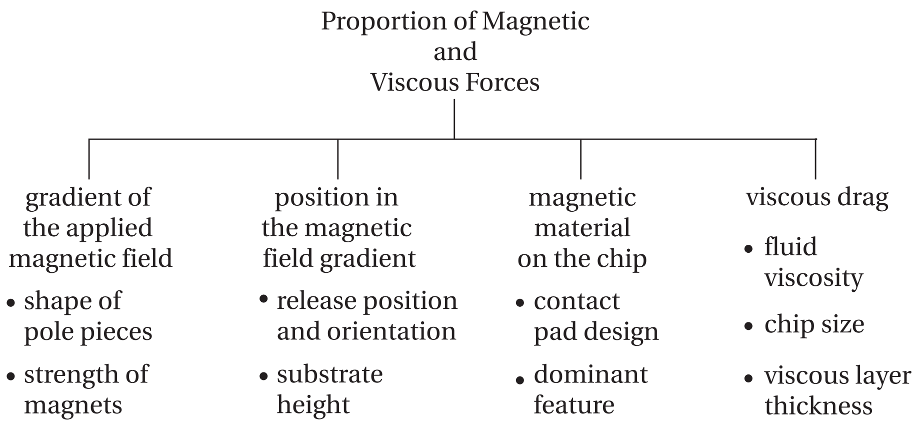

Figure 3.6: Pillars of magnetic self-assembly. A threshold between parameters related to this pillars assures unique orientation.

Before understanding the effect of each parameter and optimizing the alignment process, initial experiments were conducted with simple chips and magnet units to prove the concept of manipulating a chip that has nickel contact pads in an externally applied magnetic field. Figure 3.7 summarizes the milestones in the design development of the major components of magnetic self-assembly while pointing out their positions in the experimental timeline.

In the later stages, the alignment concept was improved by having an asymmetry on the layout of the contact pads of the chip. The magnet unit design was also changed, the magnets attached next to the pole pieces were transferred to the bottom of the magnet unit. This enabled eliminating the dominance of the strong stray flux coming out of the magnet edges, in the field gradient surrounding the self-assembly area. Finally, a unique alignment was achieved by providing a complete shape matching between the magnetic material on the chip and the applied field. The effect of changing the magnet unit and the magnetic material pattern on the chip are discussed in Sections 3.3.1 and 3.3.2, respectively.

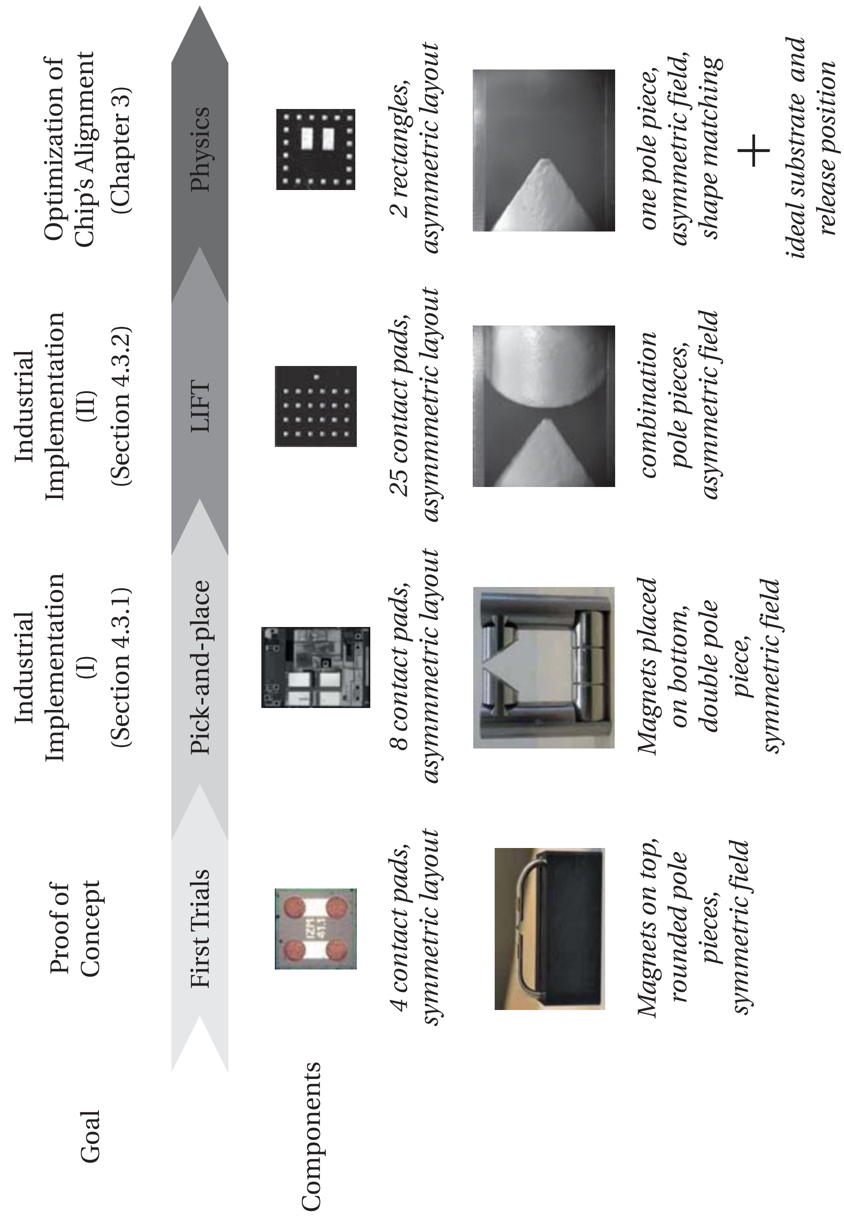

Figure 3.7: Evolution of magnetic self-assembly concept

3.3.1. MAGNET UNIT CONFIGURATION

Two main configurations for magnet units were tried out in the initial experiments (Figure 3.8). The first configuration features yoke pieces that were attached to the both ends of the permanent magnets, which guided and focused the stray flux into an air gap between two tapered pole pieces. Using such a configuration still created a symmetric field due to the two stability points at the end of the each pole piece. In the second configuration a single yoke and pole piece was used, which created a denser field on one side of the assembly area.

3

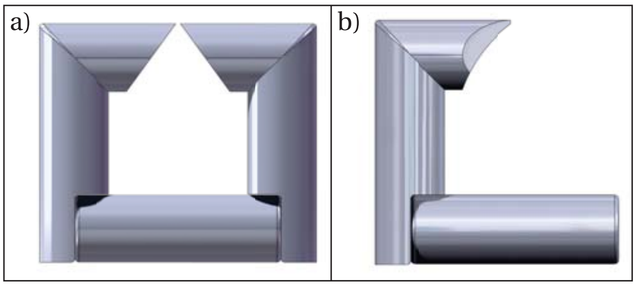

Figure 3.8: Magnet unit configurations (side view) a) Two yoke pieces attached to both end of permanent magnets. b) A single yoke piece attached to one side of the permanent magnets.

To analyze the magnetic field gradient around the magnet units different approaches were used. Initially, the field gradient was visualized by adding a small amount of ferrofluid to a glass slide positioned on top of the magnet unit (Figure 3.9). The variations in the form of the ferro-fluid such as formation of spikes showed significant changes in the direction of the magnetic field. The magnet units with a single pole piece created a field with a strong dominance in the out-of plane direction, whereas the magnet units with two pole pieces created a field with dominance in the in-plane direction.

Figure 3.9: Visualization of the magnetic field by ferrofluid. Spikes are formed on the ferrofluid since the stray flux coming out of the magnet unit is bended upwards.

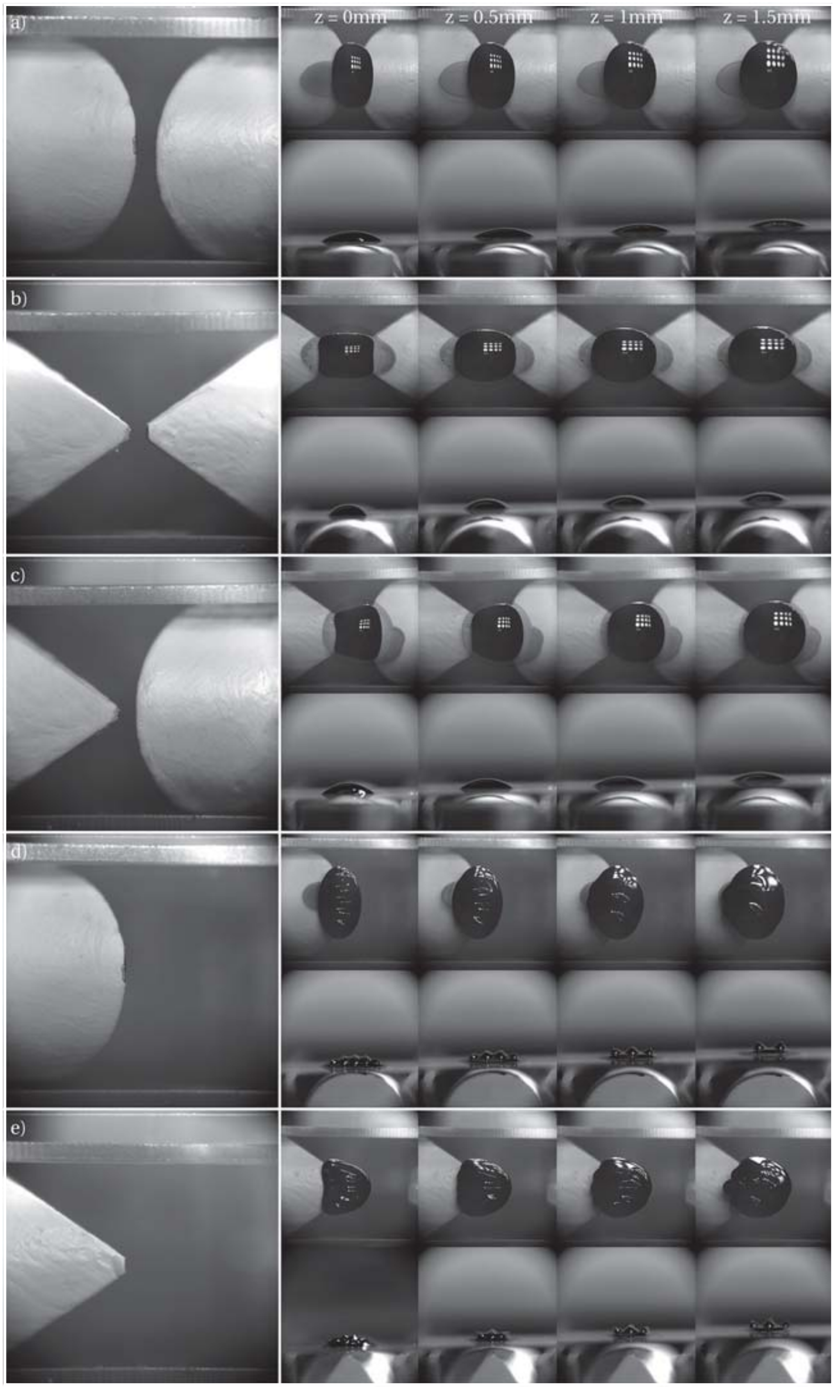

Figure 3.10: Ferrofluid patterns showing magnetic field gradients for different pole piece configurations and out-of-plane "substrate-to-magnet" distances. a) Two rounded pole pieces b) Two sharp pole pieces c) Combination of one rounded and one sharp pole pieces d) Single rounded pole piece e) Single sharp pole piece

3

Figure 3.10 shows the visualization of the magnetic field for different magnet unit configurations. In these experiments, the change in the magnetic field with respect to the out-of-plane distance between the magnet unit surface and the substrate was also examined. As the separation was increased, the magnetic field became defocussed which caused generation of multiple stable positions and eventually a decrease in the alignment precision.

In the end, a single pole piece configuration was preferred to narrow down the magnetic field into a single stability point. Furthermore, a tapered pole piece with sharp ends (Figure 3.10e) was selected to create local peak points that will potentially match the layout of the magnetic material pattern on the chip.

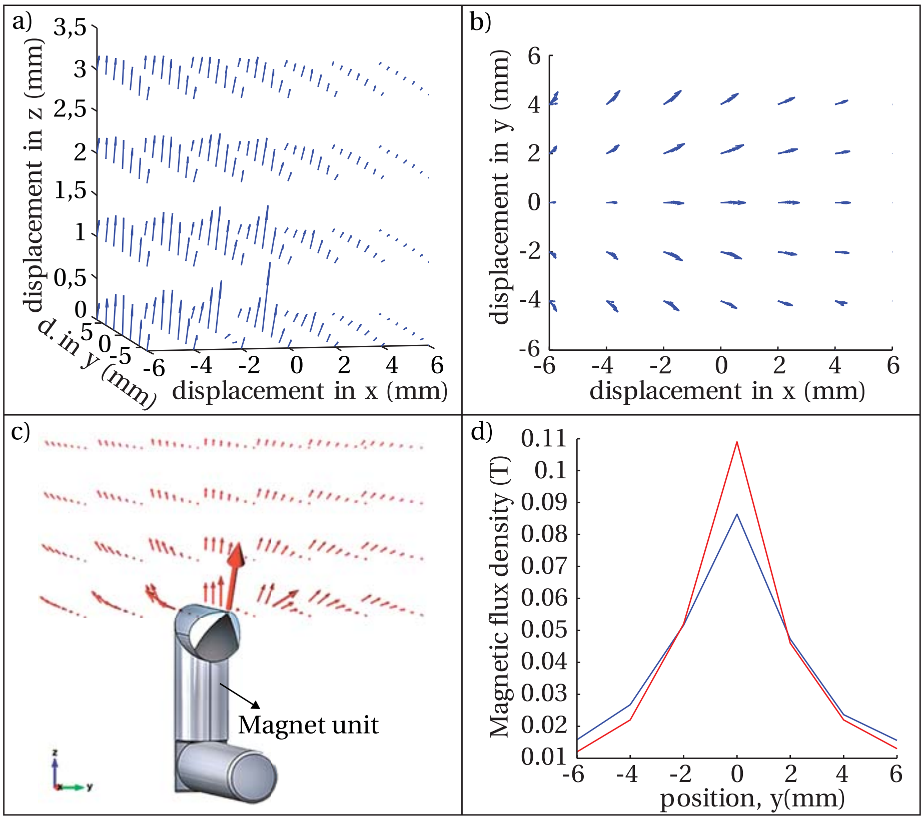

Figure 3.11: Arrow plot representations of the gradient in the magnetic field. a) 3D arrow plot of the magnetic field, measured values b) Only lateral (x, y) components of the measured values are plotted. c) 3D arrow plot of the magnetic field, FEM model d) Comparison of the magnetic flux density values calculated from the model (blue) with the gauss-meter values (red). The plotted values are along the tip of the pole piece and approximately at 1 mm above the surface, which corresponds to thickness of the gauss-meter probe

These observations were also confirmed quantitatively by measuring the magnetic field at different positions around the tip of the selected pole piece with a gauss-meter (F. W. Bell 5100 Series). Figure 3.11 shows arrow plots of the measured and modeled values, displayed from different views. The length of the arrows represent the magnitude of the magnetic flux density at the corresponding point. A good shape resemblance of the magnetic field gradient was achieved in the FEM models, although the calculated and the measured values were not completely matched (Figure 3.11d).

Several contact pad designs were generated to find different candidates that would match the shape of the magnetic field gradient. More details on these designs are explained in Sections 3.3.2 and 3.4.2.

3.3.2. USING DOMINANT FEATURES

Having an asymmetry on the layout of the contact pads is a prerequisite for reaching a unique rotational alignment. However, the common layout designs used in the commercial chips may not always be asymmetric, or the asymmetry that is present on the design may not be dominant over the total contribution of the contact pads on the chip. To create such an asymmetry or enhance the existing asymmetry, it is possible to add a dominant feature to the magnetic material pattern on the chip.

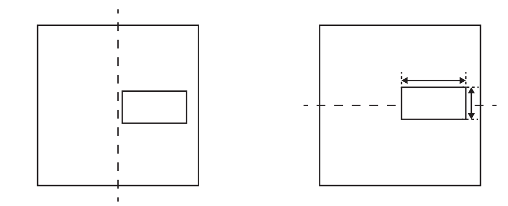

Figure 3.12: Rotation axes of chip

The dominant feature controls the rotational alignment by introducing two geometric anisotropies to the magnetic material pattern. The first anisotropy is due to layout of magnetic material, i.e., the dominant features are placed on one side of the chip. The second anisotropy is due to shape of the dominant feature. Magnetic field lines tend to align with longer edges of materials, therefore the added features should have an aspect ratio, e.g., a rectangle for rotating the chip to the desired axis (Figure 3.12).

Different shapes were tried out for finding a feature that would create a unique match with the magnetic field gradient. Figures 3.13a-c show aligned chips with rectangle, ellipse and triangle features. Regardless of the shape, the chips with a single dominant feature align into two different orientations such that the longer axis of the feature overlaps with the two sharp corners on the tip of the pole piece.

In the next set of chips, two rectangle features were used to resemble the peaks in the magnetic field gradient. The features were placed with a separation that matches the distance between the sharp ends of the pole pieces, where the magnitude of the stray flux coming out of the magnet unit reaches maximum amounts (Figure 3.13e).

The results of both single and double featured chips show that, the layout anisotropy

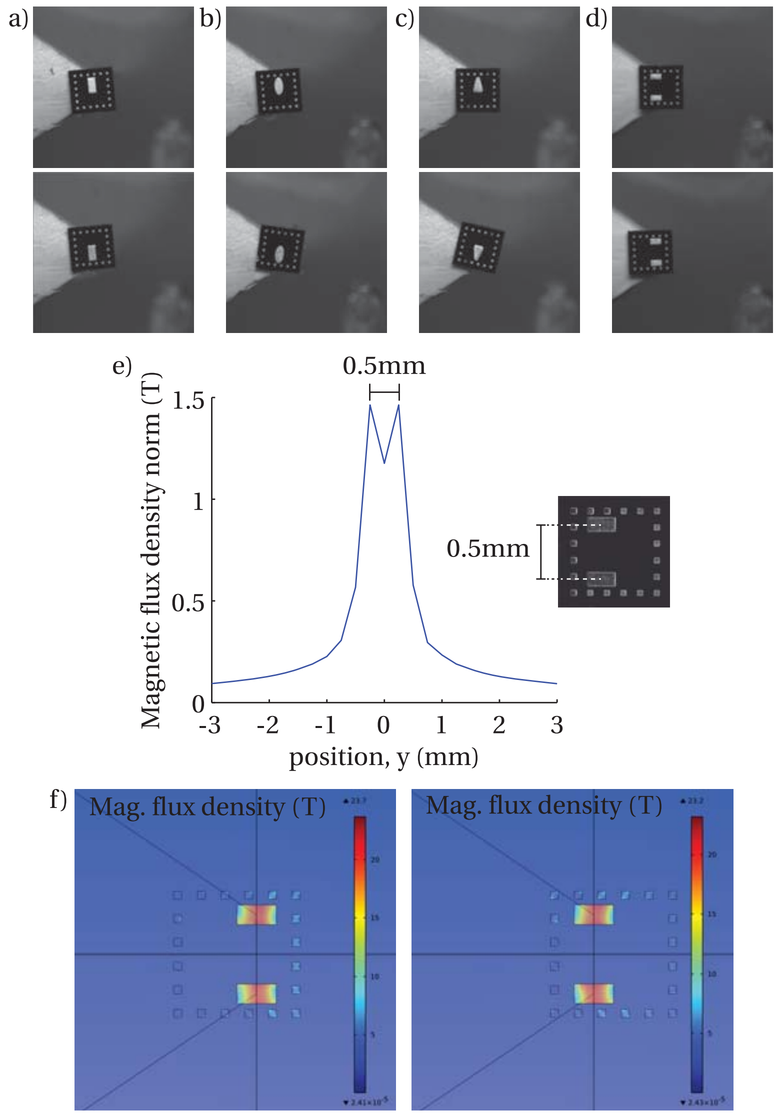

Figure 3.13: Alignment of chips with different dominant feature shapes. Chips with a) rectangle b) ellipse c) triangle d) double rectangle features. Chips that have a single dominant feature align into 0° and 270°, whereas chips with double rectangles align into 0° and 180°. e) Plot of magnetic flux density along the front edge of the pole piece (FEM model). The separation between the peaks in the plot matches the separation of rectangle features on the chip. f) Magnetic flux density plots (FEM model) of two stable orientations for the double rectangle chip and the single sharp pole piece configuration

of magnetic material on the chip becomes ineffective when the chips are released close to the pole piece. This is due to the longitudinal symmetry of the dominant features. Due to the vertical symmetry of the dominant feature shape, the chips with double rectangles align into two different stable orientations as shown in Figure 3.13f.

In Section 3.4.3 the release position is studied to find a “safe region” where the chips released from would always align with a unique orientation.

3.4. EXPERIMENTAL OPTIMIZATION

In this section, the design and process parameters are varied experimentally to optimize the performance of the magnetic self-assembly. Figure 3.14 shows a list of all the parameters related with the chip’s alignment process. The same magnet unit design (a single and tapered pole piece with sharp ends) was used in all of the experiments. For a specific set of parameters, the experiments were repeated multiple times with different chips.

$$F_{\mathrm{net}} = \overbrace{V_{\mathrm{mag}} \frac{\mu_{\mathrm{eff}}}{\mu_0} \vec{B}\nabla\vec{B}}^{F_{\mathrm{mag}}} - \overbrace{\eta A \frac{\partial v}{\partial h}}^{F_{\mathrm{vis}}}$$

magnetic material ($V_{\mathrm{mag}}\mu_{\mathrm{eff}}$)	**pattern thickness** 5 μm 3 μm	**dominant feat. geometry** triangle square doub. rectangle	**number of contact pads** 20 25	**contact pad layout** 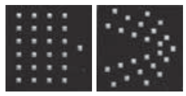
magnetic field ($\vec{B}\nabla\vec{B}$)	**field strength** N42 N35	**substrate position** z=0-2 mm	**release position** x=0-2 mm y=0-2 mm	**pole piece geometry** sharp rounded
viscous layer (ηa)	**chip geometry** 1×1 mm 2×2 mm	**viscosity** DI water glycerol		

Figure 3.14: Components used in the study

3.4.1. MAGNET STRENGTH

The speed of alignment is directly related to the strength of the magnets. When the same magnet unit configuration is used with different magnets, the form of the magnetic field gradient is not changed. However, stronger magnets have a bigger magnetic field strength. Therefore a bigger force is applied to the chip, which results in higher acceleration. The magnitude of the gradient in the field changes due to the difference in the magnetic field strength. Since the form of the gradient is preserved, a major change in the trajectory of the chip is not expected.

Two different magnet units including N42 and N35 grade rare earth magnets were investigated to understand the effects of changes in the magnetic field strength to the chip's alignment. The magnetic flux density coming out of the N42 and N35 magnets were measured to be 0.6 T and 0.52 T, respectively. Figure 3.15 shows the simulation results of the magnetic flux density of both magnet units. The FEM model allows detection of the saturation regions in the magnet unit. Magnetization curve of the yoke material was also considered in these models.

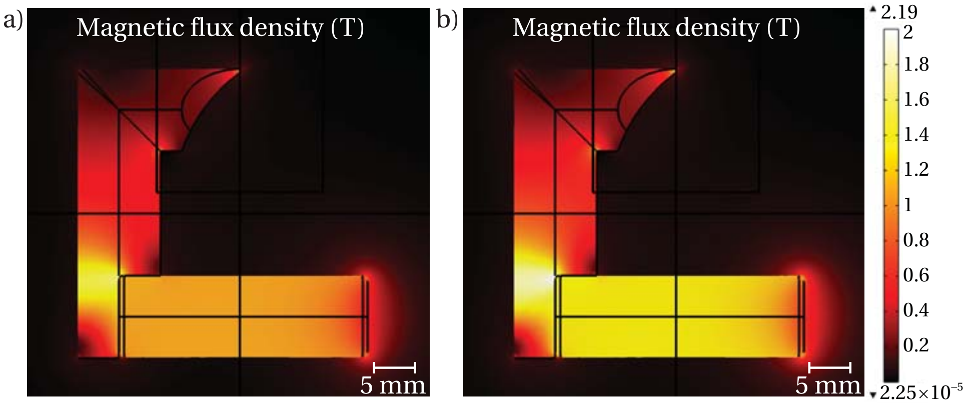

Figure 3.15: Magnetic flux density surface plots of the magnet units with N35 and N42 magnets. Brighter colored regions indicate the parts where the saturation occurs. a) N35 magnets, side view b) N42 magnets, side view

3.4.2. MAGNETIC MATERIAL ON THE CHIP

In this section, the relationship between the geometry and arrangement of the magnetic material on the chip and the applied magnetic force is investigated.

DOMINANT FEATURE SIZE

On another set of experiments the effect of changing the size of the dominant feature was studied. In these experiments the chips with ellipse shaped features and perimetric contact pads were used. Three different sizes of ellipse features were tested: a) Type I: 200 µm × 400 µm), b) Type II: 100 µm × 200 µm), c) Type III: 50 µm × 100 µm).

The results show that the dominance of the ellipse feature over the contact pads was lost as its size gets smaller. All of the chips were aligned with two different orientations as shown in Figure 3.16. The chips were released from the same position ($x_{\text{release}} = 2\,\text{mm}$, $y_{\text{release}} = -1\,\text{mm}$) and to reach the same final rotational alignment after each experiment, the release angle was differed between 0 – 180°.

LAYOUT OF CONTACT PADS

In some cases, it might not be possible to use dominant features because of the layout of the electronic circuit on the chip. However, a layout anisotropy can already be present on the chip, due to the location of the bumps. Such chips can align into multiple stable

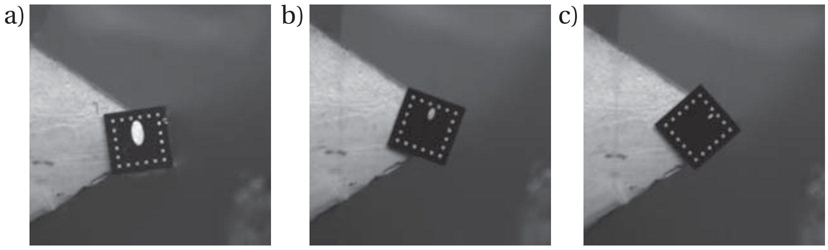

Figure 3.16: Final orientations of chips with different size ellipse features. a) Type I b) Type II c) Type III

orientations, as result of the matching between the anisotropy on the chip and the magnetic field gradient. In this case, the release angle should be limited accordingly in order to achieve the preferred orientation.

To examine this phenomena, the number and location of contact pads were changed in the test chips, while keeping the volume of the magnetic material fixed. Three different designs were considered as shown in Figure 3.17.

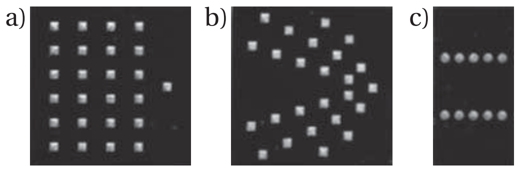

Figure 3.17: Chips with different contact pad layouts. a) A single contact pad placed on the side of evenly distributed group of contact pads. b) Contact pads distributed over the chip resembles the shape of the pole piece. c) Two rows of contact pads. For this design the separation between te rows was varied.

In the first design the anisotropy was created by a single bump placed on the side of the chip. The second design resembled the tapered shape of the pole piece. For both of the designs, multiple stable orientations were observed (Figure 3.18). The layout anisotropy did not create a dominance in these chips: the shape matching condition was satisfied every time the contact pads on the middle of the chips overlapped with the two sharp corners of the pole piece tip.

In the third set of experiments, chips that include two rows of contact pads were used. The size of the gap between the rows is altered to match the size of the distance between the sharp ends of the pole piece, as in the chips with double rectangle features (Figure 3.19). The rotational alignment of chips with gap sizes between 0.4 – 1.4 mm were used in the experiments. The results show that the chips with gaps bigger than 0.6 mm repeatedly aligns into a vertical orientation: the chips are aligned with the long axis of the rows (Figure 3.19f). It was also observed that the chips with a gap size bigger than the pole piece tip (1.4 mm) aligns diagonally such that one of the rows matches the slope at the side edge of the pole piece (Figure 3.19g).

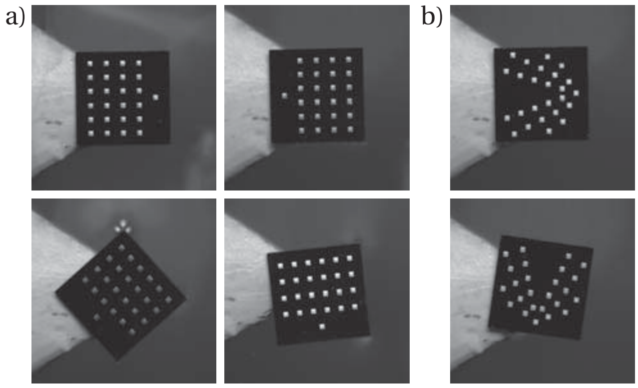

Figure 3.18: Different final orientations were observed in the experiments. a) Chip with a single contact pad on the side b) Chip with a contact pad layout that resembles the pole piece shape.

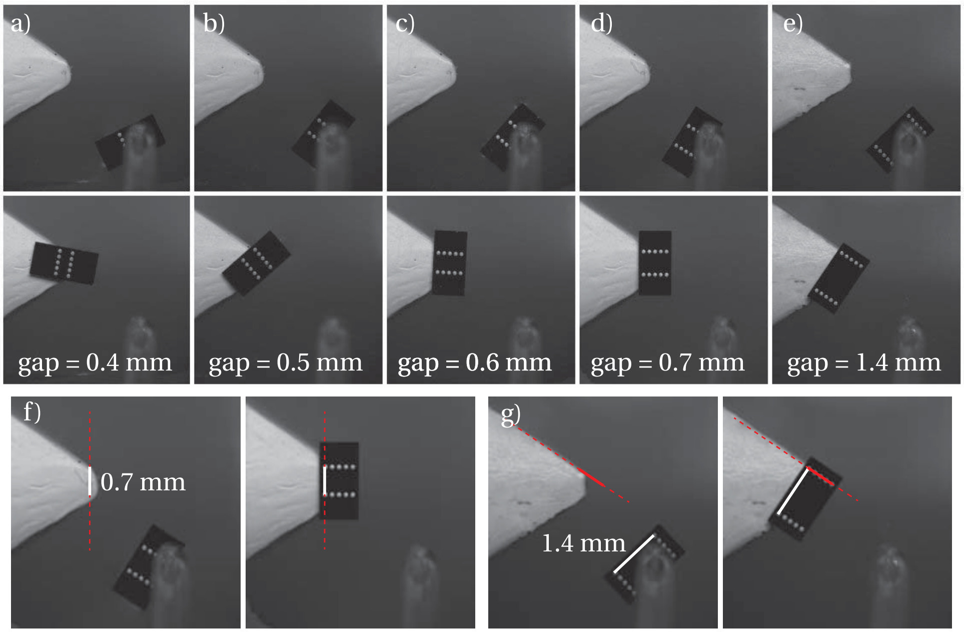

Figure 3.19: Alignment of chips with two rows of contact pads. a-e) The size of the gap between rows is changed between 0.4 to 1.4 mm. Top pictures show the chips' orientation at the beginning of alignment and bottom pictures show the aligned chips. f) The chip with 0.7 mm separation between the rows of contact pads aligns to a vertical orientation. The size of separation in this chip matches the size of pole piece at the alignment position. g) The chip with 1.4 mm separation align on the side of the pole piece.

NICKEL LAYER THICKNESS

Thickness of the electroless nickel layer in the contact pads is directly proportional to the magnetic force applied to the chip. Two different thicknesses; 3 – 5 μm were tested experimentally. The results show that the difference in bump thickness in this range does not affect the alignment duration significantly, both sets align within 0.16 sec, when released at 2 mm away from the pole piece, in all lateral dimensions. However, the chips with a 3 μm nickel layer, did not always align with the same orientation (Figure 3.20).

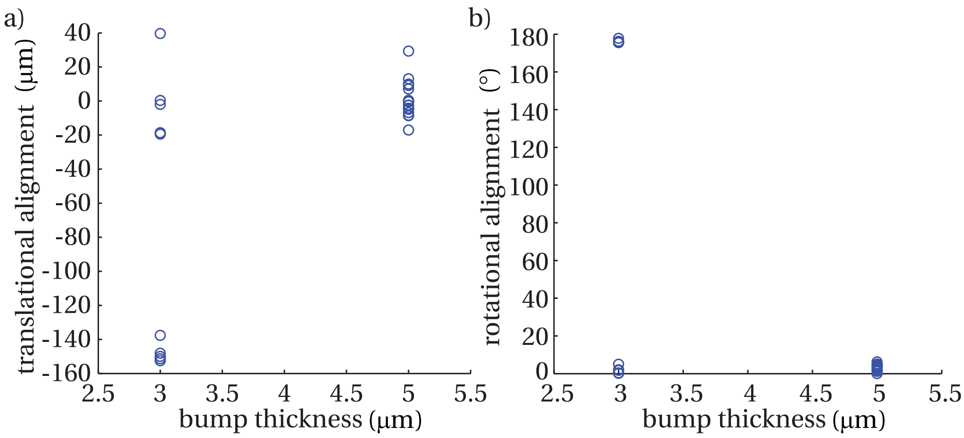

Figure 3.20: Effect of nickel layer thickness on alignment, substrate was positioned just above the surface of magnet unit. Chips were released from $x_{\text{release}} = 2\,\text{mm}$, $y_{\text{release}} = -2\,\text{mm}$ and align at the $z = 0$ plane. The blue circles represent the position or orientation of the chip after each experiment. a) Translational alignment b) Rotational alignment

3.4.3. WORKING SPACE IN THE MAGNETIC FIELD

The working space in the magnetic field defines which portion of the magnetic field gradient will be used during self-assembly. By changing the substrate or the release position, the working space is relocated in the surrounding field which also affects the trajectory of the chip's alignment.

SUBSTRATE POSITION (Z)

The out-of-plane distance between the substrate and the magnet unit is adjusted by a translational stage in order to be able to define the position of the magnetic field with respect to the top-surface of the substrate.

When the substrate is further away from the surface of the magnet, the magnetic field becomes defocussed, which diminishes the significant peaks in the field. As a result, the amount of positions that correspond to a global energy minimum is increased, i.e., the shape matching principle between the field and magnetic material on chip is satisfied in more than one location. Figure 3.21a shows the change in the magnetic flux density at different points along the tip of the pole piece, while increasing the distance between the magnet unit surface and the substrate.

Figure 3.21c shows the results of experiments, while the substrate was positioned at a variety of out-of-plane distances from the magnet unit ($z_{\text{substrate}}$ was varied between 0–2 mm with 0.5 mm steps). The distribution of the final positions reached after each experiment, indicates the defocussing in the magnetic field as the distance between the substrate and the top surface of the magnet unit is increased. A unique rotational and positional alignment is reached when the substrate is positioned at 0 – 0.5 mm above the magnet unit.

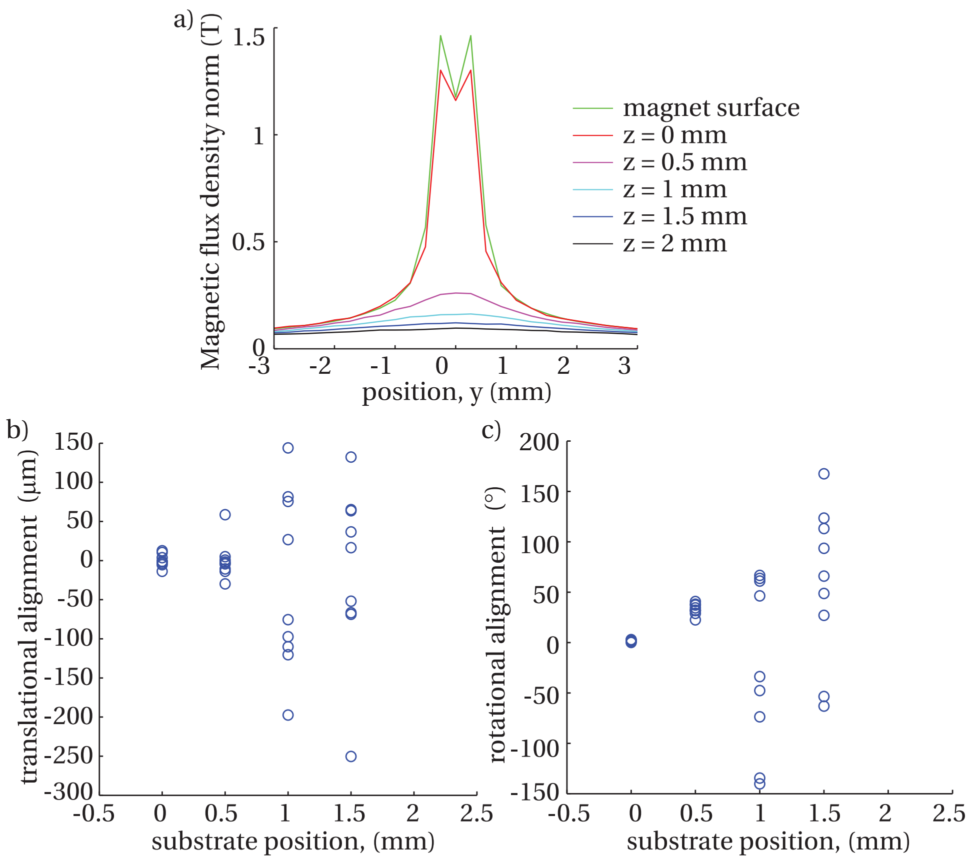

Figure 3.21: Alignment performance at different substrate positions. a) Change in magnetic flux density along the tip of the pole piece, with respect to the out-of plane distance from the magnet surface, modeled values. The peaks in the plots disappear as the out-of plane distance between the substrate and the magnet unit is increased. The position $z = 0$ mm refers to the top surface of the substrate, which has a thickness of 0.12 mm. b) Translational alignment and c) Rotational alignment at different substrate positions

RELEASE POSITION (XYZ)

All the geometric asymmetries of the magnetic pattern on the chip should be used effectively in order to reach a unique orientation and high precision alignment. Normally, the chip relocates itself into the nearest energetically favourable position. It is possible to determine a “safe region” of release, where the layout asymmetry of the magnetic material pattern is always effective regardless of the release angle, and the chip always rotates into a unique orientation.

Figure 3.22 shows all the release positions that were tried out. The initial trials have shown that the chips released from the top of the magnet unit ($x_{release} < 0$) are guided directly by the strong stray flux coming from the edge of the pole pieces. Consequently, the chips are aligned with the same orientation they have at the time of the release. To ignore the saturated edges of the pole piece, the chips should be released from the opposite side of the magnet unit.

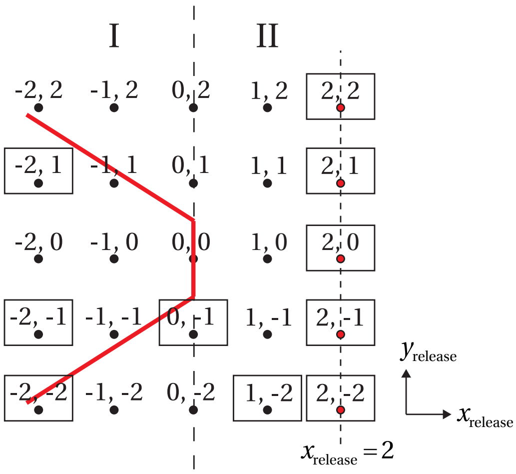

Figure 3.22: Experimentally tried release positions. The edges of the pole piece is indicated with red lines. The chips should be released from region II, to ignore the saturated edges of the magnet unit.

Release position	**Orientation I** (0°)	**Orientation II** (180°)
$x = 2, y = 2$	8	0
$x = 2, y = -2$	21	0
$x = 2, y = 1$	10	3
$x = 2, y = -1$	7	2
$x = 2, y = 0$	11	1

Table 3.1: Number of experiments at each release position

After initial trials, a series of experiments were conducted, along the $x_{release} = 2\,\text{mm}$

line, to collect statistical data and to determine the size of the safe region. Figure 3.23 shows the experimental results achieved while changing the release position of the chip. The number of experiments conducted for each release position is presented in Table 3.1. The initial orientations of the chips were varied between $0-360°$ in the experiments. The results show that, as the chips are released further from tip of the pole piece, the layout asymmetry of the rectangle features always forces the chip to rotate into the preferred orientation. Whereas, at the closer release positions, the chips align with two different orientations.

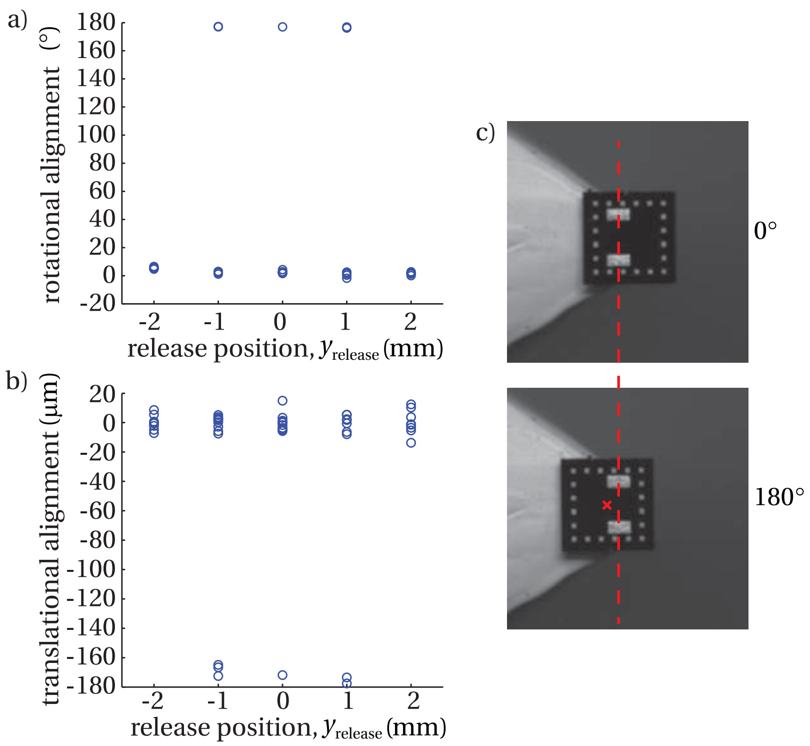

Figure 3.23: Alignment performance of the chips at different release positions along $x_{release} = 2\,\text{mm}$. a) Rotational alignment b) Translational alignment c) The red crosses show the displacement of chip center at different stable orientations (0° and 180°)

.

The distribution of the rotational alignment of the chips with respect to release position is shown in Figure 3.23a. The plot indicates that chips align into two different orientations (0° and 180°) and the rotational alignment precision is within a few degrees for the chips aligned with the same orientation. The effect of release position is also observable in the translational alignment plot (Figure 3.23b). The chips released from $x_{release} >= 2\,\text{mm}$, $y_{release} >= -2\,\text{mm}$ align with the 0° orientation. There is a clear difference between the final positions of chips for different orientations. This is due to the displacement of the chip centers, since the two rectangles tends to be positioned evenly on the edge of the pole piece. (Figure 3.23c).

Final alignment of the chips are compared in detail, for two different release positions in Figure 3.24.

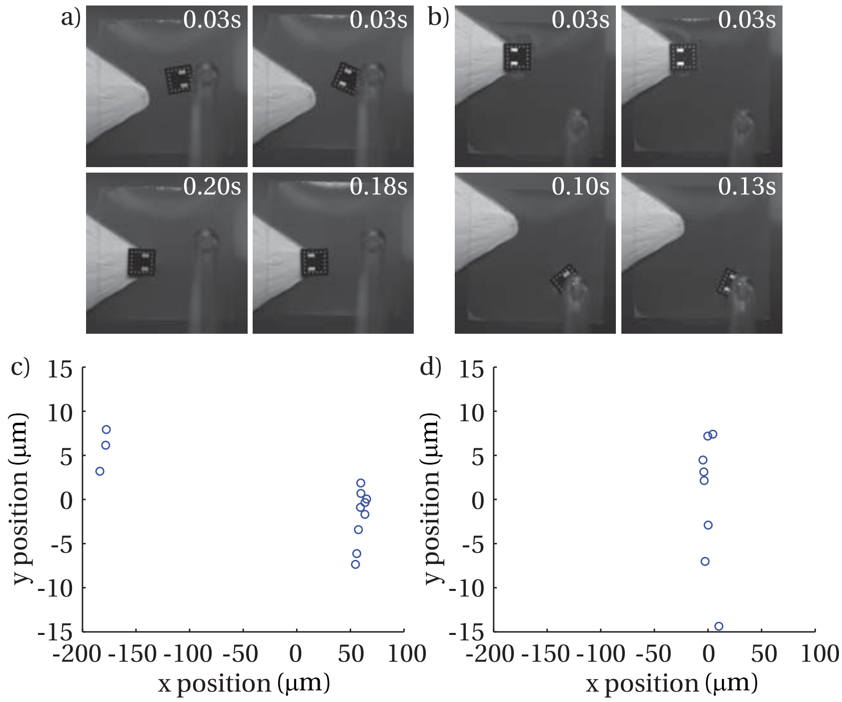

Figure 3.24: Final alignment of the chips released from a, c) $x_{\text{release}} = 2\,\text{mm}$, $y_{\text{release}} = 1\,\text{mm}$ and b, d) $x_{\text{release}} = 2\,\text{mm}$, $y_{\text{release}} = -2\,\text{mm}$. (a-b) Top pictures show the rotation of the chips after 0.03 s from the time of release and the bottom pictures show the chips at their final locations.

3.4.4. VISCOUS LAYER

The viscous layer has two major effects on the self-alignment of the chips. The first effect is lubrication of the substrate surface, which creates a lower friction force compared to the adhesion forces applied by the dry surface of the substrate. The second effect is the damping against the magnetic force applied to the chip. As a consequence, both the angular and translational acceleration of the chip is reduced, which changes the path that the chip follows in the magnetic field. The amount of the viscous drag is directly proportional to the characteristics of the viscous layer, i.e., the viscosity and the layer thickness. The effects of changing these characteristics is discussed in the following sections.

Solutions with different glycerol percentages (10 %, 25 %, 50 %, 75 % by volume) were tested as viscous layer to determine the effect of the viscosity on the chip's alignment process, which is one of the main factors determining the speed of the chip. Figure 3.25 shows the change in the chip's alignment duration when different glycerol solutions were used.

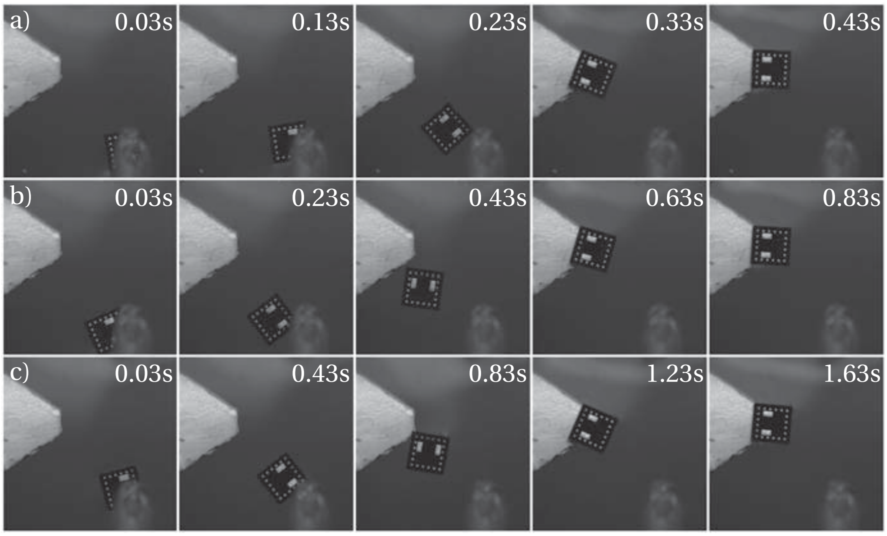

Figure 3.25: Change in alignment duration with respect to viscosity a) 25 % (v/v) glycerol solution b) 25 % (v/v) glycerol solution c) 25 % (v/v) glycerol solution

By adjusting the viscosity of the fluid it is possible to change the size of the "safe region" to release chips. Normally, the chips with a 3 μm nickel layer does not align into a unique orientation even if they are released from $x_{\text{release}} = 2\,\text{mm}$, $y_{\text{release}} = -2\,\text{mm}$. This situation changes when solutions that have more than 50 % glycerol is used; it is possible to align the chips uniquely regardless of the release angle (Figure 3.26).

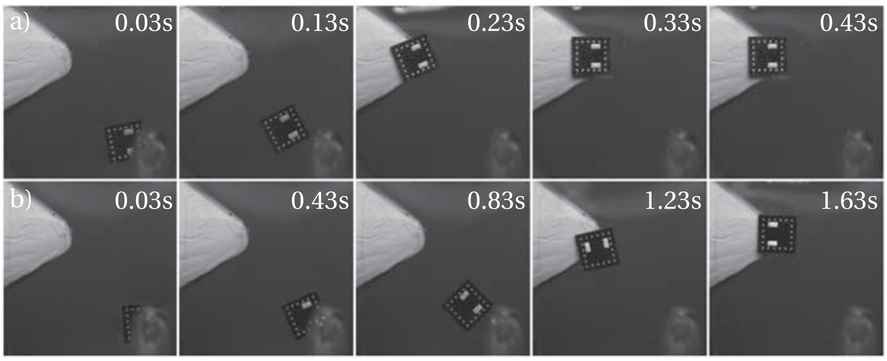

Figure 3.26: The chips aligns to preferred orientation as the viscosity is increased. a) 10 % (v/v) glycerol solution b) 50 % (v/v) glycerol solution

3.5. CONCLUSION

The following conditions should be satisfied to align chips with a unique orientation.

- The magnetic field gradient and the magnetic material pattern on the chip should be asymmetric and match in terms of geometry, i.e., the peaks in the field match the two rectangle features on the chip.
- Chips should be released away from the magnet unit, from a region where the saturation of the sharp edges does not interfere with alignment.
- To reach unique orientation regardless the release angle, the chips should be released from a "safe region" where the layout asymmetry is still effective, i.e., the 1×1 mm chip used in the experiments described in this chapter, is released from at least 2 mm away from the pole piece in both lateral dimensions ($x_{\text{release}} > 2$ mm and $y_{\text{release}} > 2$ mm).
- If the chips can not be released from the safe region, or if the asymmetry on the chip is not matching the magnetic field gradient, then the release angle should be controlled and limited. For instance, the chips released from $x_{\text{release}} = 2$ mm and $y_{\text{release}} = -1$ mm with an angle of $0° < \alpha_{\text{release}} < 90°$ or $270° < \alpha_{\text{release}} < 360°$ ends up aligning at 0° orientation (Figure 3.24).

Table 3.5 shows a summary of the experiments conducted within the scope of this chapter and their major outcomes.

		Parameter	Outcome
3.2.1 Magnetic field gradient	3.3.1	Pole piece design	Single sharp pole piece creates an asymmetric field.
	3.4.1	Magnet strength	Stronger magnets decrease alignment duration.
3.4.2 Magnetic material on the chip	3.3.2	Dominant feature shape	Having a dominant feature that has a shape and layout anisotropy matching the shape of the external magnetic field provides unique orientation.
	3.4.2	Dominant feature size	A smaller feature lose dominance over the contact pads.
	3.4.2	Bump layout	An asymmetric layout decreases number of stable orientations.
	3.4.2	Thickness	Lower thickness does not affect alignment duration drastically, however effects the final alignment orientation.
3.4.3 Position in the magnetic field gradient	3.4.3	Release position	To reach unique rotational alignment regardless the release angle, chips should be released from a region which is defined by the gradient in the proportion of magnetic and viscous forces applied.
	3.4.3	Substrate position	The substrate surface should be located at a position where the peaks in the magnetic field are matching the magnetic material layout on the chip.
3.4.4 Viscous layer	3.4.4	Viscosity	Higher viscosity slows down the process and changes the size of the “safe region”.

3

REFERENCES

[1] S. O. Kasap, *Principles of electronic materials and devices* (McGraw-Hill, 2006).

[2] D. C. Jiles, *Introduction to Magnetism and Magnetic Materials*, 2nd ed. (CRC Press, 1998).

[3] W. Wesley, *Plating,* (1950).

[4] J. Sudagar, J. Lian, and W. Sha, *Electroless nickel, alloy, composite and nano coatings - a critical review,* Journal of Alloys and Compounds **571**, 183 (2013).

[5] J. Wesselinowa, *Size and anisotropy effects on magnetic properties of antiferromagnetic nanoparticles,* Journal of Magnetism and Magnetic Materials **322**, 234 (2010).

[6] H. Li, H. Z. Wu, and G. X. Xiao, *Effects of synthetic conditions on particle size and magnetic properties of* $NiFe_2O_4$*,* Powder Technology **198**, 157 (2010).

[7] C. A. F. Vaz, J. A. C. Bland, and G. Lauhoff, *Magnetism in ultrathin film structures,* Reports on Progress in Physics **71**, 056501 (2008).

[8] C. Nacereddine, A. Layadi, A. Guittoum, S.-M. Cherif, T. Chauveau, D. Billet, J. B. Youssef, A. Bourzami, and M.-H. Bourahli, *Structural, electrical and magnetic properties of evaporated Ni/Cu and Ni/glass thin films,* Materials Science and Engineering: B **136**, 197 (2007).

[9] H. Du, P. Wu, E. Jiang, Z. Li, C. Zhao, and H. Bai, *The influence of experimental procedures on the structural and magnetic properties of rf sputtered Fe-Ni thin films,* Journal of Magnetism and Magnetic Materials **292**, 227 (2005).

[10] C. C. Huang, H. C. Hsu, and Y. C. Tseng, *Structural morphology and magnetism of electroless-plated NiP films on a surface-modified Si substrate,* Thin Solid Films **520**, 1102 (2011).

[11] N. A. Lange and J. A. Dean, *Lange's handbook of chemistry* (McGraw-Hill, 1979).

[12] G. Kissinger and W. Kissinger, *Hydrophilicity of silicon wafers for direct bonding,* physica status solidi (a) **123**, 185 (1991).

3

4

FABRICATION AND ALIGNMENT PERFORMANCE

It doesn't matter how beautiful your theory is,
it doesn't matter how smart you are.
If it doesn't agree with experiment, it's wrong.

Richard P. Feynman

The agreement of this law with nature
will be better seen by the repetition of experiments
than by a long explanation.

Hans Christian Ørsted

The following activities were performed during the experiments for extensive understanding of the magnetic self-assembly process: I) Recording the chip's motion in the magnetic field to gain detailed information on chip's trajectory II) Collecting statistical data for evaluation of the process performance. Experiments show that a repeatability of $3\sigma = \pm 25\,\mathrm{um}$ *and* $3\sigma = 2°$ *is reachable with fastest alignment duration of* $0.2\,\mathrm{s}$ *while using water as a viscous cushion. The industrial implementation was demonstrated by installing a magnetic self-assembly tool box into two separate chip presentation machines using different methods to release chips.*

Parts of this chapter is based on article E. E. Kuran, Y. Berg, M. Tichem, Z. Kotler, *Integration of laser die transfer and magnetic self-assembly for ultra-thin chip placement*, Journal of Micromechanics and Microengineering, (2015).

This chapter consists of three parts. In the first part, an introduction is made by describing the experimental process flow. Subsequently, fabrication of the components used in the experiments and the construction of the research setup are discussed. The second part is about the experiments done for understanding the dynamics concerning the chip's alignment, where an analysis on the performance is made based on the experimental results. The third part is about industrial implementation, i.e., combination of magnetic self-assembly with two different chip presentation techniques: I) conventional die bonding with pick-and-place tools II) laser-based die transfer. Figure 4.1 shows the outline of the experimental work done in this thesis.

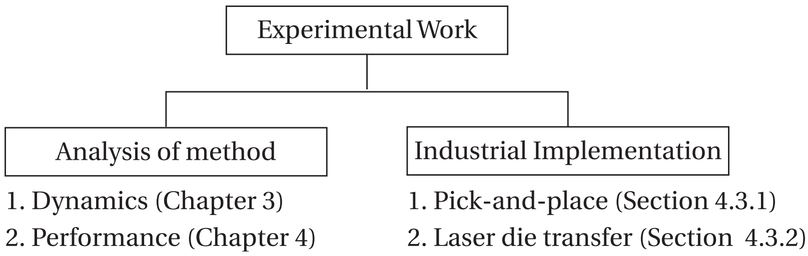

Figure 4.1: Experimental chapter outline

4.1. RESEARCH SETUP AND EXPERIMENTAL PROCESS FLOW

The research setup shown in Figure 4.2 consists of:

- Two high speed cameras to observe the experiments from top and side views (IDT Inc. NX4S1 cameras with Edmund Optics 1x silver series telecentric lenses)
- A release tool which is used for directed presentation of the chips to the magnetic field
- A magnet unit
- Several XYZ linear translation stages to position the substrate, the release tool and the cameras (Thorlabs Inc., 25 mm travel translation stages with 149.4 μm resolution).

Releasing chips with a short pulse of air is one of the common methods used in the die bonding machines [1]. However because of the high adhesion between the tool and an ultra-thin chip, a high pressure has to be applied for release which causes a considerable air flow around the viscous layer on the substrate. The high air flow deforms the viscous layer and at sometimes may even result in blowing away the fluid. A special tool was designed for releasing chips with a lower impact force. The tool consists of a fiber needle inserted inside of a glass capillary tube (Figure 4.2b). The chips are picked by vacuuming the glass capillary tube and released by turning off the vacuum. A small plastic ball is attached to the fiber needle to block the air flow when the vacuum is turned on. When the vacuum is turned off, the fiber needle falls down by its weight and mechanically pushes away the chip.

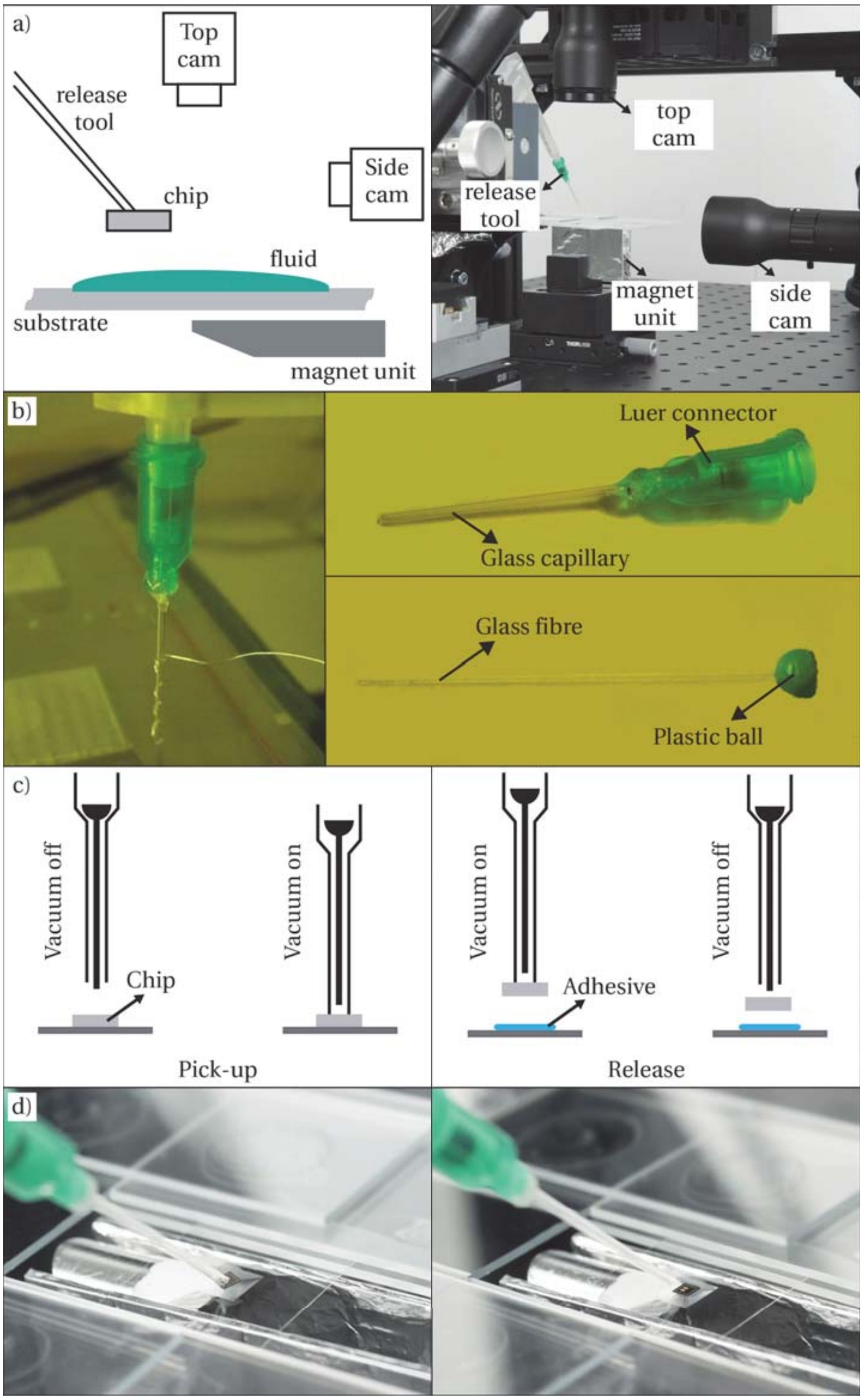

Figure 4.2: a) Experimental setup b) The release tool with capillary tubing and glass fiber needle c) Working mechanism of the release tool d) Pictures showing a chip picked-up and released.

The experimental flow chart is shown in Figure 4.3. Before starting an experiment, the stages in the setup are adjusted to desired positions and the cameras are calibrated. Afterwards, the chip is picked up by the release tool and the substrate, with a fixed amount of liquid dispensed on the binding site (Section 4.1.1), is placed on the substrate holder. Finally, the recording is started and the chip is released respectively. If bonding of the chip is required, an adhesive is used as the liquid layer and the chip is fixed at position by UV curing after the alignment is finished.

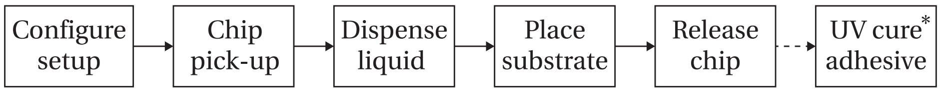

Figure 4.3: Experimental flow, * The UV curing step is added in the cases where the chip is fixed after alignment. In the industrial implementation experiments (Section 4.3.1) the substrate was placed on the self-assembly tool at first, and the viscous layer was dispensed afterwards.

4.1.1. FABRICATION

In this section, the fabrication processes of components such as the chips, the magnet unit and the substrates used are discussed. The design parameters of these components were altered during the experiments in order to analyze their influence on the chips alignment.

CHIPS

Chips with a variety of sizes in the milliliter range and with thicknesses of 20–100 µm were used in the experiments. The majority of the chips, except the commercial ones mentioned in Section 4.3.1, did not have a functionality besides having a soft-magnetic material pattern. The fabrication procedure of the chips is shown in Figure 4.4. The process starts with deposition of a silicon oxide layer (100 nm) on one side of a thick silicon wafer. Then a layer of aluminum (2 µm) with a small content of silicon was sputtered as a seed layer for electroless nickel deposition. The layer was structured with lithography and dry etching. The process was followed with addition of the nickel layer (5–2 µm) by electroless plating. Finally, the nickel features were protected from oxidation by a thin layer of immersion gold (100–200 nm). After patterning, the wafers were thinned down to (50 µm ± 1–2 µm) and subsequently diced by dicing before grinding (DBG) method. (DISCO Corp.) In the DBG process, the wafer is partially cut in advance to prevent initiation of cracks during the die singulation process. Afterwards, the dies are separated by polishing the wafer from the backside, down to the desired thickness.

Several aspects were considered for the design of magnetic features on the chip. In semiconductor industry, adding a thin layer of nickel to the contact pads of the chips is a common solution for enhancing the electrical connectivity and reliability. [2, 3] Nickel is also chosen for its compatibility with standard micro-machining processes.

The trends in IC floor planning were explored to gain knowledge on common bond pad layouts used in the semiconductor industry. [4] The following parameters were considered to achieve a design resemblance with commercial chips: standard pitch sizes used in wire bonding and solder bumping, bond pad size and thickness, I/O number and materials used for robust electrical interconnection. Distribution of bumps over the perimeter of the chip is one of the common layout arrangements for chips with smaller amount of functionalities. When the functionality number is increased, the I/O number is also increased and a ball grid array design is preferred.

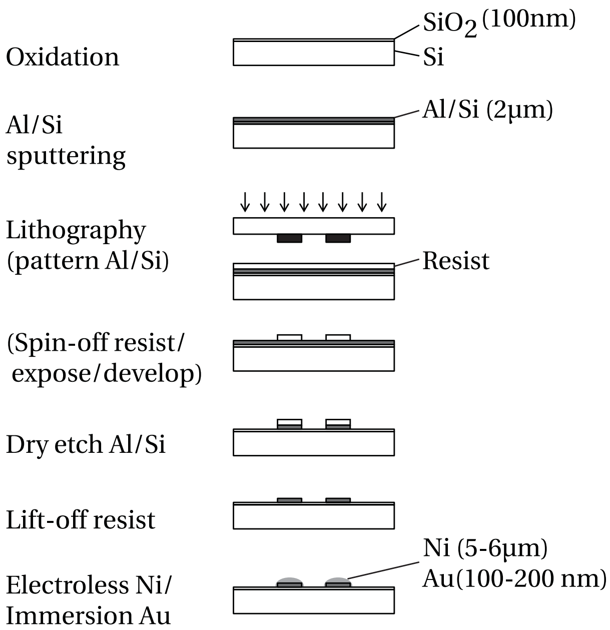

Figure 4.4: Fabrication steps of chips

MAGNET UNIT

The main magnet unit used in the experiments consists of permanent magnets (cylindrical Ø10x10mm, NdFeB/N52 grade magnet, HKCM Engineering) and a soft iron yoke with a single sharp pole piece (Figure 4.5). Permanent magnets were chosen to utilize a strong magnetic field in a compact way. For further applications, an active control of the field can be reached by using an electromagnet as discussed in Chapter 5.

The parts of the magnet unit were attached to each other by the magnetic attraction coming from the permanent magnets. This enabled building different combination of magnets, yokes and pole pieces easily, to investigate the effect of changing magnet unit design on the applied magnetic field. (See details in Section 3.2.1.) The yoke and pole pieces were fabricated by water jet cutting. The design assured to avoid sharp edges in the self-assembly area, except in the end of the pole-pieces, which focuses the magnetic field and creates high flux density points to define the chip's final alignment position. The magnet unit was fixed to the research setup by a mechanical clamp.

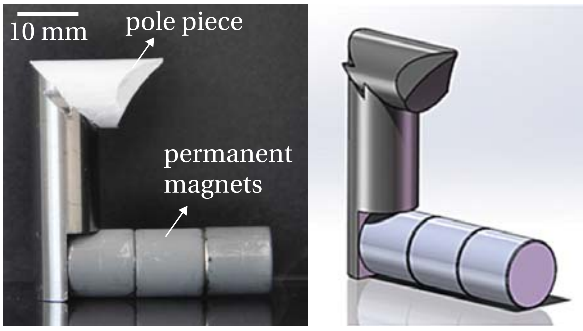

Figure 4.5: Magnet unit

VISCOUS LAYER AND THE SUBSTRATE

Different fluids were chosen for the viscous layer based on their functionality. The experiments mentioned in Section 4.3.1 involved fabrication of smart-blister demonstrators for the Chip2Foil project, which required fixation of chips after alignment. Therefore, an UV curable adhesive was used to provide initial bonding of the chip. For the experiments mentioned in Chapter 3 and in Section 4.3.2, fixation of the chips was not necessary. The chips and the substrates were recycled at these experiments and to avoid contamination DI water was used as the viscous layer.

For smart-blister demonstrators, chips were assembled to a polymer foil substrate (Polyethylene terephthalate(PET), 65 µm, Agfa-Gevaert N.V.). At locations where the self-assembly was performed, an area with a size of 5×5 mm was treated with oxygen plasma cleaning to increase the wetting and to confine the die-attach adhesive. To avoid oxidation of the web circuitry and to protect the rest of the foil during the plasma treatment, a gel-film mask is used (WF Gel-film with X0 level retention, Gel-Pak). For die-attach adhesive selection, the following criteria were considered:

- low viscosity
- compatibility with the substrate and the glob-top adhesive
- strong bonding to the silicon and the polymer substrate
- low curing temperature
- short curing time
- flexibility after curing

Low viscosity and low curing temperature were the most important requirements in the selection. The curing temperature of the adhesive to be chosen had to be below the glass transition temperature of the PET foil (70–80° [5]). Therefore, UV curable adhesives were preferred to avoid heating of the substrate. Additionally, after a brief search through commercially available adhesives, it was observed that low-viscosity was not a common characteristic for die-attach adhesives. Therefore, in-house made acrylate adhesives were used in the initial trials (hexanediol diacrylate: isobornyl acrylate (HDDA:iBoA), 1:1w/w%, viscosity=11.4 mPa·s) which caused problems in terms of compatibility with the glob-top adhesive and dispensing. Finally, to provide reliable bonding and to avoid heating of the foil a commercial UV curable adhesive was chosen (Vitralit 7641, Panacol-

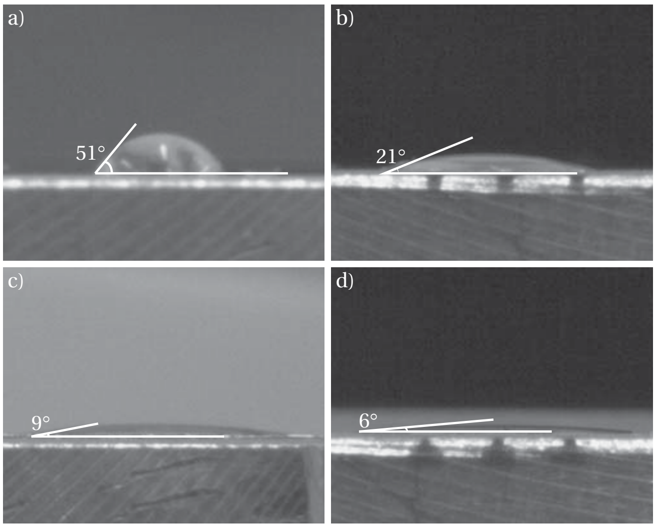

Figure 4.6: Contact angle measurements. Top and bottom pictures shows a water and an adhesive droplet, respectively. a,c) untreated foil and b,d) treated foil.

Elosol GmbH). An air pressure dispenser integrated inside the die-bonding machine was used to dispense controlled volumes of the die-attach adhesive. The adhesive was cured after alignment by a fiber optic UV source (bluepoint 4 ecocure, Dr. Hönle AG UV Technology).

Microscope cover slips were used as substrates in the rest of the experiments (Gerhard Menzel GmbH, Nr.0 glass cover slips, 0.08–0.12 mm thick). Recesses were engraved on top of the cover slips with an UV laser, to contain the viscous layer (Coherent Avia, wavelength = 266nm, pulse repetition rate = 30kHz, $V = 100\,\mathrm{mm\,s^{-1}}$, average power = 0.4 W). A micro-pipette was used for dispensing the viscous layer.

4.2. ALIGNMENT PERFORMANCE

Some of the results of the experiments discussed in this section were already introduced in Chapter 3. The following results explain the performance of the method based on the alignment repeatability and duration. Additionally, the challenges faced during the experiments and the potential failure mechanisms are explored.

The performance of the method was investigated through analysis of the videos taken during the experiments. The recordings from the top camera were used for quantitative analysis such as tracking the chip's motion during the alignment and measuring the final position and orientation the chip takes after each experiment. The side camera was used for observation of chip's fall after the separation from the release tool. The details of the image processing of the videos is discussed in Appendix-A.

The following performance parameters were analyzed in the experiment videos:

- repeatability of the alignment: The final positions and rotations that the chips reaches after the experiments were compared with each other. The repeatibilty of the alignment was determined by calculating the standard deviation of the final positions.

- cycle time: The time interval starting from the release to the end of chip's motion was measured for each experiment. The cycle time was calculated by taking average of these alignment durations.

It was observed that the chips were mostly released with a tilt, due to impact of the needle pushing the chip and the chip's attraction to the magnet unit. In most cases, as the chip fell to the viscous layer a little amount of air was trapped, which formed bubbles underneath the chip (Figure 4.7). Occasionally, the escaping air moved the chip, while the restoring magnetic force returned the chip back to its position. The time that took the air to escape from under the chip was not included in duration calculations.

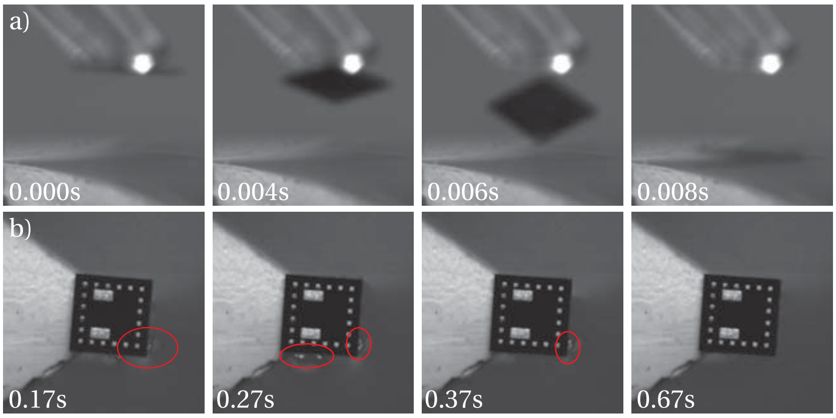

Figure 4.7: a) Tilted release of the chip, side view b) Formation of bubbles due to air entrapment underneath the chip, top view. The regions with bubbles are marked with red circles.

The coordinate system of the fixed camera is used for calculations. The last 20 frames were extracted from the video of each experiment, and the position of the chip in this videos were found by image processing. For each experiment, the average position of the chip was calculated to decrease the measurement error. Then the average positions from all experiments were compared. The repeatability of the experiment results is calculated by, the corrected sample standard deviation formula (Equation 4.1), which is suggested for experiments with small sample numbers. Additionally, the standard deviations of the experiments with same conditions were combined by using the pooled standard deviation method (Equation 4.2), to increase the sample number for each type of experiment. [6]

$$\sigma = \sqrt{\frac{1}{1-N}\sum(x_i - \overline{x})^2} \tag{4.1}$$

$$\sigma = \sqrt{\frac{\sum(n_i - 1)^2 \sigma_i^2}{\sum(n_i - 1)^2}} \tag{4.2}$$

Figure 4.8 shows the final positions reached after a set of experiments with use of ideal conditions for reaching a unique positional and rotational alignment. (Substrate is positioned at the surface of the magnet unit, the chips are released from a “safe region”, i.e., $x_{release} > 2$ mm, $y_{release} < -2$ mm & $y_{release} > 2$ mm, and 2 µl DI water was used as viscous layer.)

Out of 29 experiments that was conducted within the safe region, all the chips were aligned with the desired and unique alignment (0°), regardless of the initial release orientation. However, in one of the experiments the chip was aligned with 30 µm and 4° off the average translational and rotational alignments. This experiment was considered to be an outlier (Figures 4.8a-b) and was excluded from the standard deviation calculations.

In all of the 28 experiments conducted within the safe region, the chips ended up at same orientation regardless of the release angle.

For these experiments, the repeatability of the alignment was calculated to be $3\sigma = 25$ µm, with a rotational alignment of $3\sigma = 2°$. The average alignment duration was 0.2 s. The details of all the measurement results are included in Appendix C.

4.3. INDUSTRIAL IMPLEMENTATION

In this section implementation of magnetic self-assembly with two different chip presentation techniques is demonstrated. The first technique is pick-and-place which is a commonly used assembly method in the electronics industry. The second technique is laser die transfer, which is a relatively new technology used for micro-assembly.

4.3.1. EXPERIMENTS WITH A CONVENTIONAL PICK-AND-PLACE MACHINE

The experiments done in this part are related to demonstrator preparations in the Chip2Foil project. The general process flow for fabrication of “Smart Blister” was explained in Section 1.3. Magnetic self-assembly was used for positioning and initial bonding of an NFC chip on the smart blister package. (M24LR64, 1.5 × 2 mm size, 25 – 35 µm thickness, 10 I/Os, ST Microelectronics). The chips were assembled into a PET foil, and a commercial die-attach adhesive was used to provide initial bonding, as mentioned in Section 4.1.1).

To experimentally investigate the process, a setup as shown in Figure 4.9 is realized. Two magnet units were assembled into an aluminum box, which was placed inside the die bonder Besi EVO2200. Acrylate plates with flexure hinges were used for fine positioning of the magnet units inside the box. The foil substrates were fixed to the tool by vacuum applied from the through holes of an acrylate top plate. The foils was positioned on the top plate manually, by using registration marks printed on the foil and the self-assembly box. The set-up was placed in an UV protective cover which is used to prevent uncontrolled curing of the adhesive by the ambient light.

To start an experiment, the chip was picked up from a waffle box and subsequently, a droplet of die-attach adhesive was dispensed over the plasma treated area on the foil. Afterwards, the chip was released to the alignment area with its contact pads facing upwards, from a height of 1.5 mm and a lateral displacement of 1 – 2 mm. Finally, magnetic self-assembly brought the chip to the target position and the die-attach adhesive was UV cured for mechanical bonding of the chip to the polymer foil. The curing was done in two steps: First, a pre-curing step (1 s) was performed to fix the chip in place. Af-

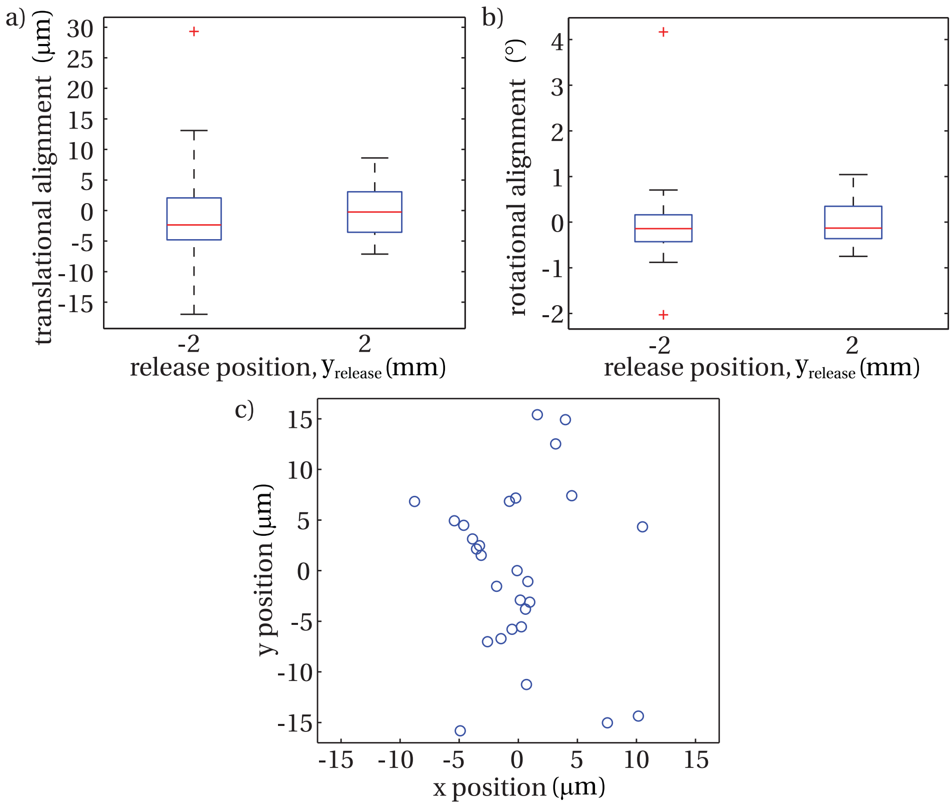

Figure 4.8: Experiment results at ideal release and substrate position, ($x_{release} = 2\,\text{mm}$, $y_{release} = 2\,\text{mm}$, $z_{substrate} = 0\,\text{mm}$) figures 4.8a-b Box plot representation of the results. The red plus marks represent the outliers. The experiment which is an outlier in both of the translational and rotational alignment plots was excluded from standard deviation calculations. The whiskers covers approximately 99:9% of the data. a) Translational alignment b) Rotational alignment. c) Final positions of chips' released from safe region.

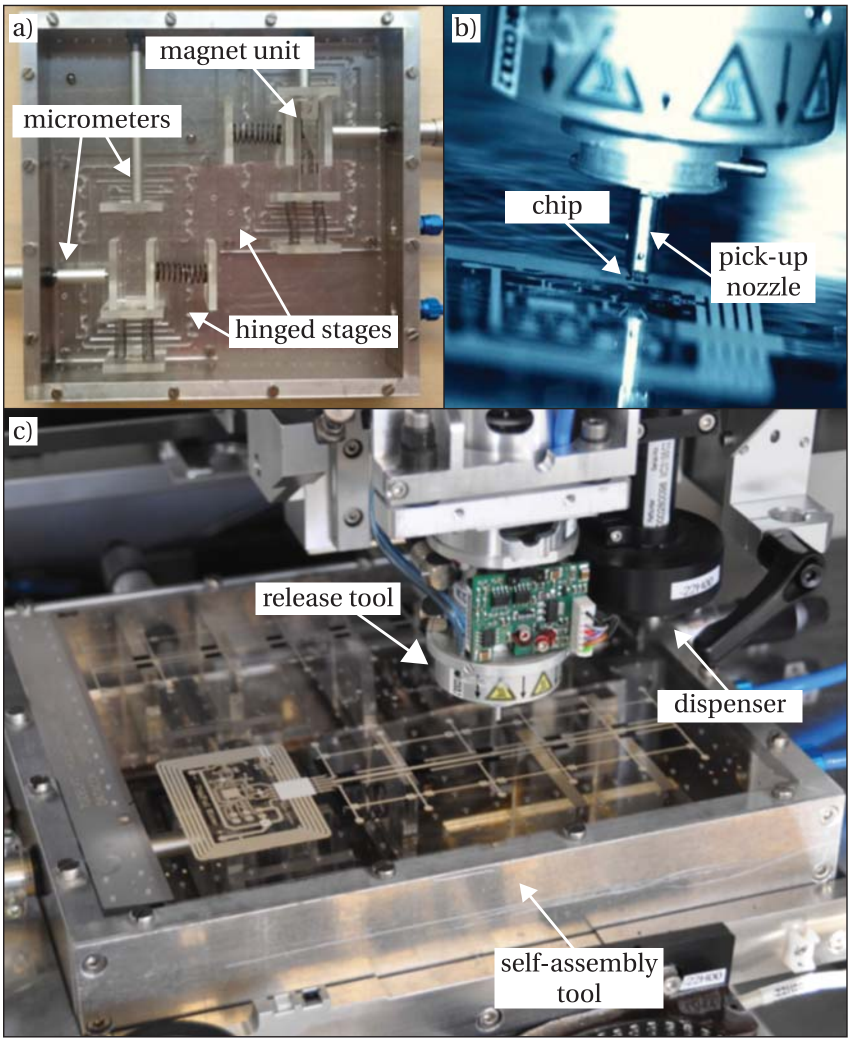

Figure 4.9: Implementation of self-assembly with pick-and-place tool. a) Self-assembly toolbox b) Close-up view of the pick-up tool with a chip c) The toolbox inserted into Besi EVO2200 die bonding machine

4

ter pre-curing, the foil could be moved from the self-assembly tool without losing chip's alignment. Subsequently, the bonding of the chip was completed by a final curing step (1 min).

Initially high air pressures were used to release the chip, which resulted a blast of air after the chip was freed from the pick-up head and eventually deformed the adhesive layer. Therefore the tool was modified to have push-through mechanism similar to the release tool mentioned in Section 4.1.

Table 4.1 shows the calculated precision values for the position of the chip with respect to the targeted position on the foil defined by the registration marks. The values include the error coming from manually placing the foil and the misalignment of the magnet unit with respect to the registration marks on the tool. There is a clear difference between the precision achieved in the first magnet unit compared to the second one. We suspect that this is due to a less well focused magnetic field in the first magnet unit. In addition, these experiments were conducted before the optimization of the magnetic self-assembly alignment concept. Even though the contact pads on the chip were positioned asymmetrically, the magnet unit created an symmetric field due to the two identical pole pieces. Therefore, shape matching requirement for reaching a unique orientation was not satisfied. The desired rotational alignment was achieved with controlling the release angle. Despite the insufficient conditions, the achieved precision values are within the acceptance range of the adaptive interconnection process.

	Position I	Position II
Number of experiments	13	12
Repeatability (1σ)	X: ±235µm Y: ±135µm	X: ±90µm Y: ±80µm

Table 4.1: Results of industrial implementation experiments with a pick-and-place tool

In the earlier experiments without self-assembly, an average cycle time of 0.83 seconds/die was achieved while assembling chips with a size of 0.9 × 0.9 mm and a thickness of 20µm. This accounts for a throughput of 4337 chip/hour, for this particular type of chip. Magnetic self-assembly allows releasing the chips with low accuracy which decreases the machine travel time of the pick-up tool. For example, a separate set of trials for chip presentation shows that, releasing the chip from a height of 1 mm results with 40 ms of decrease in cycle time of the pick and place process, which amounts to a throughput increase of 100 chips/hour.

FAILURE MECHANISMS

All the failure modes observed in the experiments were related with the adhesive, starting from the deposition to the curing step. The first failure mode was the variation of the form of the die-attach adhesive layer, due to problems occurred in plasma treatment. As mentioned before, a gel-film mask was used to pattern hydrophilic areas on the foil surface. To achieve a uniform pattern, the mask should be attached to the foil tightly to prevent leakage of the plasma to the inside of the mask. However this was not the case in most of the experiments: the height difference between the web circuitry and the foil surface created openings on the edges of the square holes on the gel-film masks. This lead to leakage of plasma and eventually oxidization of the ends of the web circuitry (Figure figures 4.10a-c).

The variations on the thickness of the die-attach layer caused failures on the interconnection of the chip, i.e., the topography of the die-attach layer was transformed to the glob-top adhesive which led to problems in the via-filling process.

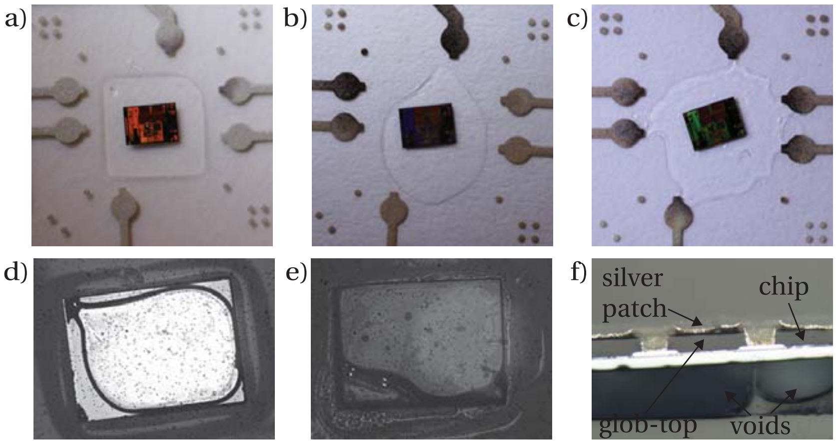

Figure 4.10: Adhesive related failure modes a-c) Defects due to the leakage from gel-film masks during plasma treatment a) Well-defined coverage of the die-attach layer b) Insufficient spreading c) Over-spreading d) Air cavity formed under the chip after curing e) Chip detached during handling due to low adhesion f) Cross-section view of the chip in the interconnection process: vias opened on the glob-top layer is filled with screen-printed silver patch. The voids underneath the chip is clearly visible on the figure. Courtesy of the Chip2Foil consortium [7].

Another failure mode was the low adhesion due to the big air cavities formed underneath the chips. The entrapment of air under the chip as it falls to the adhesive layer and the degassing during the curing step were considered to be the reasons behind the formation of the air cavity. Besides, the wettability of the chip was decreased due to the contamination of the chips by the wax used in the thinning process. The cavity formation decreased the bonding area of the chip such that the already warped chip was only adhered to the adhesive on the corners. As a consequence, some of the chips were detached from the demonstrators while handling (Figure 4.10e).

4.3.2. EXPERIMENTS WITH LASER INDUCED FORWARD TRANSFER (LIFT)

Lasers have been widely used in different micro-fabrication processes, e.g., lithography, mask generation, wafer dicing, trimming, scribing via drilling and material deposition [8, 9]. Laser induced forward transfer (LIFT) is a printing technique for direct writing of materials [10]. First, the material to be printed is deposited on a donor substrate which is transparent to the wavelength of the laser used in the process. Then by laser ablation, the material is removed and transferred to a receiver substrate which is placed closely underneath the donor.

LIFT is also used for the transfer of micro-electric components; which is referred as laser die transfer. In this case, the components are attached to the donor substrate by a sacrificial adhesive layer. Later, the adhesive is ablated by a laser beam and subsequently the micro-component is detached from the donor substrate [11–15]. Laser die transfer enables direct ejection and presentation of chips without a mechanical contact that would cause adhesion problems as in a pick-and-place process. Additionally, it provides a high speed chip placement, i.e., the whole process including the release and landing of the chip on the target substrate is accomplished within a millisecond.

4

However, the precision of the process is dependent on the separation between the donor and the target substrates. After the ablation of the sacrificial adhesive, it can be assumed that the component's motion takes place within a fictional release cone as shown in Figure 4.11. The chip, accelerated by the impact from the ablation deviates from its normal path and lands to an arbitrary position on the donor substrate with an arbitrary orientation. For reaching a high precision, the gap between the donor and target substrates has to be fairly small, which is a disadvantage because of the machine control demand. Karlitskaya et. al. [12] shows the relation of the donor-to-target substrate gap to the release angle and achieved accuracy. With a gap of 0.5 mm, the allowable release angle is 4°, and the accuracy is 35 µm. With a gap of 0.2 mm, the allowable release angle increases to 9° while the accuracy stays at the same level. Pique et. al. [13] mentions that a lateral precision smaller than 50µm can be achieved for short travel distances (< 1 mm). Initial trials in our work with (1 × 1 mm) components has shown that a precision of σ = 120 µm and σ = 8.8° can be achieved at a transfer distance of 1 mm, without implementation of self-assembly.

The experiments discussed in this part aims to improve the alignment precision by addition of magnetic self-assembly to the system. The combination of the laser die transfer and self-assembly enables handling of delicate parts in a fully non-contact approach. Besides, the dependence of the alignment precision to the donor-to-target substrate gap is eliminated, and the release angle allowance demands are relaxed.

Figure 4.11 shows the concept of the laser die transfer assisted with magnetic self-assembly. The chip is presented by laser die transfer to the magnetic field surrounding the assembly area and lands on the viscous layer. Then the magnetic self-assembly brings the chip to the final precision.

The self-assembly box mentioned in Section 4.3.1 was used again to realize experiments inside the LIFT setup (Figure 4.12a). To start the experiments, a donor substrate with chips was flipped and attached to a 3-axis motorized stage, which was used to roughly position the donor substrate above the magnet unit. The separation distance between the donor and the target substrates was adjusted to 1 mm and the chips were released approximately 1.4 mm away from the targeted position of assembly (1 mm in each lateral direction.

The magnet unit configuration, the chips and the substrates used in the experiments are shown in Figure figures 4.12b-c. Two different types of magnetic material patterns were used in the chips. In the first type, the contact pads were distributed over the perimeter of the chip and an ellipse feature was added to this pattern to create an asym-

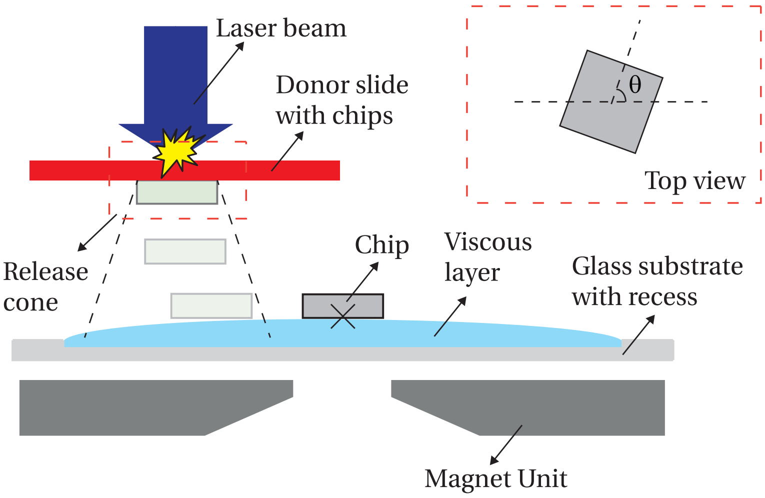

Figure 4.11: Concept of laser die transfer integrated with magnetic self-assembly. The zoomed area shows that the chips are released with a random angle, θ from the donor substrate.

metric layout of magnetic material. The shape anisotropy of the ellipse (width/length) and the asymmetric layout allows aligning chips with specific orientations. This pattern was experimented with both 1×1 mm and 2×2 mm chips. In the second type the asymmetry is created by the layout of contact pads and addition of two rectangles on the right corners of the chip. This type was experimented only with 2×2 mm chips.

In these experiments, DI water was used as viscous layer to prevent contamination chips and substrates which were re-cleaned and used repeatedly. The recess size on the glass substrates and the volume of the water was changed according to chips size. The combinations of the components used in the experiments are listed in Table 4.2. A micro-pipette was used to dispense a controlled volume of DI water onto the engraved cavity on the substrates.

Chip size	Size of recess on substrate	Volume of DI water
1×1 mm	5×5 mm	2 µl
2×2 mm	8×8 mm	7 µl

Table 4.2: Properties of the components used in the experiments

The chips were manually placed on the donor substrate (glass slide, 1 mm) with a dynamic release layer (DRL) of triazene (250 nm) as shown in Figure 4.13. Triazene is an exothermic polymer which undergoes full decomposition into volatile water vapor and CO_2. A $4wt\%$ solution of triazene polymer was prepared in a 1:1 w/w mixture of chlorobenzene and cyclohexanone. The solution was mixed overnight and then spin coated onto the soda lime glass microscope slides for 30 seconds at a speed of 800 rpm.

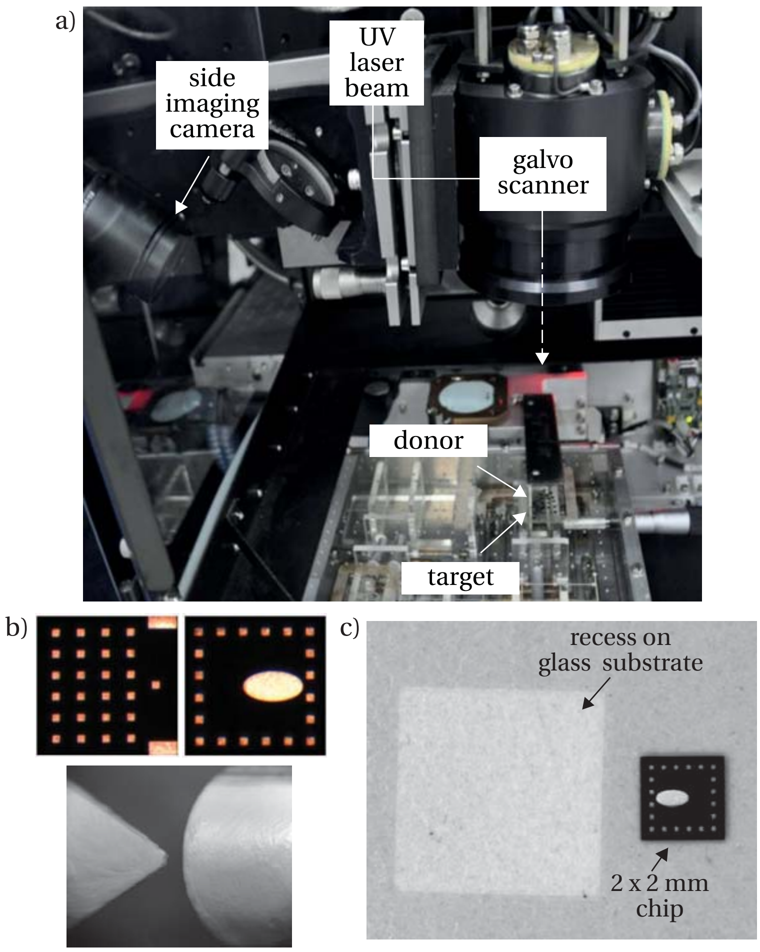

Figure 4.12: Research setup and components used in laser die transfer experiments a) Self-assembly toolbox inserted into the laser die transfer setup b) Chips with different magnetic material patterns and magnet unit with combination of tapered and rounded pole pieces were used in the experiments. c) Glass substrate with a recess

The chips were placed face-down on the freshly spun layer and the donor substrates were then dried for 4 hours at 50 °C. The final film thickness was determined by a Bruker ContourGT-K 3D microscope to be approximately 250 nm.

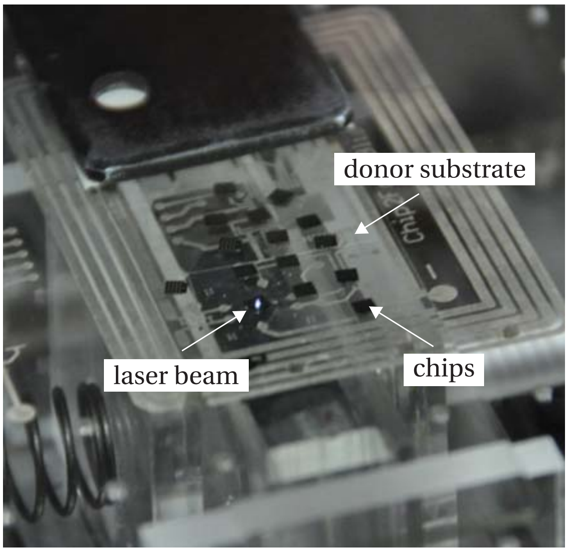

Figure 4.13: The donor substrate with the chips

An optimized release process was achieved by varying parameters such as laser energy per pulse, beam diameter and transfer height. A single pulse of laser was sufficient to release the 1 × 1 mm chips. For bigger chips (2 × 2 mm), a circular path was used instead of a single pulse. In order to detach the chip from the DRL's adhesion force, three rings with diameters of 50 µm, 1 mm, 2 mm were patterned, starting from the center of the chip. The beam size used was 120 µm and the scanning speed was adjusted to 400 mm/s.

The assembly process was recorded with a camera that was positioned at an angle with respect to the substrate plane (Mightex Systems, USA, BTE-B013-UW camera, recording speed: 28 fps). The tilt of the camera caused distortion in the images as shown in Figure 4.14. The distortion was corrected by image processing and repeatability of the process was calculated by comparing the final position of the chips after each experiment. More details on the correction of images can be found in Appendix- A.

The initial orientation of the chip at the time of the release was arbitrary, since the chips were randomly placed on the donor substrate. The initial orientation that the chips can have is divided to four ranges ($\alpha_1, \alpha_2, \alpha_3, \alpha_4$) as shown in Figure 4.15.

After self-assembly, the chips align into four different final orientations (Figure 4.16). The distribution of the final rotational alignment of the chips in Figure 4.17 shows the relationship between the initial orientation of the chips on the donor substrate and the final orientation on the target substrate. The chips released within the same angle range always aligns with the same final orientation. More fundamentally, this indicates that the multiple stable final orientations of a chip can be reduced to a single final orientation by controlling the initial release angle.

4

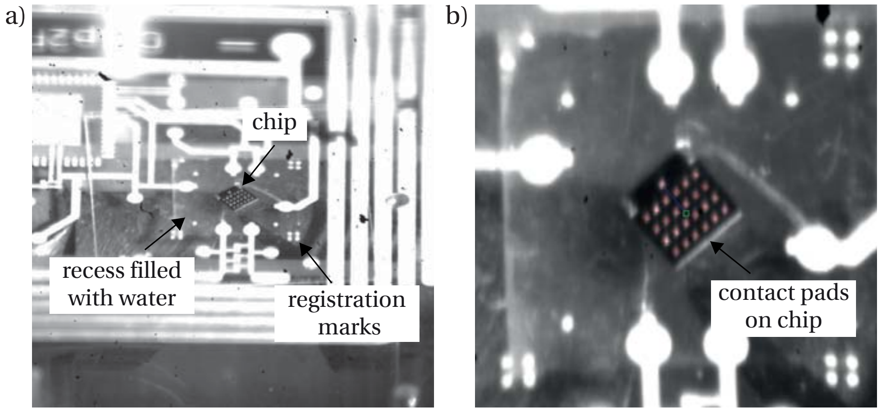

Figure 4.14: Pictures of an aligned chip a) Image acquired by a camera placed at an angle of 40° in relation to the receiver substrate's plane b) Image after correction

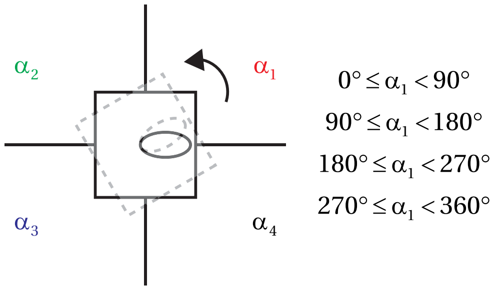

Figure 4.15: The initial orientations that the chips can have at the time of the release are represented with four angle ranges.

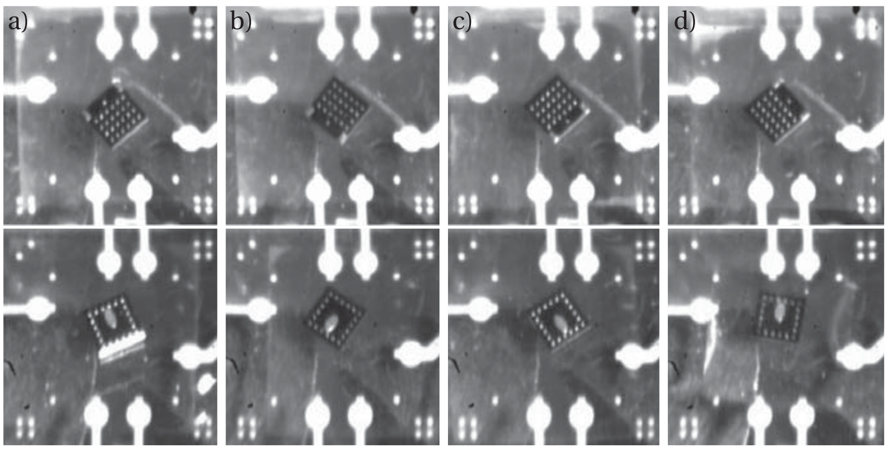

Figure 4.16: Four stable orientations that the chips take after alignment, approximately a) 45°, b) 135°, c) 225° and d) 315°.

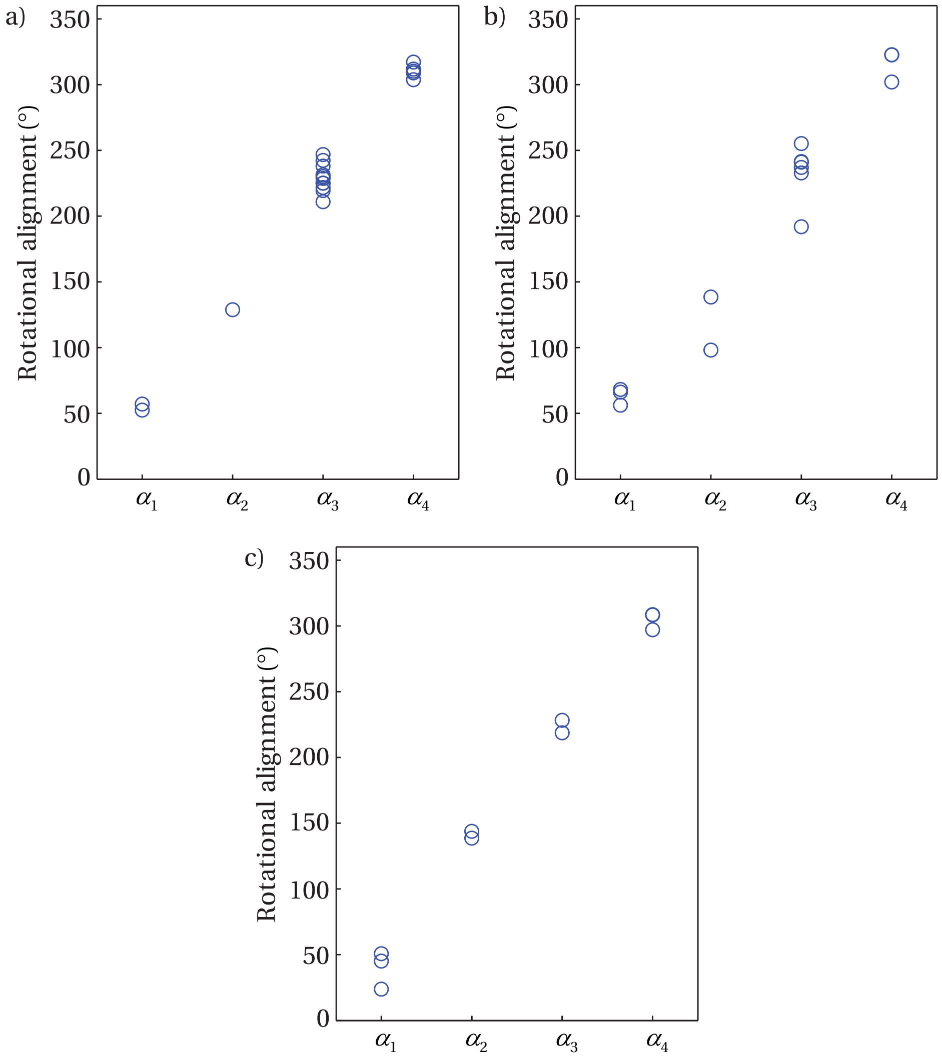

Figure 4.17: Alignment performance of magnetic self-assembly with laser die transfer. The blue circles represent the orientation (rotational alignment) of the chips on each image. a) 1 × 1 mm chips with ellipse feature b)2 × 2 mm chips with ellipse feature c) 2 × 2 mm chips with asymmetric contact pad layout

The repeatability values of the process is calculated regarding to the release angle of the chips in Table 4.3. The alignment performance of the process differs between the release angle ranges for the same type of chip, especially for the chip with asymmetric contact pads. The major cause of this difference is expected to be the small number of experiments. The alignment performance is also affected by the shape matching between the magnetic material on the chips and the magnetic field gradient. Due to the mismatch between the geometry of the magnet unit and the magnetic material patterns used on the chips, four different stable orientations were observed. Another factor that is affecting the shape of the magnetic field gradient is the out-of plane distance between the magnet unit and the target substrate. In the current setup, the minimum distance that can be reached is limited by the thickness of the cover plate of the self-assembly box (1 mm). The change in the magnetic field gradient is limited by this gap: As the distance is increased, the magnetic field gets defocused, which creates multiple stability points in the field for the chip to align. Eventually the repeatability of the translational and rotational alignment decreases.

Chip type	**Release angle range**	**Translational** σ (µm)	**Rotational** σ (°)	**Sample number**
ellipse feature (1 × 1 mm)	α_1	53.91	3.2	2
	α_2	N/A	N/A	1
	α_3	55.28	10.4	11
	α_4	38.96	4.8	5
ellipse feature (2 × 2 mm)	α_1	116.44	6.39	3
	α_2	91.66	19.73	2
	α_3	39.57	19.66	6
	α_4	51.68	11.92	3
asymmetric contact pads (2 × 2 mm)	α_1	60.57	14.20	3
	α_2	9.76	3.69	2
	α_3	48.21	6.80	2
	α_4	24.38	6.57	3

N/A means there was only one or no chips released from that angle range, therefore there is no standard deviation.

Table 4.3: Repeatability of the process with respect to release angle ranges

The exact time for release could not be determined since the process was faster than the recording speed of the camera. As a consequence, the process is expected to be in the sub millisecond regime. The cycle time for the whole process, including the release and the alignment, is approximately 0.33 s.

FAILURE MECHANISMS

The chips were attached to the donor substrate by pressing against the triazene layer with a tweezer. This method of manual placement caused difference in the adhesion force over the area of the chip. Consequently, some of the chips were not ejected properly: The triazene layer was removed from the areas on the path of the laser beam, nonetheless the adhesion of the remaining areas was strong enough to hold the chip in place.

The chip or bumps were not damaged by the laser beam during the release process. However, debris were formed on top of the chip after the triazane layer was ablated (Figure 4.18). It was observed that this debris layer can be cleaned easily after assembly, to prevent any potential problems in the interconnection process.

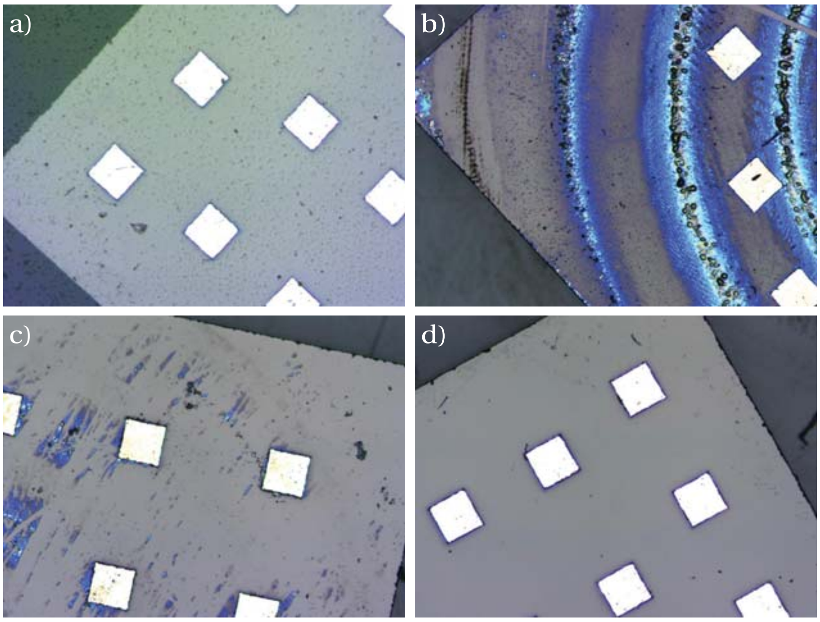

Figure 4.18: Optical investigation of chips after and before ejection a) A chip attached to the donor substrate b) Debris formed on the chip's surface after ejection c) Debris were removed easily by cleaning. d) Picture of another chip detached from the donor substrate before ejection. The surface of the chip was not contaminated by the triazene layer.

4.4. CONCLUSION

The experimental results are summarized in Table 4.4. The difference in the experimental results is due to the mismatch between the magnetic material on the chips and the applied magnetic field, rather than the method of chip presentation. The decision on using a single pole piece and matching bump layouts was made after the industrial implementation experiments.

The duration, which refers to the total time spent on the chip presentation and self-alignment was investigated only in the experiments done for understanding the chips alignment. Viscosity of the fluid is the major parameter that effects the alignment speed: when a commercial adhesive is used the alignment duration can go up to 4 s. However, this time obstacle could be removed by increasing the number of assembly positions handled at the same time, which requires a high speed chip presentation process.

Out of the two chip presentation methods, the LIFT process provides faster chip presentation (within milliseconds) and direct ejection of chips. Additionally, the chips are handled without a direct mechanical contact throughout the assembly process.

Experiment type	**Components**	**Results** (1σ)		
		Translational	Rotational	Duration
Magnetic self-assembly with pick-and-place	double pole piece NFC chip (1.5×2.0 mm) Vi7641 PET foil	120 µm	N/A	N/A
Magnetic self-assembly with laser die transfer	combination pole piece ellipse chip DI water glass substrate with recess	60 µm	15°	N/A
Experiments for understanding chip's alignment	one pole piece double rectangle chip DI water glass substrate with recess	10 µm*	0.6°*	0.2 s

Table 4.4: Comparison of experimental results. *The exact values of the alignment performance in "safe region" are $\sigma = 7.38$ µm* and $\sigma = 0.62°$* for a sample number of, $N = 28$ experiments.

REFERENCES

[1] F. X. Lihui Wang, *Smart Devices and Machines for Advanced Manufacturing* (Springer Science & Business Media, 2008).

[2] B. T. Ng, V. Ganesh, and C. Lee, *Optimization of gold wire bonding on electroless nickel immersion gold for high temperature applications,* in *Electronics Packaging Technology Conference* (2006) pp. 277–282.

[3] J. Herbsommer, T. Teutsch, and A. Strandjord, *The electrochemical effects of immersion Au on electroless nickel and its consequences on the hermetic reliability of a semiconductor device,* IEEE Transactions on Device and Materials Reliability **12**, 317 (2012).

[4] ITRS, *The next step in assembly and packaging: System level integration in the package (SiP),* http://www.itrs.net/papers.html (2007).

[5] W. S. Wong and A. Salleo, *Flexible Electronics: Materials and Applications*, Electronic Materials: Science & Technology, Vol. 11 (Springer, 2009) pp. 78–79.

[6] A. D. McNaught and A. Wilkinson, *UPAC Compendium of Chemical Terminology, 2nd ed. (the "Gold Book")* (Blackwell Scientific Publications, Oxford, 1997).

[7] http://www.chip2foil.eu/ (Last visited on 30/01/2015).

[8] E. J. Swenson and C. N. Berglund, *Lasers in microelectronics manufacturing: past, present, and future,* Proceedings of the IEEE **90**, 1611 (2002).

[9] C. M. Dunsky, *Laser material processing in microelectronics manufacturing: status and near-term opportunities,* in *Proceedings of SPIE*, Vol. 5713 (2005) pp. 200–214.

[10] R. Baseman, A. Gupta, R. Sausa, and C. Progler, *Laser induced forward transfer,* in *Symposium Laser and Particle-Beam Chemical Processing for Microelectronics*, MRS Proceedings, Vol. 101 (1987).

[11] A. Holmes and S. Saidam, *Sacrificial layer process with laser-driven release for batch assembly operations,* Journal of Microelectromechanical Systems **7**, 416 (1998).

[12] N. Karlitskaya, J. Meijer, D. De Lange, and H. Kettelarij, *Laser propulsion of microelectronic components: releasing mechanism investigation,* in *Proceedings of SPIE*, Vol. 6261 (2006).

[13] A. Pique, N. Charipar, R. Auyeung, H. Kim, and S. Mathews, *Assembly and integration of thin bare die using laser direct-write,* in *Proceedings of SPIE*, Vol. 6458 (2007).

[14] R. Miller, V. Marinov, O. Swenson, Z. Chen, and M. Semler, *Noncontact selective laser-assisted placement of thinned semiconductor dice,* IEEE Transactions on Components, Packaging and Manufacturing Technology **2**, 971 (2012).

[15] V. R. Marinov, O. Swenson, Y. Atanasov, and N. Schneck, *Laser-assisted ultrathin die packaging: Insights from a process study,* Microelectronic Engineering **101**, 23 (2013).

5

TOWARDS R2R FABRICATION

Imagination is more important than knowledge.

Albert Einstein

One of the major goals in the industrial implementation of the self-assembly process is to fulfill the high-volume manufacturing demand for large-area electronics. To achieve a complete extension of the magnetic self-assembly into R2R manufacturing, all the relevant processes such as the chip presentation, the deposition of the viscous layer and the bonding of the chip should be adapted to the continuous manufacturing.

This chapter mainly focuses on the feasibility of implementing magnetic self-assembly into R2R manufacturing. Additionally the compatibility of the method with the newest packaging trends is discussed in the beginning of the chapter. Afterwards, the flexible electronics manufacturing steps related to the chip integration are addressed individually. In an effort to integrate the magnetic self-assembly process into high volume and continuous manufacturing, the industrial equivalents of the research level techniques used in the experiments are suggested.

5.1. COMPATIBILITY WITH THE NEW PACKAGING TRENDS

Having magnetizable material on a chip is obligatory for manipulation of the chip with magnetic self-assembly. The nickel content present on the contact pads of the chip are suitable for this purpose. Nickel is a standard material used for increasing electrical performance and reliability of the contact pads [1, 2]. However with the new type of packaging technologies entering the market, usage of materials that have low magnetic permeabilities such as copper is also becoming popular for the contact pads. For example, the finer pitch flip chips (FPFC) have an increased number of functionalities and relatively a higher I/O density compared to the standard flip chips with solder bumps and the chips with the perimetric contact pad layouts. Copper pillar bump technology allows fabrication of well-defined bumps with a small contact area (50–80 μm compared to the 150 μm pitch in traditional solder bumps [3]), and has many advantages over the standard solder bumping [4]. In addition, especially for 3D stacking of bare dies, it is possible to use bumpless interconnections [5]. For the chips that do not have nickel contact pads adding a small feature of nickel might be enough to move chip in an acceptable speed . The addition of the nickel features to the chip can be performed on wafer-level, together with the micro-fabrication of other metalization layers. Although addition of a new nickel pattern would require a new set of lithography and deposition steps and eventually increase the fabrication costs, it is essential for benefiting from the advantages of the magnetic self-assembly.

One of the difficulties in UTC integration is the warping of the chip due to the stresses that arise from the wafer thinning and the mismatch of metallic layers (Figure 5.1). The bending causes problems in electrical performance of the chip, such as piezoresistive offset [6]. These factors should be considered in the floor planning step, such that the addition of a dominant magnetic feature or the layout of the bumps may contribute to decreasing the warpage of the chip.

5.2. ADAPTATION INTO ROLL-TO-ROLL MANUFACTURING

In this section we propose different designs and logistic concepts for implementing self-assembly to an R2R manufacturing scheme. Figure 5.2 shows an illustration of a manufacturing line built for the industrial processes suggested in the following sections.

The effect of the dynamics of a moving web such as stretching between the rolls has not been investigated for the processes discussed in the following sections. Additionally, it is not possible to match the cycle times of all the processes. Therefore the speed of the

The commercial NFC chips used in the Chip2Foil demonstrator packages had a 6 μm layer of Ni.
Alignment of a 1×1 mm chip with a $100 \times 50 \times 5$ μm ellipse feature is achieved within 0.5 s.

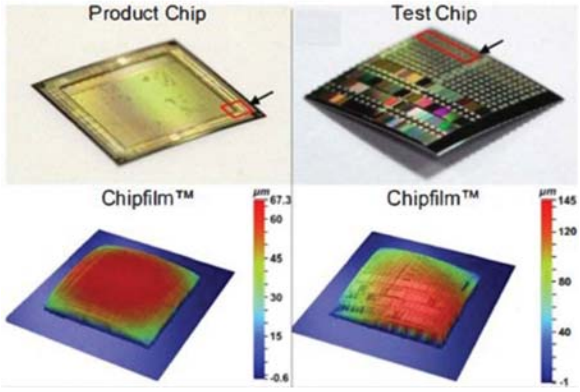

Figure 5.1: Warpage in UTCs due to the mismatches in the layout of CMOS layer. Reprinted from [6].

web might be altered or the web might be fully stopped at different manufacturing steps.

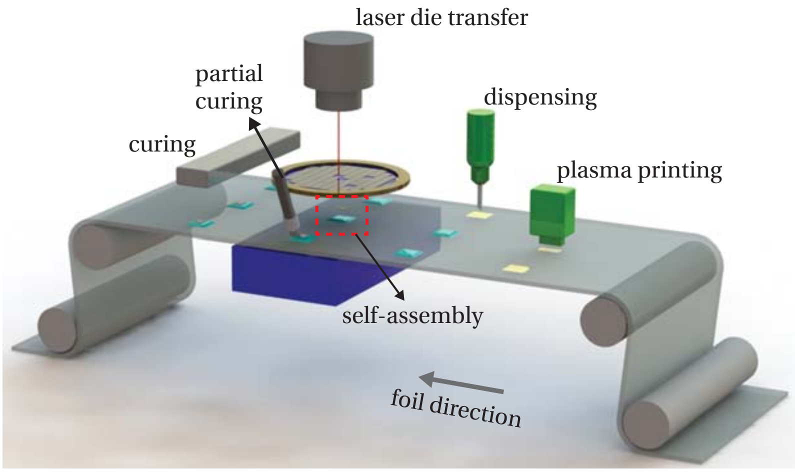

Figure 5.2: R2R implementation of self-assembly: Illustration of the R2R manufacturing line with industrial equivalents of the experimental processes studied in this thesis.

5.2.1. CHIP PRESENTATION

The industrial process of releasing chips from a wafer mounted on a blue tape involves the following steps: At first, the wafers are optically or electrically inspected to identify damaged chips. Subsequently, a digital map of the wafer showing the chips in good condition, i.e. “known good dies” is created. Afterwards, the good chips are pushed out from the blue tape individually, with a separate ejection tool. Finally, the ejected chips are picked up by a pick-and-place tool to be directly assembled onto a substrate or to be collected in a station, e.g. a waffle box.

The choice of exploiting self-assembly as a serial or a parallel process is dependent on the separation between the assembly positions (Figure 5.3a) and the method of chip presentation. Stochastic presentation by agitation is advantageous for flexible substrates with densely populated components. Usually, in the batch presentation approach, the good chips are collected at an initial station by conventional release processes and distributed by agitation or vibration systems afterwards.

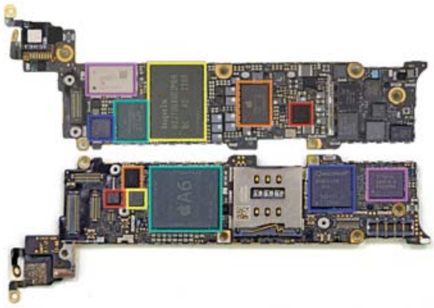

(a) The circuit board inside an apple iphone5 [7].

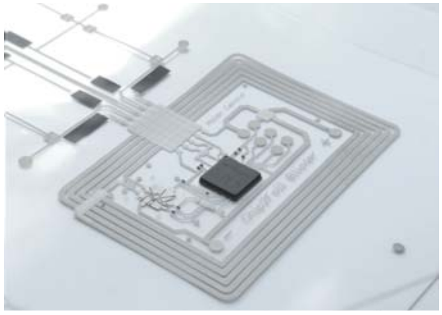

(b) C2F smart blister package with two chips and passive components

Figure 5.3: Densely and sparsely populated substrates

For large area electronics that have a low density of components (Figure 5.3b), a fast and serial chip presentation method such as laser die-transfer is more beneficial compared to the stochastic presentation method. In contrast to the pick-and-place method, the laser die transfer process provides simultaneous ejection and presentation of chips as demonstrated in Section 4.3.2. By elimination of a separate ejection tool, the LIFT process is expected to reduce the machine costs. Besides, the optical path of the laser beam used in the LIFT process can easily be changed within milliseconds, which enables high speed chip presentation and creates a possibility for batch handling of the chips in the self-assembly process.

The proposed magnetic self-assembly method can also align chips that have symmetrically distributed contact pads with a unique orientation, without the addition of other magnetic features: The chips used in the experiments discussed in Section 3.4.2 aligned with the same orientation as long as the rotation of the chip at the release orientation was limited to 0 – 180° (Figure 3.19). This requirement is easily satisfied for the industrial case, since all the diced chips on a blue tape have the same orientation.

5.2.2. FOIL ALIGNMENT

Substrate misalignment with respect to the magnet units is a major failure mechanism that affects the accuracy of the current process. In the experiments where Chip2Foil demonstrators were fabricated, the repeatability of the process was calculated by measuring the final position of the chips with respect to the fiducial markers on the foil. The foils were aligned to the self-assembly toolbox manually in these experiments, which is

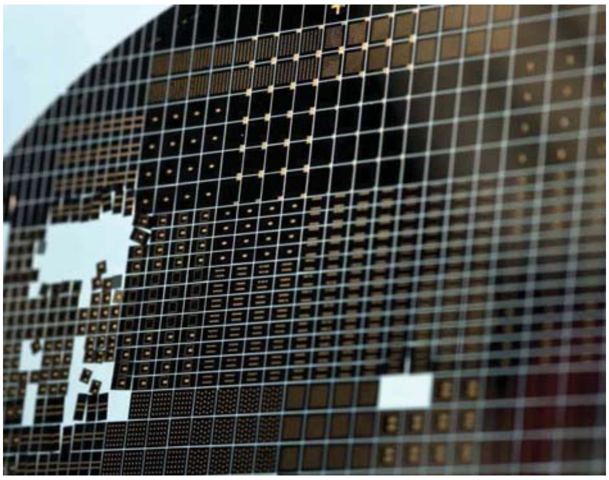

Figure 5.4: Chips on the blue tape have same orientation.

one of the reasons behind the large amount of deviation in the alignment repeatability (X: ±235μm(1σ), Y: ±135μm(1σ) for the first assembly position and X: ±90μm(1σ), Y: ±80μm(1σ) for the second assembly position). Another cause of the foil placement errors was the dislocation of the fiducial markers due to the deformation of the foils and the toolbox surface. It is expected that the foil alignment in a mass manufacturing environment would be more accurate with the use of automation on the visualization of the registration marks both on the foil and the self-assembly tool. For example, the laser micro-gages used in the printing industry allows detecting web alignment errors down to ±3μm [8].

The effect of the foil alignment to the final accuracy of the magnetic self-assembly process can also be eliminated by addition of magnetic features to the foil substrate. These features, so-called flux guides, create local gradients in the applied magnetic field, which are correctly positioned with respect to the circuitry on the foil. Preliminary experiments were performed in an earlier study to demonstrate the usage of flux guides to assist magnetic self-assembly [9] (Figure 5.5). In this method, the saturated edges of the magnet unit should be positioned further away to assure that the maximum flux density in the assembly area is only created at the tips of the flux guides: When the magnet unit is placed underneath the flux guides, the magnetic field created by the sharp ends of the pole piece dominate over the local gradients created by the flux guides. In this case, the chips prefer to align to the pole pieces rather than the flux guides.

Similar to the addition of the magnetic features to the chip, the flux guides might be added to the foil during the printing of the web circuitry. LIFT of metal layers is another method for patterning the flux guides; LIFT will provide a pure magnetic layer with a higher permeability compared to the commercial magnetic inks used in printing.

Repositioning of the magnetic field with respect to the foil can be another solution to the substrate misalignment problem. In this case, first the position of the foil should be found by detection of registration marks on the foil. Then the magnetic field should

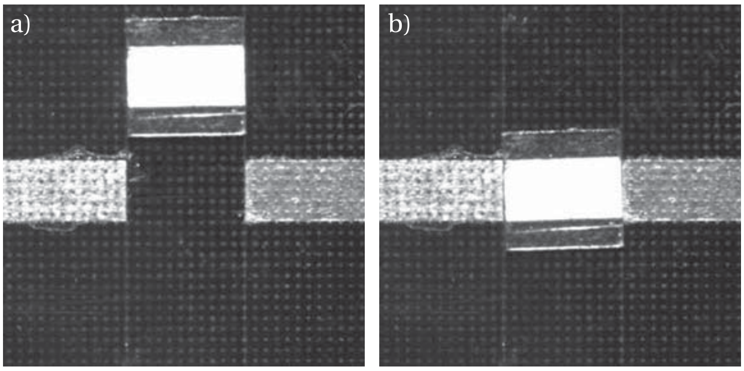

Figure 5.5: Magnetic self-assembly assisted with flux guides on foil. Reprinted from [9]. a) The flux guides on foil and a PET part with a rectangular nickel pattern b) The PET part aligned with the flux guides

be relocated either by moving the magnet unit to the correct position mechanically, or by using a set of electromagnets that can actively control the magnetic field.

5.2.3. DISPENSING AND CONTAINING THE ADHESIVE

The positional accuracy demand for dispensing the adhesive is quite low, but the surface of the binding site should be covered completely to have a flat and homogeneous layer. In the industrial implementation experiments, it was observed that the coverage of the entire binding area by the dispensed adhesive takes up to several seconds which is longer than the total of the presentation and the alignment durations for the chip. The wettability of the binding sites with die attach adhesive should be high enough for fast and homogeneous spreading. Stamping or screen-printing could be alternatives to the jet dispensing, however both of these methods require adhesives with high viscosities. For adhesives with low viscosity, inkjet printing is suggested. As mentioned before, majority of the items in the failure spectrum of prototypes were related to the adhesive compatibility and plasma treatment. The poor adhesion between the gel-film masks and the foil substrates used in the experiments, caused leakage of plasma to the inside of the masks. Therefore, the plasma treated areas were merged into the web circuitry and the square shape of the adhesive was lost. Eventually, the difference in the die-attach layer thickness caused defects on the adaptive circuitry process.

As an alternative to the treatment of the foil by using masks, plasma printing is a direct patterning method that allows local modification of surfaces at atmospheric pressure [10, 11]. A conventional plasma printing station [12], can create patterns with a minimal size of $200\mu m \pm 20\mu m$, by scanning the area to be treated with a plasma printing head at a speed of 60mm/s. This method does not require a mask or usage of inert gases and it is compatible with R2R manufacturing.

5.2.4. CURING

For polymer substrates used in the flexible electronics industry such as PET and PEN, the glass transition temperature is an important parameter for choosing the curing method. Thermally curable adhesives, often require higher temperatures compared to the glass transition of these polymers (85 °C for PET foil) and longer curing times. UV curing is preferred over thermal curing, since the UV light only affects the adhesive and does not heat the polymer foil substrate.

In the Chip2Foil demonstrator preparation, an intermittent curing step was demonstrated. After the self-assembly, the bonding of the chip was performed with a two-step curing process. In the first step, the die-attach adhesive was exposed to the UV light for short time (1 s), while keeping the foil on top of the self-assembly tool. This was sufficient to fix the chip at its position, and since the magnetic field was still active the alignment of the chip was preserved. After the pre-curing step the foil was ready to transferred to another location to continue the curing. The aim of a two step curing process was to increase the throughput of the system: Instead of waiting for the adhesive to be fully cured, self-assembly could continue with the new chips fed to the system.

REFERENCES

[1] B. T. Ng, V. Ganesh, and C. Lee, *Optimization of gold wire bonding on electroless nickel immersion gold for high temperature applications,* in *Electronics Packaging Technology Conference* (2006) pp. 277–282.

[2] J. Herbsommer, T. Teutsch, and A. Strandjord, *The electrochemical effects of immersion Au on electroless nickel and its consequences on the hermetic reliability of a semiconductor device,* IEEE Transactions on Device and Materials Reliability **12**, 317 (2012).

[3] D. S. Patterson, *Transforming mobile electronics with copper pillar interconnect,* Advancing Microelectronics **39**, 18 (2012).

[4] B. Appelt, H. Chung, C. Chen, and R. Wang, *Fine pitch flip chip chip scale packaging,* in *European Microelectronics and Packaging Conference (EMPC)* (2011) pp. 1–4.

[5] C. Lin, S. Chiang, and T. Yang, *3D stacked high density packages with bumpless interconnect technology,* in *IEEE Nuclear Science Symposium Conference Record*, Vol. 1 (2003) pp. 73–77.

[6] M.-U. Hassan, E. Angelopoulos, H. Rempp, S. Endler, and J. Burghartz, *Packaging challenges associated with warpage of ultra-thin chips,* in *Electronic System-Integration Technology Conference (ESTC)* (2010) pp. 1–5.

[7] *iPhone 5 teardown,* https://www.ifixit.com/Teardown/iPhone+5+Teardown/10525 (Last visited on 30/01/2015).

[8] *Roll & web alignment with a laser microgage,* http://pinpointlaser.com/resources/technical-papers/roll-web-alignment-with-a-laser-microgage/ (Last visited on 20/11/2014).

[9] T. Poiesz, *Magnetic Alignment of Ultra-thin Chips*, Master's thesis, Delft University of Technology (2010).

[10] C. Penache, C. Gessner, T. Betker, V. Bartels, A. Hollaender, and C. P. Klages, *Plasma printing: patterned surface functionalisation and coating at atmospheric pressure,* Nanobiotechnology, IEEE Proceedings **151**, 139 (2004).

[11] A. Mobius, D. Elbick, E.-R. Weidlich, K. Feldmann, F. Schussler, J. Borris, M. Thomas, A. Zonker, and C.-P. Klages, *Plasma-printing and galvanic metallization hand in hand: A new technology for the cost-efficient manufacture of flexible printed circuits,* Electrochimica Acta **54**, 2473 (2009).

[12] Innophysics, *μ - plasmaprint station,* http://www.innophysics.nl/index.php/products (Last visited on 31/1/2015).

5

6

CONCLUSION

I do not think there is any thrill that can go through the human heart like that felt by the inventor as he sees some creation of the brain unfolding to success... Such emotions make a man forget food, sleep, friends, love, everything.

Nikola Tesla

The scientific man does not aim at an immediate result. He does not expect that his advanced ideas will be readily taken up. His work is like that of the planter - for the future. His duty is to lay the foundation for those who are to come, and point the way. He lives and labors and hopes.

Nikola Tesla

The future of electronics industry holds great challenges towards development of new devices and materials. Nevertheless, carrying the manufacturing to a high volume level is crucial to bring these new inventions into the consumer markets. There is a big demand for improvement on micro-assembly and packaging, especially on forthcoming topics such as ultra-thin chips, bare die assembly and 3D integration. Self-assembly tries to address the challenges in the handling and high precision placement of these new types of chips, with a considerable potential of providing an increase in manufacturing throughput.

6.1. CONTRIBUTION TO THE FIELD

For flexible electronics, self-assembly suggests a bottom-up fabrication scheme which is expected to improve the throughput while lowering the manufacturing costs [1]. Although the ultimate goal of self-assembly is to enable high-volume manufacturing of small-scale components, most of the literature only focuses on the development of the self-assembly approach and overlooks the compatibility of the suggested method with a real manufacturing process. There are a few research groups that have offered machine designs for implementing self-assembly into R2R fabrication [2–4]. In these machines, the components are mobilized by agitation or mechanical vibration and brought to a relatively small area. These self-assembly methods address the flexible electronics applications with densely populated components, such as flexible displays.

The magnetic self-assembly method demonstrated in this thesis, carries out a hybrid placement strategy for sparsely populated substrates, which complements to the manufacturing of flexible electronics applications with a small amount of components such as disposable products. Since batch presentation in such cases is not feasible, an intermittent manufacturing scheme was followed to realize the industrial implementation of magnetic self-assembly with two different chip presentation methods: pick-and-place and LIFT. In the LIFT process the chips are released from the donor substrates within a few milliseconds, which is expected to be more compatible with R2R manufacturing.

We also demonstrate the integration of magnetic self-assembly into the complete manufacturing flow of a flexible electronics prototype: the smart blister (Section 4.3.1). This case study enabled looking into the entire perspective of the challenges that can be faced in the industrial implementation of self-assembly.

Major advantages of the method are handling of the ultra-thin chips without a direct physical contact and the distribution of the precision budget with a low accuracy demand on chip presentation. Moreover, the chips are remotely released from a height above the substrate which prevents overflow of adhesive to the top of the chip and protects the chip release tool from contamination. Finally, the chips are aligned with high precision and a specific orientation. The experiments with a 1×1 mm chip show that the repeatability of the process, i.e., the variation in the final alignment positions of the chips with respect to the magnet unit, goes down to $3\sigma = 25$ µm and $3\sigma = 2°$.

Having magnetic material on the chip is necessary for controlling the chip. However, the nickel content already present on the contact pads of the chip is enough for magnetic manipulation. Based on the layout of the bumps, it is possible to reach a unique rotational alignment. If the layout is not asymmetric, the first solution suggested is adding a magnetic feature to the chip that will create a dominance over the total contribution of the all contact pads on the chip in terms of applied magnetic force and torque. The same solution holds for chips without magnetic material.

The second solution for chips that have nickel content and that has a layout of contact pads without a significant asymmetry is adjusting the process parameters such as release position and angle. The details of the conditions for reaching a unique rotational alignment was discussed in Section 3.5.

6.2. FUTURE WORK

Further work should be done to realize a machine that will combine high speed chip presentation with LIFT and magnetic self-assembly for continuous manufacturing schemes. In addition, the direct release of chips from the wafers mounted on blue tape carriers should be studied. This will provide a higher throughput, compared to the conventional methods where the chips are ejected from the blue tape in a different location and transferred to the assembly position afterwards by a pick-and-place tool.

Additional to the development of a high speed chip presentation method, the dynamics of the chip's fall should be investigated more carefully. As discussed in Chapter 5, the falling velocity of the chip and the release-cone can be adjusted by controlling the impact force applied to the chip at the moment of release. This might enable increasing the release height, and consequently completing alignment of the chip during its fall through the air. As a result, the area of the viscous layer can be decreased, which will also decrease material costs in the cases where a die-attach adhesive is used. Another advantage will be the decrease in the cycle time of alignment per chip, since the drag force applied against the movement of the chip will be smaller in the air than the drag force applied in the viscous layer. A robust chip presentation process will also minimize or more preferably eliminate the air entrapment underneath the chip, which is one of the major failure mechanisms discussed in Section 4.3.

Alignment precision could further improved by optimizing the shape of the pole pieces and magnetic features on the chip. Topology optimization was not studied in the course of this thesis, however it should be considered as a powerful numerical method for creating new designs. Optimization of the pole piece shape is more practical compared to the contact pads on the chip, since it may not be feasible to change the design of a commercial chip.

As an alternative to the static magnetic field created by the permanent magnets, active control of the magnetic field with electromagnets could be considered. This will enable active repositioning of the magnetic field gradient with respect to the web circuitry.

Further improvements should also be made on the viscous layer addition to the substrate. The open issues discussed on Section 5.2.3 such as compatibility of adhesives, wettability of the substrate surface should be addressed comprehensively.

Possibilities to exploit magnetic self-assembly for handling different type of microelectronic components should be investigated further. For example, magnetic self-assembly could be used for 3D integration of UTCs. Since the magnetic forces have a long working range, it might be possible to align multiple chips at the same location. The metalization in through silicon vias on the chip (TSV) could be used as alignment features. The magnetic interactions between the vias in each chip will contribute to the force applied by the external magnetic field. Self-assembly could also be used for assembly of passive components, such as the 01005 sized capacitors which commonly have nickel content.

REFERENCES

[1] L. Cademartiri, K. J. M. Bishop, P. W. Snyder, and G. A. Ozin, *Using shape for self-assembly,* Philosophical Transactions of the Royal Society A: Mathematical,Physical and Engineering Sciences **370**, 2824 (2012).

[2] S. Shet, V. Mehta, A. Fiory, N. Ravindra, and M. Lepselter, *The magnetic field-assisted assembly of nanoscale semiconductor devices: A new technique,* JOM **56**, 32 (2004).

[3] R. Rivero, S. Shet, M. Booty, A. Fiory, and N. Ravindra, *Modeling of magnetic-field-assisted assembly of semiconductor devices,* Journal of Electronic Materials **37**, 374 (2008).

[4] S. C. Park, J. Fang, S. Biswas, M. Mozafari, T. Stauden, and H. O. Jacobs, *A first implementation of an automated reel-to-reel fluidic self-assembly machine,* Advanced Materials (2014), 10.1002/adma.201401573.

A

ACCURACY MEASUREMENT ALGORITHM

A.1. FINDING CHIP'S POSITION IN AN IMAGE

The camera recording the alignment process was fixed throughout the experiments. Therefore, the coordinate system of the camera was used to calculate the position of the chip relative to the center of the camera's frame.

To calculate an accurate estimate of the repeatibilty of the alignment process, the measurement errors coming from the image processing should be minimized. Therefore, for each experiment, the chip's final position is calculated by averaging the data gathered from a set of 20 images. Additionally in each image the contact pads on the chips were used as registration marks.

The process flow of calculating the repeatibilty and post-processing of images is shown in Figure A.1. The calculation of the chip's final position after an experiment is performed in two steps: First, the center of the chip in each image is calculated by averaging the location of the contact pads. Then, the chip centers found in all of the 20 images are averaged to find the correct final position of the chip. In addition, the dominant features on the chip were used to determine the rotation of the chip. The same process described above is followed the location of the dominant features in all images. Then the rotation of the chip is found by finding the angle of an imaginary line is drawn between the calculated center of the chip and the center of the dominant feature. Finally, the repeatibilty of the alignment process is determined by calculating the standard deviation of the chips' final positions and rotations for all of the experiments.

The post-processing involved the following steps: First, the frames where the chip's motion has ended is determined manually by observing the videos. Then, 20 frames next to determined end frame is extracted from the videos as single images. Afterwards, these images are cropped to remove the excess parts and to decrease size of the data to be handled in further steps. In the next step, the pictures were scaled up and a Gaussian filter was used to blur the image which enhanced the gray value difference between the

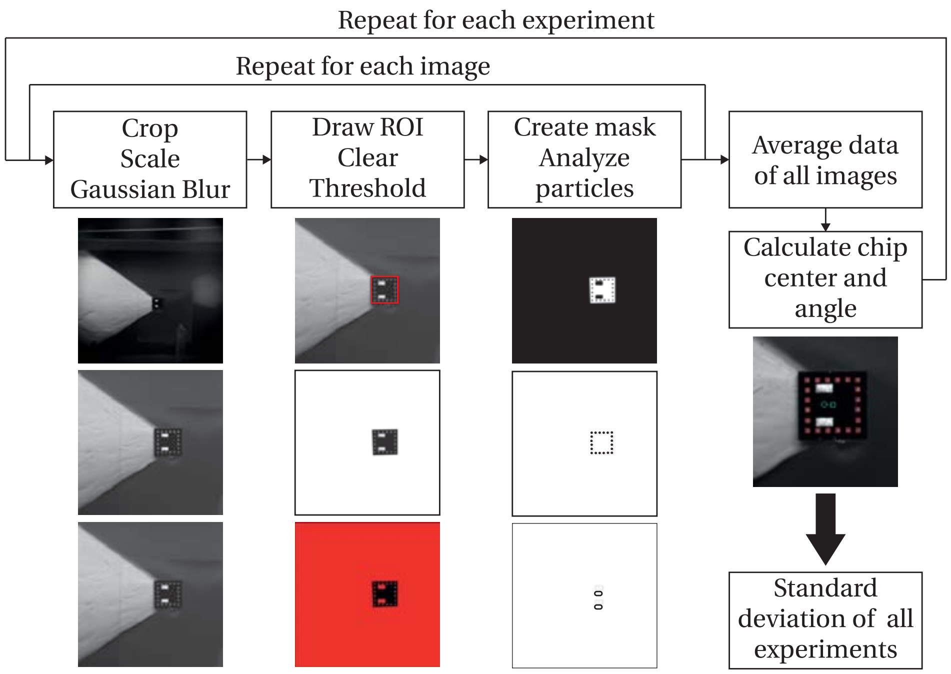

Figure A.1: Steps of image post-processing and repeatibilty calculation pixels. This allowed making a more accurate estimate of the positions of the contact pads in the image.

Finally, a binary mask is created by thresholding the image which is used as a guide to find the contact pads. The mask selects the bright pixels in the image to form separate region of interests (ROI) showing the contact pads. By analyzing the original image with the binary mask, information such as the location or size of the contact pads were found.

The repeatability of the process is calculated by comparing the final position of the chips after each experiment. The camera was fixed throughout the experiments, therefore the coordinate system of the camera was used.

A.2. DISTORTION CORRECTION IN PICTURES

The experiments mentioned in Section 4.3.2 were recorded by a camera positioned at an angle with respect to the substrate plane (Mightex Systems, USA, BTE-B013-UW camera, recording speed: 28 fps). Due to the camera projection, the frames taken from the video were distorted which was corrected by re-stretching the frames according to an undistorted reference image.

The distortion correction was performed before finding the chip's position in the images and involved the following steps (Figure A.2): First, the registration marks on the reference image were defined as fixed control points. Then, the misplaced and stretched registration marks on the distorted images were found with the same post-processing procedure that was used for an undistorted image (See Section A.1). Afterwards, the distances between the registration marks on the reference image was calculated to form a transformation matrix. In the final step, by using the transformation matrix, the pixels in the distorted image are relocated to match the reference image.

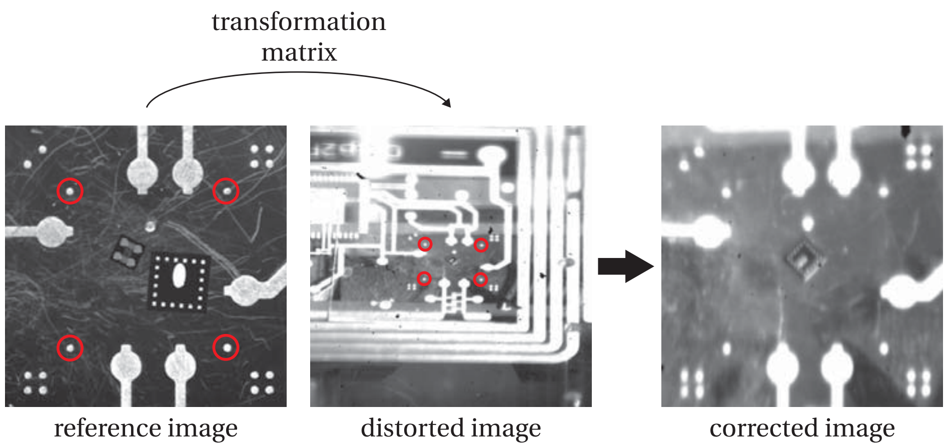

Figure A.2: Steps of correcting the distortion in the images

B

Magnetometer Measurements of Electroless Nickel

The magnetization of the chips was measured with a SQUID magnetometer (Quantum Design Inc., MPMS XL Magnetic Property Measurement System). Chips with and without contact pads were used in the measurements, to analyze the individual magnetization of the EN layer. Figure B.1 shows the in-plane and out-of plane magnetization curves derived from the measurements. The magnetization curve of the EN layer was obtained by subtracting the data of chips without the contact pads from the data of chips with contact pads.

The aim of the measurements was to show that the in-plane magnetization curve gets saturated faster compared to the out-of plane axis: With the same amount of applied field, the in-plane axis would get a bigger magnetization, and thus would be the magnetization easy-axis. However, the plots contained a lot of noise, since the chip was misplaced within the sample holder during the measurements.

In the next measurements, the chips were fixed to the sample holder with a teflon tape. Figure B.2 shows the in-plane magnetization of the samples. In this measurement the saturation and the small hysteresis confirmed the ferromagnetic behavior of the electroless nickel layer.

B

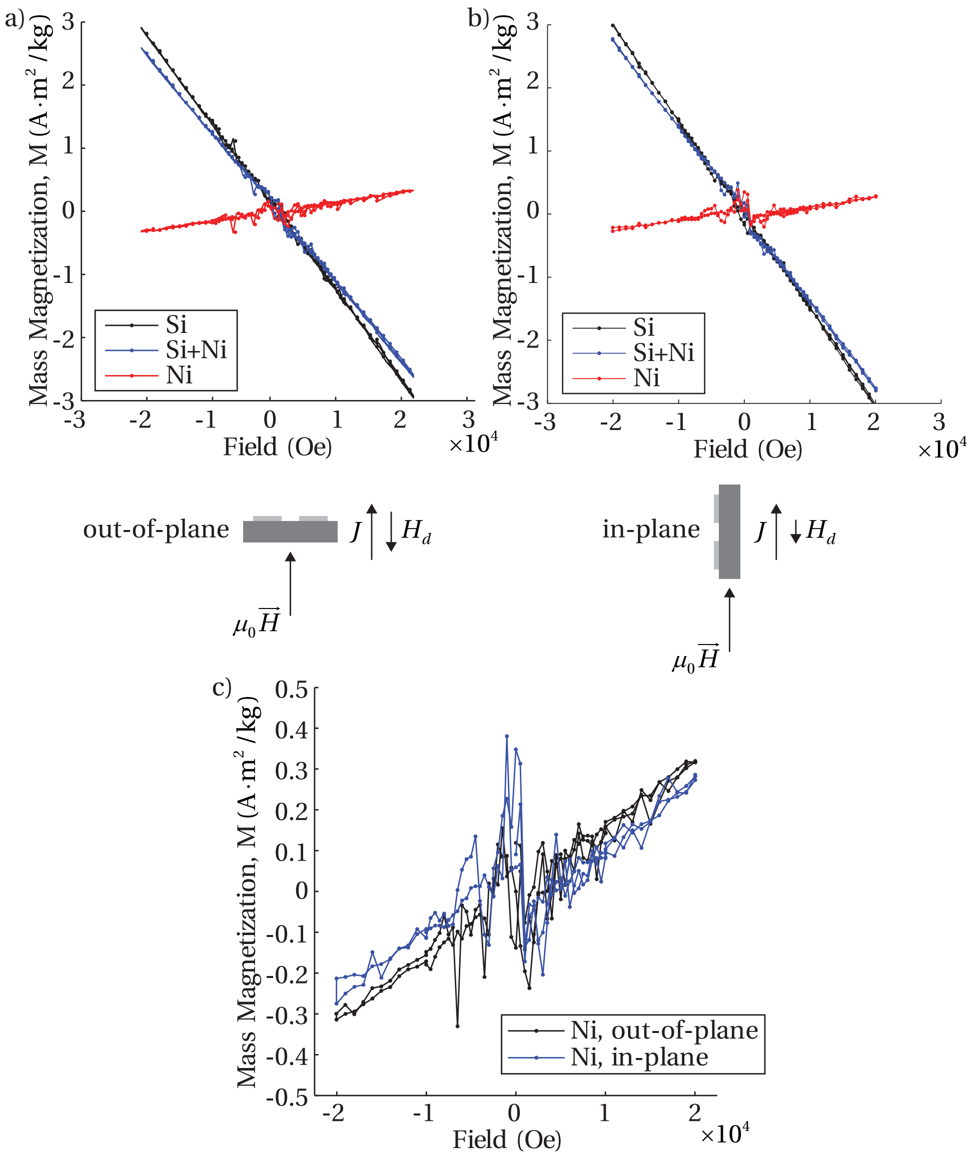

Figure B.1: Magnetization curves of chips with and without contact pads. The subtractions of the two curves gives the magnetization of electroless nickel layer individually. a) Out-of-plane magnetization b) In-plane magnetization c) Comparison of in and out-of-plane magnetization of electroless nickel

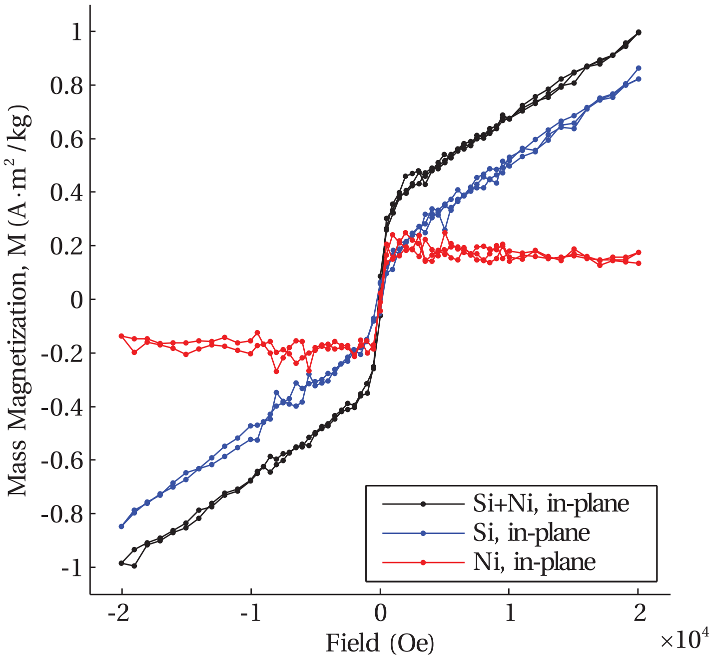

Figure B.2: In-plane magnetization curves of chips with and without contact pads, 2nd measurement.

C
EXPERIMENTAL DATA

The following results were achieved in the experiments where the chips were released in the safe region. 1×1 mm chips with two rectangle features were used in this experiments. The rectangles were positioned 0.375 mm away from the center of the chip, with a 0.5 mm separation. Each rectangle has a size of 125×250 µm (Figure C.1).

The magnet was consisting of N42 grade magnets and a sharp pole piece. Finally, the substrate (thickness 0.1 mm) was positioned adjacent to the magnet unit.

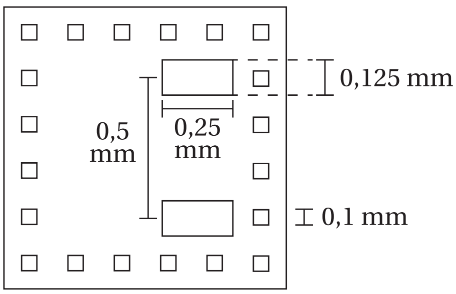

Figure C.1: Design of chip with two rectangle features

The exact position and angle of the chips at the time of the release can not be calculated, because the features on the chips, which are used as registration marks, are blocked by the release tool. Therefore, the initial positions and rotations given in the following table are calculated from the first frame where all the features are visible.

The accuracy of alignment for each experiment refers to the difference of the chip's final position on that particular experiment from the mean value of all the final positions. For example, for the nth experiment in the dataset, the accuracy in x direction equals to,

$$Acc_{X_n} = X_{f_n} - \frac{\sum_{i=1}^{N} X_{f_i}}{N}$$

where N is the total number of experiments.
The following parameters are used in Table C.1 to represent the data;

n	Experiment number
x_0	Initial position of the chip in x direction
y_0	Initial position of the chip in y direction
θ_0	Initial rotation of the chip
x_f	Final position of the chip in x direction
y_f	Final position of the chip in y direction
θ_f	Final rotation of the chip
Acc_x	Accuracy of the translational alignment in x direction
Acc_y	Accuracy of the translational alignment in y direction
Acc_{xy}	Accuracy of the translational alignment, x and y components combined
Acc_θ	Accuracy of the rotational alignment
Δt	Alignment duration

	n	x_0(pixel)	y_0(pixel)	θ_0(°)	x_f(pixel)	y_f(pixel)	θ_f(°)	Acc_x(µm)	Acc_y(µm)	Acc_{xy}(µm)	Acc_θ(°)	Δt(s)
$x=2, y=-2$	1	1711.00	1720.00	54.49	1236.09	991.44	1.80	0.17	−2.91	−2.19	−0.75	0.24
	2	1739.79	1704.09	52.38	1235.22	992.74	2.80	10.00	−14.37	−4.93	−0.22	0.26
	3	1712.80	1687.62	144.51	1237.00	993.47	1.76	−3.00	−7.02	−7.13	1.04	0.20
	4	1750.00	1670.00	50.75	1235.41	984.82	1.58	0	7.17	5.49	−0.05	0.20
	5	1718.11	1583.17	79.36	1236.73	988.3	1.67	−3.88	3.12	0.04	0.74	0.25
	6	1717.50	1654.37	252.14	1238.81	996.56	2.15	−3.54	2.14	−0.52	−0.09	0.19
	7	1712.91	1692.46	53.37	1238.5	995.64	1.67	−4.62	4.47	0.64	−0.5	0.21
	8	1755.82	1728.23	25.20	1237.66	989.67	0.07	5.00	7.39	8.60	−0.18	0.17
	9	1764.69	1591.03	112.30	1240.17	985.12	1.22	−3.14	1.51	−1.51	0.17	0.15
	10	1221.76	1460.09	291.20	736.04	934.99	5.1	−5.41	4.92	−1.15	1.17	0.22
	11	1188.22	1432.63	274.49	734.17	930.05	4.36	−0.76	6.84	3.68	0.12	0.13
	12	1187.57	1493.86	105.46	735.52	926.99	4.74	−4.92	−15.82	−13.73	−0.05	0.19
	13	1166.45	1477.23	93.81	735.69	924.81	4.53	−1.46	−6.72	−5.35	0.03	0.18
	14	1121.75	1494.87	261.47	735.38	929.11	4.96	3.99	14.91	12.44	0.51	0.16
	15	1190.43	1493.84	32.85	735.73	928.70	4.81	3.17	12.51	10.29	0.04	0.15
	16	1137.91	1418.10	161.82	754.98	928.59	3.9	0.97	−3.12	−1.20	−1.57	0.16
	17	1079.67	1505.75	124.33	751.20	925.49	3.69	7.54	−15.03	−3.48	−0.42	0.14
	18	1086.39	1538.71	121.98	750.26	926.35	3.31	1.62	15.41	13.09	0.35	0.18
	19	1206.89	1390.03	121.14	747.61	929.55	4.25	−3.28	2.47	−0.11	−0.39	0.18
	20	1179.88	1417.25	119.34	750.76	924.73	3.61	0.26	−5.56	−4.20	−0.01	0.12
$x=2, y=2$	21	1094.41	394.24	105.64	736.93	931.20	4.72	0.70	−11.25	−8.38	−0.22	0.18
	22	1130.47	416.09	93.61	740.75	926.83	5.25	−0.10	0.01	−0.06	0.21	0.26
	23	1079.46	496.06	261.47	735.87	929.63	6.51	0.81	−1.07	−0.34	0.06	0.13
	24	1115.21	465.05	264.94	736.79	935.05	5.43	10.52	4.32	9.98	0.15	0.13
	25	1091.39	367.09	108.30	735.39	933.51	6.21	0.61	−3.81	−2.58	−0.06	0.18
	26	1058.32	418.98	18.30	735.52	933.13	5.38	−1.83	−1.55	−2.36	−0.44	0.19
	27	1018.84	503.09	302.36	735.11	934.02	4.97	−8.78	6.83	−0.20	0.5	0.14
	28	1063.37	404.38	300.73	738.60	935.14	5.30	−0.53	−5.80	−4.84	−0.14	0.16

Table C.1: Experimental data for safe region

SUMMARY

This thesis focuses on developing a magnetic self-assembly method for high precision placement of parts with micro-scale thicknesses, i.e. ultra-thin chips (UTCs), without a direct mechanical contact. The chips are manipulated by the magnetic interactions between an externally applied magnetic field and nickel contact pads present on the chips. The method enables aligning the chips into a unique rotation by using shape matching between the asymmetric arrangement of nickel features on the chip and the gradient in the applied field.

The majority of flexible electronics applications require integration of thin chips on low-cost polymer substrates, with a high volume manufacturing fashion. However, handling thin parts (below $< 100\,\mu m$) with contact-based micro-assembly techniques is challenging due to the strong adhesion forces at micro-scale. This situation slows down the traditional assembly methods, i.e. pick-and-place machines, because of the following reasons: In contact based placement, the chip is squeezed between the pick-and-place tool and the substrate. The force applied to release the chip, which should compensate the strong adhesion, might damage the delicate chip. Additionally, in the cases where a die-attach adhesive is present on the substrate, there is a potential risk of contaminating the chip and the tool due to the capillary forces. Therefore, to prevent contamination or any potential damage to the chip the machine slows down while reaching the substrate.

The proposed approach enables combining directed micro-assembly methods with self-assembly, which lowers the precision demand required at the part presentation stage and allows releasing parts at a height above the substrate. After part presentation, self-assembly performs the fine positioning of the chip: the nickel layer becomes magnetized and forces the chip to relocate itself to the energetically most favorable position. The chip floats on a liquid layer during the alignment to decrease the friction at the substrate surface.

The relation between the magnetic field gradient, the magnetic material on the chip and the viscous layer are studied by modeling and experimentation. By changing different design parameters a guideline is developed for aligning the chips into a unique orientation. The experiments with optimized process parameters has shown that, the repeatability of the process is $3\sigma = 25\,\mu m$ in translation and $3\sigma = 2°$ in rotation, with an average alignment duration of 0.2 s.

The implementation of magnetic self-assembly was demonstrated with two different directed part presentation approaches. The first approach, implementation with pick-and-place showed that the machine travel times can be lowered by decreasing the precision required from the pick-and-place tool. In the second approach, laser die transfer provided direct ejection of chips and high speed part presentation.

In conclusion, the magnetic self-assembly method demonstrated in this thesis, enables trapping parts from a long range and aligns them to final precision with a unique rotation. The combination of the method with directed part presentation offers a hybrid

micro-assembly technique especially suitable for sparsely populated flexible electronics applications, such as smart packaging of disposable products.

Samenvatting

Dit proefschrift richt zich op de ontwikkeling van een magnetische zelf-assemblage methode voor het met hoge precisie uitlijnen van mechanische componenten met diktes in het micrometer bereik, in het bijzonder ultra dunne chips (Ultra Thin Chips, UTC's), zonder direct mechanisch contact. De chips worden gemanipuleerd door de magnetische interacties tussen een extern aangelegd magnetisch veld en de nikkel contacten die op de chips aanwezig zijn. Deze methode maakt het mogelijk om de chips met een unieke rotatie uit te lijnen door de asymmetrische plaatsing van de nikkel contacten te matchen met de gradiënt van het magnetisch veld.

Het merendeel van de toepassingen van flexibele elektronica vereist de integratie van dunne chips op goedkope polymeersubstraten, in een hoog-volume productieproces. Het hanteren van dunne onderdelen ($< 100\,\mu m$) met contact-gebaseerde microassemblage technieken is een uitdaging, vanwege de relatief sterke adhesiekracht op de microschaal. De traditionele assemblage methode, d.w.z. 'pick-and-place', wordt hierdoor ernstig vertraagd vanwege twee hoofdoorzaken: bij contact gebaseerd plaatsen wordt de chip wordt ingeklemd tussen het pick-and-place instrument en het substraat. De kracht die moet worden uitgeoefend om de sterke adhesie te compenseren en de chip los te laten, kan de chip beschadigen. Bovendien is er, in het geval er een 'die-attach' lijm aanwezig is op het substraat, een mogelijk risico om de chip en de nozzle te vervuilen vanwege de capillaire krachten. Om vervuiling en schade aan de chip te voorkomen moet de plaatsingsbeweging langzamer worden uitgevoerd.

De voorgestelde benadering maakt het mogelijk om discrete microassemblage technieken te combineren met zelf-assemblage en verlaagt daarbij de vereiste nauwkeurigheid in de 'part-presentation'-fase en maakt het mogelijk om onderdelen op een kleine hoogte boven het substraat los te laten. Na de part-presentation wordt de fijne positionering van de chip uitgevoerd door middel van zelf-assemblage: de nikkel laag wordt gemagnetiseerd en dwingt de chip in de richting van de energetisch meest gunstige positie. Tijdens het uitlijnproces drijft de chip op een vloeistoffilm om de wrijving met het oppervlak van het substraat te verminderen.

De relatie tussen de gradiënt van het magnetisch veld, het magnetisch materiaal op de chip en de viskeuze laag worden bestudeerd aan de hand van modellering en experimenten. Door het veranderen van verschillende ontwerpparameters worden de voorwaarden beschreven waaraan voldaan moet worden om de chips uit te lijnen met een unieke rotatie. De experimenten met de geoptimaliseerde procesparameters hebben laten zien dat de herhaalnauwkeurigheid van het proces $3\sigma = 25\,\mu m$ is wat betreft translatie en $3\sigma = 2°$ wat betreft rotatie, met een gemiddelde uitlijnduur van 0.2 s.

De implementatie van magnetische zelf-assemblage is gedemonstreerd met twee discrete part-presentation benaderingen. De eerste benadering, implementatie met een pick-and-place machine liet zien dat de machine translatietijd kan worden verminderd door de benodigde precisie van het plaatsingsinstrument te verkleinen. Bij de tweede benadering werd 'laser die transfer' gebruikt voor het direct losmaken van chips en presentatie op hoge snelheid.

Concluderend, de magnetische zelf-assemblage methode die in dit proefschrift wordt gedemonstreerd maakt het mogelijk om onderdelen aan te bieden vanaf een relatief grote afstand en lijnt ze uit met een unieke rotatie. De combinatie van deze methode met discrete part-presentation biedt een hybride microassemblage techniek die in het bijzonder geschikt is voor flexibele elektronische toepassingen met een lage dichtheid van componenten, zoals slimme verpakkingen van wegwerpproducten.

CURRICULUM VITÆ

Emine Eda KURAN

05-01-1986	Born in Hatay, Turkey.

EDUCATION

2004–2008 BSc. Systems Engineering
Yeditepe University, Istanbul, Turkey
Thesis: Sea Water Desalination by Forward Osmosis
Supervisor: prof. dr. M. Tunç

2008–2010 MSc. Mechanical Engineering
Columbia University, New York, USA
Research focus: Fabrication and mechanics of nano-porous gold thin films
Supervisor: prof. dr. J. W. Kysar

2010–2015 PhD. Mechanical Engineering
Delft University of Technology, Delft, Netherlands
Thesis: Magnetic self-assembly with unique rotational alignment
Promotor: prof. dr. U. Staufer
Co-promotor: dr. ir. M. Tichem
The research was a part of EU funded collaborative project, Chip2Foil.

LIST OF PUBLICATIONS

1. **E. E. Kuran**, Y. Berg, M. Tichem, Z. Kotler, *Integration of laser die transfer and magnetic self-assembly for ultra-thin chip placement*, Journal of Micromechanics and Microengineering, (2015).
2. **E. E. Kuran**, M. Tichem, *Magnetic self-assembly of ultra-thin chips to polymer foils*, IEEE Transactions on Automation Science and Engineering, **10**, 536 (2013).
3. **E. E. Kuran**, M. Tichem, U. Staufer, *Magnetic force driven self-assembly of ultra-thin chips*, Electronic System-Integration Technology Conference (ESTC), (2012).
4. M. Tichem, M. Cauwe, Z. Hajdarevic, **E. E. Kuran**, B. Naveh, A. Sridhar, P. Weissel, *Towards reel-to-reel integration of ultra-thin chips to polymer foils*, Electronic System-Integration Technology Conference (ESTC), (2012).

Acknowledgments

Doing a PhD is much like living in the movie "Risky Business": The well-known catchphrase of a doctoral study, "being self-independent" can be taken as, your parents going on vacation and leaving the keys to the Porsche at home. Being drunk off freedom, you drive in the town of science recklessly, with a slight idea of where to go and how to go there. At this point, someone needs to control your intake of alcohol, before you dump your car into the sea of literature. Thanks to my supervisors, no Porches were damaged during the first two years of my PhD.

In the third year, empowered by my new ability to control my thirst for trying out new things, (in reality, pushed by the upcoming deadlines), I became more conscious of what I am doing and started to get the first real results of my research. In the end of the third year, while I was getting drowsy by the closing of the EU project that my research was part of, my new chips arrived and the most exhausting year of my PhD had begun. With new chips, new ideas rushed into my mind. Again, at this point, I needed someone to ravel my thoughts. And again, thanks to my supervisors, my monkey mind was tamed in no time.

The fourth year was indeed exhausting, however it was also the most surprising and rewarding one. Now, I finally got to the end. And what an delightful end this is...

There were many great people traveling beside me on this exciting journey and no words can express my gratefulness to these people. However, since this will be my only chance to shout out my thanks to the world, I will give it a humble try in the following sentences.

First, I would like to thank my promoters Marcel Tichem and Urs Staufer. Marcel, you have been a constant source of encouragement and support. I can not express how lucky I have felt throughout my PhD, that I have a supervisor, "world's best boss", who has always believed in me and assured me of my potential. Even at the hardest moments, Marcel always says "You will get there!". While being modest, I can say that I am "there" finally, and your trust is one of the biggest reasons behind this. You stand as a great example for me both with your academic and personal attributes, especially your relation with your colleagues and your cheer up mode even in the most challenging moments of my PhD are some of the things that I am going to hold onto in my future career.

Urs, you have been always an inspiration, with your intelligence and generosity. Regardless of your busy agenda, you have always had time for me. I appreciate the enlightening discussions we had on the movement of my tiny chips. Thank you for your guidance and for teaching me how to observe things from the window of physics.

I also would like to express my sincere gratitude for our lab technicians Rob Luttjeboer, Harry Jansen and Patrick van Holst for their generous assistance and for being patient with my endless questions and wills. They showed me the way to do things right and transferred me from just a PhD student to an engineer that understands how to build a research setup. Patrick and Harry, I admire the way you work and your perfectionism.

Rob, I admire your "to do list", your patience and your willing to help everyone queuing at your door. It would have been impossible for me to go through all the details about how to build a “working” experimental setup without these great people.

I would like to thank Ron Van Ostayen and Matthijs Langelaar, for their extensive support on modeling with COMSOL. Dear Ron, I very much appreciate our fruitful discussions and your guidance even on the last minute. The stellar advices you have given me was very helpful in the last months of my PhD.

For the first three and half years, I had the chance to be a part of the Chip2Foil team, where I collaborated with incredible people from a variety of reseach areas. Here, I gratefully acknowledge my colleagues from the Chip2Foil consortium; Jeroen van den Brand, Henri Fledderus and Ashok Sridhar from TNO/Holst Centre, Netherlands; Zvi Kotler, Yuval Berg, Benny Naveh and Michael Zenou from Orbotech, Israel; Hannes Kostner, Zlatko Hajdarevic, Fabian Schnegg and Michael Lerchster from Besi, Austria; Philipp Weissel and Andreas Tanda from Plastic Electronics, Austria; Maarten Cauwe, Johan De Baets and Tomas Podprocky from IMEC, Belgium; and finally, Hajo Janse from Qolpac BV, Netherlands. Some of these remarkable people deserve extra credits for their direct contributions to my research.

Foremost, I must thank Zvi, for his enthusiasm on making a collaboration to combine self-assembly with laser die transfer, and for giving me the opportunity to do experiments at Orbotech. Special thanks goes to Yuval, it was a great pleasure to have your assistance during the experiments. There is still plenty of work to be done on this area, but we have made a strong step forward and I am very much pleased with our accomplishments. During my visit to Orbotech, I also met Michael Burdinov, whom I would like to thank for getting me started on the image analysis work.

I would also like to thank Hannes Kostner for opening me the doors of their labs in Austria. Fabian and Michael, thank you for the welcoming atmosphere and your help on the problems we encountered during the experiments. Zlatko, it has been great pleasure to work with you, thank you so much for the long hours you spend along with me in the lab. At sometimes, the experiments became enormously overwhelming that they required four highly skilled researchers at once, to do “high-performance” tasks; me fixing a foil into a setup, Zlatko pressing the start button, while Marcel is holding the light for the camera and Ashok running the UV source to cure the adhesive. I would say, this is the kind of true collaboration and synergy that every high-tech project should have nowadays, in order to succeed. Our striving for fabricating the demonstrators, and the fun lab moments we had are etched in my memory.

In the beginning of my research, we have tried finding alternative ways to fabricate parts/chips with nickel features. I am grateful to Henri, Andreas and Ashok for their help with preparing the first samples.

I am greatly indebted to Ashok, who have helped me a lot throughout the project. Ashok supplied me chips, foils, he helped me with creating the gel-film masks and screen printed the cover of my setup. Ashok, thank you also for your interest in self-assembly, our stimulating discussions have inspired me to try out new things for improving the method. Thank you so much for being there, whenever I needed help.

Furthermore, Maarten and his collegue Kristof Dhaenens helped me in the fabrication of the new chips, with electro-less nickel deposition. Dear Maarten, I should also thank you for the very practical but incredibly precious tool that you have given me to handle the thin chips. Funnily, those needles with silicon tips have been one of the most useful tools I have ever used during my PhD.

I also owe my sincere thanks to Luana Caron and Anton Lefering from the Radiation Science & Technology group (TNW), for squezing me in their tight schedules and making the SQUID magnetometer measurements of the eletroless nickel on the chips.

Coming back to the MNE group, I would like to thank former master student, Thomas Poiesz for his previous developments on magnetic self-assembly and for helping me to start up with the project. I would also like to thank Daan Stam for taking up the torch, I appreciate his enthusiasm to contribute to magnetic self-assembly research in our group.

I am grateful to the members of MNE academic staff, Guido Janssen, Murali Ghatkesar and Merlijn Spengen for their insight and the stimulating discussions in our group meetings. I would also like to thank Merlijn, along with Jaap Kokorian, for helping me with taking my first steps into image analysis.

I also owe a debt of gratitude to the support staff of the PME; our department manager Gaby Offermans, and PME secretary, Marli Guffens, Corinne duBurck, Marianne Stolker, Birgit Rademakers, Eveline Matroos (it was fun to share an office with you in the last days) for their continuous assistance. Marli, I should especially thank you for your patience with my “control freak” situations while doing my shipments.

I would like to thank the PhDs of the ever growing MNE group (the name order is earned by success in laser-tag and go-kart sessions); Hugo Perez Garza, Federico Buja, Venkata Girish Kotnur, Yueting Liu, Jaap Kokorian, Tjitte-Jelte Peters, Shou-En Zhu, Enrique Rull Trinidad, Kai Wu, and the former collegues; Adnan Noor, Friedjof Heuck, Iwan Kurniawan, Hans van Gurp, Ronald Stoute, Zhong Chonghe, Alexandre Beck and officemate, Jonathan Tigelaar. Each one of these wonderful people have played a significant role in my version of the “Days of our PhD lives” which involved: the smell sticking to one’s clothes after a lunch at Aula, an office booth filled with balloons, a man-sized private office made out of paper (up to the detail of curtains, an exit sign and an air conditioner control box), an RC helicopter occasionally buzzing around, a football appearing out of nowhere, stains on a coffee table and 4 egg chairs, vast amounts of free food and a broken air conditioner. I would not be able to stand in a small office with other 5 people for long hours, if it wasn’t fun. We had no windows seeing the direct sunlight, but the joy inside the room was bright enough. Special thanks goes to Jaap and Tjitte-Jelte, thank you for provoking me to learn LaTeX and for your help on the Dutch translations of the summary and propositions in this thesis.

The stereotypical PhD gets to prove that she/he has a fulfilling social life outside of faculty, by thanking friends and family in the last paragraphs of the acknowledgments. I will follow the tradition with no doubt, here is my bulletproof list of people who have been my support system for the last months; Jess, for her precious friendship, Neslihan and Nalan, for shushing away the gremlins in my mind for the past few months and giving me great advices upon graduation and Fabai, for being the cool flatmate for a year and teaching me how to cook rice cakes. The following people, accept my apologies! None of the “thank you” words would be enough for you, the great friends who have made my first years in Netherlands a blast; the ultimate triangle: Eli, Mounir and

Alessandro, the Indian couple: Nitish and Gopika, and finally sweet as french macarons, Manou. I would also like to thank my “24/7/365” true friends, whom I hope will not fight me over the order of names here; Sezgi, Irem, Sebnem, Esin and Görke and the great twins across the pond, Murcy and Mindy.

Kudos to my dear paranymphs, Elisabetta Iorfida and Alkisti Gkouzou, thank you for bearing the stress of the last bits of my PhD with me. Eli, you have come all the way from UK for my defense, and I am greatly thankful for having your support. You are one of the best things that happened to me in Netherlands, thank you so much for your friendship. And Alkisti, one of the most colorful people I have met, it has been a great pleasure to know you. You are a saga of personality, with your always smiling face and your kindness.

Finally, I would like to thank my family for all their love and for being there whenever I need them. My deepest thanks goes to my mother, my anxiety pill, whose voice always makes my worries vanish; my brother, who stands strong behind me like a tree that I can lean on without any doubts; and my sister-in-law, who has been rooting for me to succeed since the day I know her. You have been and will be my pillars of strength all my life. Making you proud is my greatest achievement.

It would be a shame if I skip mentioning my favorite cousin here; Seniz, having you around is always a tremendous blessing. Our road trips over the past years have been a breath of fresh air between my studies.

My final words belong to my father, my role model, whom I know is still around watching over his girl. I will consider myself successful, if I can become half the achiever you have been. Thank you for everything that made me who I am today.

Emine Eda Kuran
Delft, January 2015